UNIVERSITÉ LAVAL

On the function and genetic interactions of the *Caenorhabditis elegans* genes *alg-1* and *alg-2*

Thèse

Alejandro Vasquez Rifo

Doctorat en biologie cellulaire et moléculaire
Philosophiæ doctor (Ph.D.)

Québec, Canada

Résumé

La voie des microARNs est un mécanisme post-transcriptionnel de régulation génique qui contrôle divers aspects développementaux et physiologiques chez de nombreux eucaryotes supérieurs. Afin de mieux comprendre les rôles et modes d'actions des microARNs, nous avons entrepris l'exploration des interactions génétiques de cette voie chez le nématode *Caenorhabditis elegans*. Nous nous sommes ainsi concentrés sur les gènes codant pour les protéines Argonautes ALG-1 et ALG-2, qui sont les principaux constituants effecteurs de cette voie. Premièrement, nous avons caractérisé la relation entre ces deux paralogues, en étudiant respectivement leur expression spatio-temporelle, leur association avec des microARNs, ainsi que les phénotypes associés à leur perte de fonction. Nous avons ainsi pu définir des caractéristiques communes et spécifiques pour chacune de ces deux protéines Argonautes et décrire de manière précise leurs rôles essentiels lors du développement embryonnaire. En effet, nous avons démontré que l'absence d'expression zygotique des protéines ALG-1/2 provoque un arrêt du processus morphogénétique lors de l'allongement des embryons et un défaut dans les structures de fixation épidermique-musculaires. Deuxièmement, nous avons realisé un criblage génétique dans le but d'identifier des nouveaux partenaires des protéines Argonautes ALG-1/2. Nous avons découvert le gène codant pour la protéine VPS-52, qui est un composant du complexe GARP (*Golgi Associated Retrograde Protein*). La caractérisation de ce gène nous a permis de démontrer que VPS-52 interagit génétiquement avec le gène *alg-1* et se comporte comme un modulateur positif de l'activité de certains miARNs impliqués dans le développement larvaire. Les mutants de *vps-52* aggravent les défauts des cellules souches épidermales observés dans les mutants de *alg-1* et du microRNA *mir-48*. Ils augment également la létalité du mutant *let-7(n2853)* et ce dépendement de sa cible. Ces augmentations phénotypiques sont liées à une baisse des niveaux des microARNs miR-48, miR-241 et des protéines GW182. Cette étude nous amène donc à proposer que l'activité des microARNs peut être contrôlée en partie par un mécanisme de transport rétrograde dépendant du complexe GARP.

Abstract

The microRNA pathway is a post-transcriptional gene regulatory system that controls multiple developmental and physiological processes in many eukaryotes. We have undertaken the exploration of the genetic interactions of this pathway in the nematode *Caenorhabditis elegans*, with the goal of unveiling processes controlled by microRNAs and the mechanisms of microRNA action. We focused on the genetic interactions of the *alg-1* and *alg-2* genes, that encode the microRNA-specific Argonaute proteins, key effector constituents of this pathway. In the first place, we characterized the relationship between these two argonaute paralogs, with respect to their spatio-temporal expression, association to microRNAs, and loss-of-function phenotypes. Thus, we defined shared and gene-specific features of these Argonautes and defined in detail their essential role during embryonic development. The absence of zygotic *alg-1* and *alg-2* expression causes arrest during the morphogenetic process of elongation with defects in the epidermal-muscle attachment structures. Addressing another aspect, we sought to elucidate novel genetic interactors of these argonautes using a forward genetics approach. We identified *vps-52*, a component of the GARP (Golgi Associated Retrograde Protein) complex, as a genetic interactor of the *alg-1* gene and established that, through its GARP complex function, it effects a positive modulatory role on miRNA activity. Mutants of *vps-52* exacerbate the seam cell defects in the loss-of-function alleles of *alg-1* and the *let-7* miRNA family member *mir-48* and enhance the lethality of the *let-7(n2853)* hypomorph in a target dependent manner. These phenotypic enhancements related to decreased levels of the *let-7* family microRNAs (miR-48 and miR-241) and the worm GW182 protein. Furthermore, the positive effect of *vps-52* on microRNA activity seems to be conserved in mammalian cells, where VPS52 co-fractionates with miRISC components. Our analyses allow us to propose that VPS-52 as part of the GARP complex participates in membrane-related processes of the miRNA pathway, which facilitate miRNA activity and operate at the effector miRISC level.

Contents

Résumé iii

Abstract v

Contents vii

List of Tables ix

List of Figures xi

Nomenclature and Abbreviations xiii

Acknowledgments xvii

Foreword xix

1 Introduction and Review of the Literature 1
- 1.1 Post-transcriptional gene regulation . . . 2
- 1.2 The microRNA pathway . . . 3
- 1.3 The miRNA pathway and cancer . . . 15
- 1.4 The miRNA pathway in *C. elegans* . . . 17
- 1.5 Cellular aspects of microRNA function . . . 22
- 1.6 Doctoral research objectives . . . 28

2 Developmental characterization of *C. elegans alg-1* and *alg-2* **29**
- 2.1 Résumé . . . 31
- 2.2 Abstract . . . 32
- 2.3 Introduction . . . 33
- 2.4 Results . . . 34
- 2.5 Discussion . . . 47
- 2.6 Materials and Methods . . . 49

3 Implication of the GARP complex in *let-7* microRNA family function **53**
- 3.1 Résumé . . . 55
- 3.2 Abstract . . . 56
- 3.3 Introduction . . . 57
- 3.4 Results . . . 58
- 3.5 Discussion . . . 70

3.6 Materials and Methods 72

4 Concluding remarks and perspectives **77**
4.1 Developmental aspects of *alg-1* and *alg-2* 77
4.2 *vps-52*, a new genetic interactor of the *C. elegans* microRNA pathway 82

Bibliography **91**

A A primer on *C. elegans* embryonic development **109**
A.1 *Caenorhabditis elegans* 109
A.2 Embryonic development 109

B A primer on vesicular trafficking **113**
B.1 Introduction 113

C microRNAs in germ cells proliferation and differentiation **117**

D Argonaute pull-down using 2'-O-methylated oligonucleotides **129**

List of Tables

1.1 Selected core protein components of the miRNA pathway 4
1.2 Homology between the worm and human GW182 proteins. 10

2.1 Summary of ALG-1/2 expression in different organs and tissues. 36

3.1 Alae defects of vesicular trafficking mutants. 62
3.2 Alae defects for the *vps-52, hbl-1* and *mir-48* mutant animals. 63
3.3 Lethal vulva bursting phenotype observed in different mutant backgrounds. 65

List of Figures

1.1 Biogenesis of the let-7 miRNA. . . . 6
1.2 The *C. elegans let-7* family of miRNAs. . . . 6
1.3 Structural features of the core proteins of the miRNA pathway. . . . 8
1.4 Structure of the human AGO2 Argonaute. . . . 9
1.5 The miRNA binding sites in the *lin-41* mRNA. . . . 13
1.6 Schematic flow of miRNA pathway phases and processes. . . . 14
1.7 Development of the seam cells in *C. elegans*. . . . 20
1.8 Developmental course of miRNA action during *C. elegans* development. . . . 21
1.9 Model of miRNA processes affected by trafficking complexes. . . . 25

2.1 Features of the miRNA-specific Argonautes ALG-1 and ALG-2. . . . 35
2.2 Immunostaining of ALG-1 in adult *C. elegans* hermaphrodites. . . . 36
2.3 ALG-1 and ALG-2 expression profile in adult worms. . . . 37
2.4 Profile of ALG-1 and ALG-2 expression in larval stage. . . . 38
2.5 Embryonic ALG-1 and ALG-2 expression. . . . 38
2.6 ALG-1/-2 expression in somatic gonad, seam cells and neurons. . . . 39
2.7 ALG-1/-2 expression in neurons, hypodermal and muscular tissues. . . . 40
2.8 Detection of ALG-1 and GFP::ALG-2 in purified complexes. . . . 41
2.9 Relative microRNA association with ALG-1 and ALG-2. . . . 42
2.10 ALG-1 and ALG-2 are required for *C. elegans* embryonic development. . . . 43
2.11 Developmental timing of double *alg-1/2* mutant and siblings. . . . 44
2.12 ALG-1/2 function is required to maintain muscles and the epidermis. . . . 46

3.1 Seam cell-related phenotypes of the GARP mutants. . . . 59
3.2 Features and mutants of the *vps-52* gene. . . . 60
3.3 Analysis of precocious alae synthesis. . . . 64
3.4 Fractionation of VPS52 with the miRISC components in human cells. . . . 66
3.5 Effect of *vps-52* on the level of components of the miRNA pathway. . . . 67
3.6 Effect of *vps-52* on miRISC components. . . . 68
3.7 Detection of the pri- and pre-miRNA forms of let-7 family miRNAs. . . . 69
3.8 Interpretative model of GARP-mediated effects on miRNA activity. . . . 72

4.1 Immunoprecipitation of VPS-52. . . . 87

A.1 Anatomy of epidermal and muscle attachment structures. . . . 110

B.1 Schematic of the processes of vesicular traffic. . . . 114
B.2 Intracellular tethering complexes. . . . 115

Nomenclature and Abbreviations

A. thaliana *Arabidopsis thaliana*, page 26

C. elegans *Caenorhabditis elegans*, page 1

D. melanogaster *Drosophila melanogaster*, page 3

e.g. latin, for example, page 41

i.e. latin, that is, page 47

sensu lato latin, in the broad sense, page 15

AU-rich elements Adenylate-uridylate-rich elements, page 2

BLOC-3 complex Biogenesis of lysosome-related organelles complex 3, page 26

Co-IP Co-Immunoprecipitation, page 87

DSRM dsRNA binding motif, page 7

dsRNA double-stranded RNA, page 7

DTC Distal Tip Cell, page 19

ESCRT complex Endosomal Sorting Complex Required for Transport Complex, page 24

FO Fibrous organelle, page 111

GDP Guanosine diphosphate, page 113

GTP Guanosine triphosphate, page 113

miRISC miRNA Induced Silencing Complex, page 3

miRNA microRNA, page 3

mRNA messenger RNA, page 2

MVBs Multivesicular bodies, page 22

NSF N-ethylmaleimide- sensitive fusion protein, page 113

P-bodies Processing bodies, page 22

Pat paralyzed at 2-fold, page 111

PIP4,5 phosphatidyl inositol 4,5 phosphate, page 84

piRNA Piwi-interacting RNAs, page 3

poly(A) tail poly-adenylate tail, page 2

pre-miRNA precursor miRNA, page 5

pri-miRNA primary miRNA, page 5

RNAi RNA interefence, page 7

siRNA short interfering RNA, page 3

SNARE soluble NSF attachment protein receptor, page 113

TGN *trans*-Golgi Network, page 58

TS Temperature sensitive, page 19

Ub ubiquitin, page 116

UTR untranslated region, page 2

UV ultraviolet, page 77

A Maria, Alejandro, Elisa, Raul,
Eleonora, Claudia, Wiem y
Claire.

Acknowledgments

I would like to acknowledge my supervisor Dr. Martin Simard, for giving me the opportunity to join his laboratory in which I completed my graduate studies. Throughout the lows and highs of these years, his advice and determination have been essential to strengthen what I have been able to contribute to science. I would also like to acknowledge present and past lab members, Irfan, Samir, Guillaume, Sandra, Gabriel, Johannie and Evelyne who contributed in some way to what I have achieved. From the research centre community, I would like to show my gratitude to my friends Prakash, Ranjan, and Wajid, for the nice moments we shared together, and Eric Paquet for his friendly advice in bioinformatics. I am fortunate to have collaborated during my studies with Dr. Michael Labouesse, Dr. Javier Armisen, Dr. Eric Miska, Dr. Derrick Gibbings and Dr. Olivier Voinnet.

I owe special gratitude to my former professor Carmen, and to my friends Arturo, Leonardo, William and Bich. I specially dedicate this work to my family: Alejandro (*In memoriam*), Maria, Elisa, Raul, Eleonora, and also to Claudia, Wiem and Claire.

Foreword

Chapters 2 and 3 of the present thesis are constituted by research articles.

The chapter 2 is constituted by an article recently published in the journal PLoS ONE (Vasquez-Rifo *et al.*, 2012). I performed most of the experiments presented in the paper, Syed Irfan Ahmad Bukhari did the ALG-1 immunostaining of worms, Evelyne L. Rondeau performed preliminary immunoprecipitation experiments, the immunoprecipitation of Argonaute proteins was conducted by Guillaume Jannot, their associated small RNAs were hybridized to microarrays by Javier Armisen from the laboratory of Eric A. Miska. Michel Labouesse performed the immunostaining of muscle and hemidesmosomes in embryos.

The chapter 3 is constituted by a manuscript submitted for publication in the journal 'Proceedings of the National Academy of Sciences of the United States of America'. I performed most of the experiments presented in the manuscript. Derrick Gibbings from the laboratory of Olivier Voinnet carried to completion the experiments in mammalian cells. Gabriel Bossé contributed to the mutant identification and performed Northern blotting analyses. Evelyne L. Rondeau performed the random mutagenesis screen.

I am fortunate to have collaborated in several studies of my colleagues. The appendix C is constituted by an article published in the journal 'Cell research' (Bukhari *et al.*, 2012). I contributed to this study of my colleague Irfan Bukhari by generating plasmids and the corresponding transgenic reporter lines. The appendix D is constituted by a book chapter published in 'Methods Mol Biol.' (Jannot *et al.*, 2011b). I participated in the redaction of this study of my colleague Guillaume Jannot.

Chapter 1

Introduction and Review of the Literature

Foreword

The present chapter covers introductory aspects that I judged most relevant for the understanding and presentation of the subsequent chapters, namely some information on post-transcriptional gene regulation and a general description of the microRNA pathway. This is followed by the presentation of the pathway components and roles in the model organism *Caenorhabditis elegans* (*C. elegans*). The chapter concludes with a presentation of cellular aspects of the pathway, a topic of particular relevance to the chapter 3.

I have omitted historical and evolutionary aspects, which have been described in detail in these reviews (Pager *et al.*, 2009; Vella and Slack, 2005). In addition, I have focused on the miRNA pathway as it occurs in animals. The pathway in plants have considerable similarities but important differences as well (Vaucheret, 2006). It is also of note that while the pathway is found in eukaryotes, components of it, like the Argonaute proteins, are also present in archaea where they have been proposed to fulfill a function in transposon defense (Makarova *et al.*, 2009).

1.1 Post-transcriptional gene regulation

The control of genes once they are transcribed can occur by a variety of mechanisms, and, in general, specific features in the messenger RNAs (mRNA) determine the type of control used. Modifications of the translation machinery can affect the translation of many genes. This regulatory mode is exemplified by the phosphorylation of the translation initiation factor eIF2, a modification that inhibits its function and hence strongly slows translation in a widespread manner (reviewed in Proud 2005). Conferring another regulatory mode, certain mRNAs contain specific sequences downstream of the original initiation codon that allow translation to start by a initiation complex that binds to them. Sequences of this kind, known as 'Internal Ribosome Entry Sites' render translation initiation independent of the common interactions and factors. Examples of this mode of regulation are found in viruses and cellular mRNAs like that of the Bip protein (reviewed in Hellen and Sarnow 2001). Furthermore, an additional mode of post-transcriptional control that affects the translation of mRNAs is the binding of specific regulators to particular 5' untranslated region (UTR) sequence elements. This type of regulation has been demostrated by the control of ferritin mRNA translation by the regulatory form of the aconitase enzyme. This regulatory form binds a stem-loop located in the 5'UTR of the ferritin mRNA and blocks its translation (reviewed in Rouault 2006).

The stability of mRNA is a primordial factor that regulates its temporal existence. Most cellular mRNAs carry a terminal 3'UTR poly-adenylate (poly(A)) tail sequence of varied length that contributes to the stability of the messenger RNA. This tail sequence is subject to the shortening action of exonucleases that ultimately will entirely digest it, impairing translation and favoring the further nucleolytic destruction of the mRNA. The length of the poly(A) tail can be subjected to biological regulation, for example by enzymes (poly(A) polymerases) that can extend the tail in specific cells (reviewed in Richter 1999), and also as a result of multiple polyadenylation sites conferring mRNAs with alternative poly(A) tails of varied length (reviewed in Weill *et al.* 2012). A sequence feature, the adenylate-uridylate-rich elements (AU-rich elements) in the mRNA 3'UTR can also control its stability. A number of proteins recognize AU-rich elements. The mammalian HuR protein and its paralogs confer increased stability upon binding these elements. Another protein, tristetraprolin, also binds these elements and provokes mRNA deadenylation and subsequent degradation. Examples of this mode of regulation are found in the mRNAs of the cytokines IL-2, IL-3, TNF-alpha and c-myc among many others (reviewed in Barreau *et al.* 2005).

Another kind of gene regulatory mechanisms that encompasses several pathways makes use of small RNA molecules to regulate targeted RNAs post-transcriptionally. These different small RNA pathways share several features such as the sequence complementarity (partial or complete) between the small RNA and its target. This provides specificity of interaction. Another common feature is the incorporation of the small RNA molecule into a protein of

the Argonaute family to mediate its effector functions. Three major systems of this regulatory kind are those of microRNAs (or miRNAs for brevity), siRNAs (short-interfering RNAs) and piRNAs (Piwi-interacting RNAs) (reviewed in Siomi *et al.* 2011). An important difference between miRNA and siRNA in animals is that the first are partially complementary to their targets, while siRNAs are fully complementary to them [1]. A varying degree of overlap exists between the siRNA and miRNA pathways in different species, caused by the shared use of biogenesis factors (*i.e.* Dicer) and Argonautes. In *C. elegans*, these two pathways are clearly separated, and each small RNA class binds to different members of the Argonaute protein family (see section 1.2.1).

The present thesis is centered on the miRNA pathway. This pathway is a gene regulatory system that regulates mRNAs post-transcriptionally. The mRNAs that contain binding sites for miRNAs in their 3'UTR are targeted by an effector complex comprising, at its core, an Argonaute protein and its associated miRNA, termed the miRISC (miRNA Induced Silencing Complex). This complex binds mRNA and mediates the repressive processes of target expression by mechanisms that induce translational inhibition and mRNA destabilization (see section 1.2.3.)

1.2 The microRNA pathway

1.2.1 Components of the miRNA pathway

The components of the miRNA pathway can be categorized according to their role as factors of miRNA processing or biogenesis (Dicer, Drosha, Pasha/DGCR8 and the Argonautes), of miRNA effector function (Argonautes, GW182 proteins), and factors involved in recycling and termination of the miRNA response (such as the nucleases XRN1, XRN2, the exosome complex and likely additional factors). Another pertinent distinction is between core and accessory components. The main core protein components of the human, *C. elegans* and the fly *Drosophila melanogaster* (*D. melanogaster*) species are listed in table 1.1 and their features described below. For simplicity the listed generic names may be preferred hereafter where appropriate. It is noteworthy that a different number of protein paralogs are present in each species. In addition, the mentioned protein components of the miRNA pathway may additionally function in the siRNA pathway. For example, the human miRNA and siRNA pathway partially converge. Both miRNAs and siRNAs can be processed by the single mammalian Dicer protein and bound by the AGO2 Argonaute protein. In the fly, the two small RNA pathways are mostly separated with dedicated Dicer and argonaute genes for each pathway [2].

1. An exception to this generalization may be constituted by the highly complementary *mir-249* miRNA in *C. elegans* (Park *et al.*, 2013)

2. The fly AGO2 and Dicer-2 proteins affiliate mostly to siRNAs, while AGO1 and Dicer-1 do mostly to miRNA.

Generic name	Human	*D. melanogaster*	*C. elegans*
Drosha	DROSHA	Drosha	DRSH-1
Pasha	DGCR8	Pasha	PASH-1
Dicer	DICER	Dicer-1	DCR-1
Argonautes	AGO1-4	AGO1	ALG-1 and ALG-2
GW182	TNRC6A-C	GW182	AIN-1 and AIN-2

Table 1.1: **Protein components of the miRNA pathway.** The human miRNA pathway comprises four Argonautes (AGO1 to AGO4) and three GW182 homologues (TNRC6A,-B and -C). In flies, most miRNAs are associated to the AGO1 Argonaute, however a few associate with a distinct Argonaute (AGO2) more specialized in the siRNA pathway. From the expanded family of Argonautes in *C. elegans* (24 members), two associate exclusively with the miRNA pathway (ALG-1 and ALG-2). Similarly, two GW182 homologues are present in worms.

In the worm *C. elegans*, the multiple pathways mediating siRNA functions are widely separated from that of miRNAs (see also section 1.4), but there is a common partial requirement for one single Dicer (DCR-1) enzyme. The majority of the studies on the mechanisms of the miRNA pathway in animals refer to flies and mammals, so it is important to note the distinct involvement of pathway components with regard to both miRNA and siRNA function.

The core pathway components are necessary for the biogenesis and action of most miRNAs. In contrast, a number of proteins are important for the processing of specific subsets of miRNAs. Most of these proteins recognize sequence-specific features in the immature miRNA forms and promote or repress their processing (reviewed in van Kouwenhove *et al.* 2011). For example, proteins of the SMAD family promote processing of the immature primary form of the mammalian mir-21 miRNA that has a consensus sequence for SMAD binding in its stem region (reviewed in Blahna and Hata 2012). Another regulator of miRNA biogenesis is the LIN28 protein, which binds both the precursor and primary forms of the let-7 miRNA through its terminal loop sequence and prevents its processing (Heo *et al.*, 2008; Viswanathan *et al.*, 2008; Newman *et al.*, 2008; Rybak *et al.*, 2008; Piskounova *et al.*, 2011).

Variations in the process of miRNA biogenesis exist but are restricted to rather few miRNAs. A small set of miRNAs contained inside introns are transcribed as part of the mRNA that contains them, and their non-mature form released upon splicing and debranching of the pre-mRNA intron. These miRNAs do not need the processing function of the Drosha protein, but are cleaved by Dicer and are termed mirtrons (Okamura *et al.* (2007), reviewed in Westholm and Lai 2011). Four mirtrons have been reported to be contained in the *C. elegans* genome (Isik *et al.*, 2010). Another special form of biogenesis has been described for the vertebrate *mir-451*. Processing of this miRNA does not require Dicer but rather the catalytic activity of the Argonaute AGO2 (Cifuentes *et al.*, 2010; Cheloufi *et al.*, 2010). In the following sections emphasis is on the processes responsible for the biogenesis and action of the majority of miRNAs in animals, centered on *C. elegans*.

miRNAs

miRNAs are genes that are transcribed to RNA molecules that do not code for proteins, and once processed become small RNAs (20 to 24 nucleotides long). When bound to specific Argonaute proteins, they form the core miRISC. The miRISC is the effector complex that targets and regulates mRNAs in a sequence-specific manner. Most miRNAs genes have specific promoters for RNA polymerase II and transcription results in a primary miRNA form (pri-miRNA) that contains the characteristic termini: a 7-methyl-guanosine cap at the 5' extremity and a 3' poly(A) tail. The pri-miRNA transcript includes a stem-loop structure from which the miRNA will derive after two enzymatic cleavages (Figure 1.1). In the first processing step, the neighboring regions of the stem loop are removed giving rise to the precursor miRNA form (pre-miRNA). The pre-miRNA is a 60 to 70 nucleotides long stem-loop that contains 5' and 3' stem parts and a terminal loop. In the subsequent processing step, the terminal loop is cleaved. The mature miRNA can be contained in either the 5' or 3' stem regions. In certain cases, both 5' and 3' molecules can become a mature miRNA and fulfill biological functions (they are referred to as 5p miRNA and 3p miRNA) (Yang *et al.*, 2011; Okamura *et al.*, 2008). However, in most cases only one of the molecules of the duplex will become incorporated into the Argonaute protein (named the 'guide strand', the mature miRNA molecule), while the other small RNA will be degraded (named the 'passenger strand', or the miRNA-star (miRNA* molecule). In animals, the mature miRNA termini are nucleotide monophosphates and in general, no nucleotide bears other chemical modifications[3]. The 2'-o-methyl groups found in other kinds of small RNAs are absent from miRNAs, and adenosine to inosine editing seems very rare in *C. elegans*, potentially affecting only two miRNAs (Warf *et al.*, 2012).

Sequence analysis has established that the most conserved region of a miRNA is a seven nucleotide stretch starting from the second 5' nucleotide, a region termed the 'seed' region. This nucleotide stretch is generally fully complementary to a sequence in the 3'UTR of the miRNA targeted gene, and mutations in this region are much less functionally tolerated compared with mutations outside the seed region. MiRNA 'seed' families have been defined based on the conservation of this region. For example, a sequence alignment of the *C. elegans let-7* miRNA family members is shown in figure 1.2. Two additionally verified miRNAs, *mir-794* and *mir-795* and two partially verified miRNAs, *mir-793* and *mir-1821* also belong to the *let-7* miRNA 'seed' family but their function is unknown (Johnson *et al.*, 2005; Warf *et al.*, 2011).

3. However, non-templated nucleotide additions can be found in miRNAs (reviewed in Kim *et al.* 2010.)

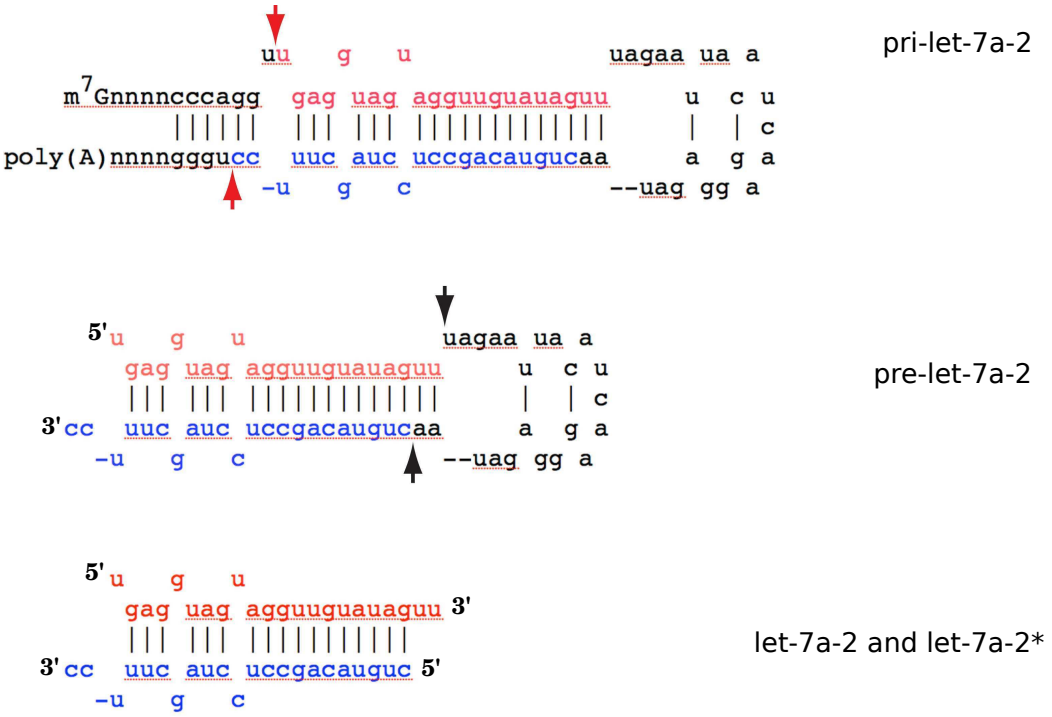

Figure 1.1: **Biogenesis of the let-7 miRNA.** The processing steps of the human *let-7a-2* miRNA are illustrated. The top molecule represents the pri-let-7 molecule that is cut by Drosha. The stem-loop pre-let-7 form (the middle) is then processed by Dicer. The mature miRNA and miRNA* molecules of the let-7 miRNA are shown at the bottom. The nucleotide sequence of the mature let-7 is colored red, while the let-7* passenger sequence is colored blue. Red arrowheads indicate sites of Drosha cleavage, black arrowheads indicate the site of Dicer cleavage. Note the 2 nucleotides overhangs produced by these enzymes and the partial complementarity between the miRNA and miRNA* molecules.

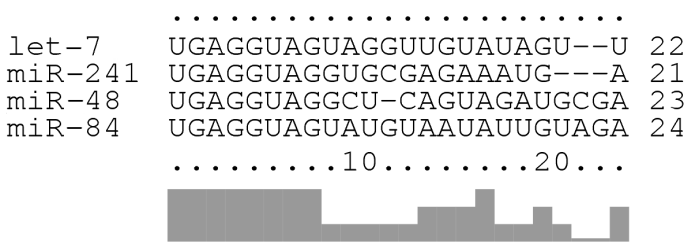

Figure 1.2: **The *C. elegans let-7* family of miRNAs.** Alignment of the mature sequences of *let-7, mir-48, mir-84* and *mir-241* obtained used the locARNA program. Gray bars below the alignment indicate the relative conservation of each position. The nucleotides 1 to 8 are identical among the family members.

The Drosha and Dicer enzymes

The Drosha and Dicer enzymes are miRNA biogenesis factors that convert the pri-miRNA into pre-miRNA and process the pre-miRNA to the mature miRNA molecule, respectively (Figures 1.1, 1.3). Both enzymes are RNase-III family endonucleases and produce two nucleotide overhangs upon cleavage. The Drosha enzyme contains a domain architecture [4] composed of two double-stranded RNA (dsRNA) binding domains and a dsRNA binding motif (DSRM) (Figure 1.3). Another factor, the Pasha protein, contains WW domains (suggested to be involved in protein-protein interactions by binding specific proline sequences (Macias *et al.*, 2002) and binds Drosha. Together, Pasha and Drosha form a complex termed the microprocessor complex (Gregory *et al.*, 2004) that cleaves pri-miRNAs in the nucleus.

Dicer is the cytoplasmic enzyme responsible for pre-miRNA processing. The protein has the following domain architecture in worms: A N-terminal helicase domain, followed by a DUF283 domain that displays a non-canonical dsRNA binding fold (Qin *et al.*, 2010; Dlakic, 2006), a PAZ domain, two ribonuclease III dsRNA binding domains and a DSRM motif (Sawh and Duchaine, 2012) (Fig. 1.3). Dicer activity is not only required for miRNA production; this enzyme is also able to cut long double-stranded (dsRNA) molecules such as those exogenously introduced into worms in order to perform RNA interference (RNAi). In addition, it is necessary for the production of a set of naturally occurring small dsRNA molecules (*i.e.* endo-siRNAs). Indeed, these additional functions involve the helicase domain, a domain that is not essential for miRNA processing (Welker *et al.*, 2010). The PAZ domain of Dicer binds the free termini of the pre-miRNA molecule. Each of the two dsRNA binding domains appears to be responsible for one of the two cuts on the pre-miRNA molecule necessary to produce the miRNA molecule and the release of the terminal loop (Gurtan *et al.*, 2012).

The Argonaute proteins

In eukaryotes, the Argonaute family of proteins bind small RNAs and function in a partnership as effector complexes. In addition, some of these proteins have RNA cleavage activity (reviewed in Hutvagner and Simard 2008). The Argonaute bound to the miRNA is considered the minimal effector miRISC that is able to bind mRNAs and induce a regulatory outcome. The Argonaute domain architecture is composed of PAZ and PIWI domains [5] (Fig. 1.3). Recently, the tridimensional crystal structure of the complete human AGO2 Argonaute was determined (Elkayam *et al.* (2012); Schirle and MacRae (2012), reviewed in Sasaki and Tomari 2012). The PAZ domain (also found in the Dicer enzyme), harbors a binding pocket for the 3' hydroxyl

4. Considered as the linear arrangement of the set of domains present in a protein. The structural features of the proteins are taken from the SMART domain annotation database (Letunic *et al.*, 2012).

5. Additionally, protein 'N-term domain' and 'Mid domain' (in between the PAZ and PIWI domain) are commonly incorporated in the Argonaute domain architecture.

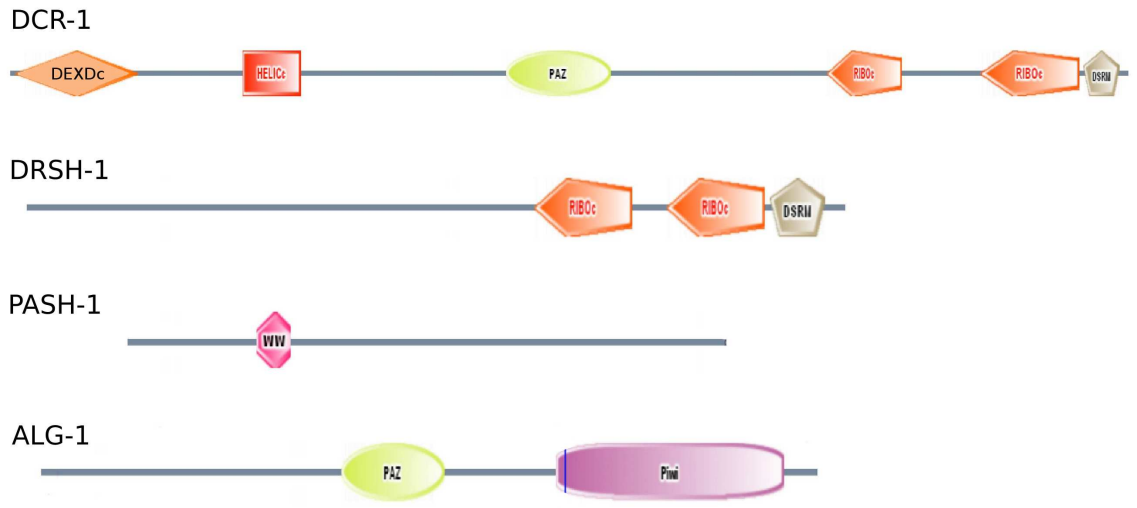

Figure 1.3: **Structural features of the core proteins of the miRNA pathway.** Domains of the core proteins involved in the *C. elegans* miRNA pathway. The features are presented as found in the domain annotation SMART database (Letunic *et al.*, 2012). DCR-1 contains a helicase domain (DEXDc), DUF283 (HELICc), dsRNA binding domains (RIBOc) and dsRNA binding motif (DSRM). DRSH-1 contains the two RIBOc and DSRM. PASH-1 contains a WW domain. ALG-1 (and ALG-2 as well) contain PAZ and PIWI domains.

end of the miRNA. A second binding pocket, localized in the PIWI domain, recognizes the 5' monophosphate of the miRNA, and also contacts the base of the first 5' nucleotide. The miRNA is thus anchored by its two extremities, and the miRNA seed region (nucleotides 2 to 8) is prearranged inside the Argonaute in a conformation that favors target binding. The PIWI domain harbors core aminoacids that are necessary for the catalytic activity exhibited by some Argonautes, as well as tryptophan binding pockets that likely mediate the binding to GW182 proteins (Figure 1.4).

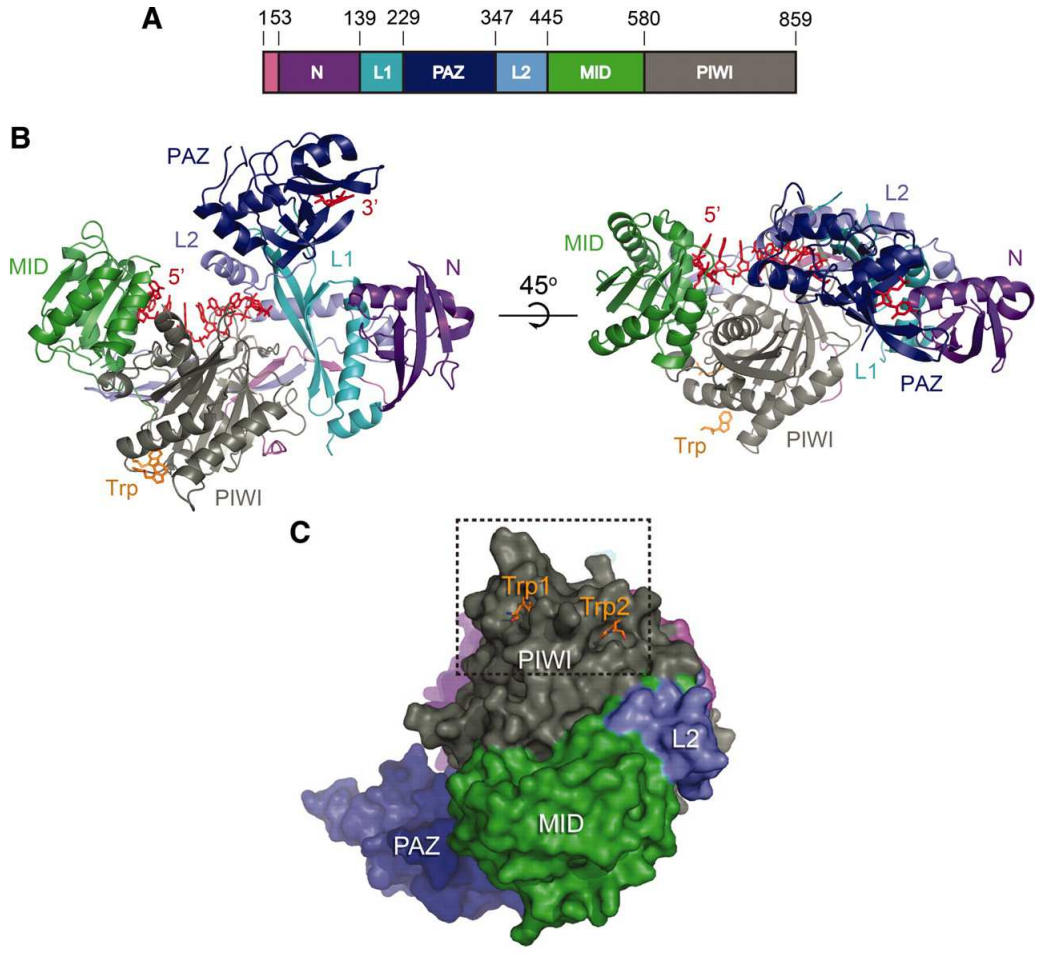

Figure 1.4: **Crystal structure of the human AGO2 Argonaute protein. A)** AGO2 domain architecture. **B)** The AGO2 Argonaute protein has a bi-lobed form with a groove pocket that separates the 'Mid' and PIWI from PAZ and 'N-term'. This groove accommodates the RNA molecule. The co-crystalized small RNAs (indicated in red color) display a distinctly organized conformation for the first eight nucleotides starting from the 5' binding pocket (at the MID-PIWI interface). They then become disorganized (not visible) and their 3'-end nucleotide binds into the PAZ domain. **C)** Two closely located trypthophan binding pockets (surrounding the Trp1 and Trp2 molecules in orange color) are located in the PIWI domain. Figure reproduced with permission from Schirle and MacRae (2012).

A

	TNRC6A	TNRC6B	TNRC6C
AIN-1	24%	24%	23%
AIN-2	21%	24%	23%

GW/WG motifs

B

TNRC6A	39/60
TNRC6B	25/58
TNRC6C	34/56
AIN-1	7/22

Table 1.2: **Homology between the worm and human GW182 proteins.** The worm GW182 proteins, AIN-1 and AIN-2 display weak homology to the human GW182 homologues TNRC6A-C. **A)** The percentage of sequence identity over the length of the shorter protein is displayed for pairwise sequence alignments of the proteins TNRC6A-C with AIN-1 or AIN-2. **B)** The number of GW/WG motifs divided over the total number of tryptophan (W) aminoacids is indicated for each GW182 protein (data from Ding and Han (2007)).

GW182 proteins

The GW182 proteins fulfill an effector role, they bind the Argonaute proteins and recruit complexes that promote mRNA decay. GW182 proteins do not participate in the processes of miRNA biogenesis, and do not impair miRNA stability (*e.g.* Jiang *et al.* (2012),Zhang *et al.* (2007)). The most prominent feature of these proteins is the presence of a series of Glycine(G) and Tryptophan(W) repeats, the GW/WG/GWG motifs. Their domain architecture in mammals and flies includes a ubiquitin associated domain, RNA recognition motifs and Glutamine-rich stretches (reviewed in Eulalio *et al.* (2009)). In contrast, the nematode GW182 homologs, AIN-1 and AIN-2 (Ding *et al.*, 2005; Zhang *et al.*, 2007), do not have any of these domains and display only a distant sequence homology to their mammalian counterparts. The only prominent signatures of the AIN-1/AIN-2 proteins are the GW/WG/GWG motifs themselves (Table 1.2). These motifs are considered sufficient to mediate a direct physical interaction of GW182 with the Argonaute protein. The binding of GW182 to the miRISC contributes to the miRNA-mediated repression of mRNA expression as explained below.

Other components

The proper function of the miRNA pathway depends on additional cellular processes, like transcription, nuclear export systems, and cytoplasmic nucleases. Upon transcription of the miRNA gene by the polymerase II, and processing by the microprocessor complex (Drosha and Pasha) in the nucleus, the pre-miRNA is exported to the cytoplasm in a process mediated by the Exportin 5 protein (Lund *et al.*, 2004; Bohnsack *et al.*, 2004; Yi *et al.*, 2003). In the cytoplasm, the pre-miRNA is processed and the mature miRNA bound by an Argonaute protein. The miRISC engages molecular complexes important for the degradation of mRNAs,

like the CCR4-NOT complex and the PAN2-PAN3 deadenylase complex. These nucleolytic complexes have been proposed to be recruited by the GW182 proteins to degrade the mRNA targeted by the miRISC (reviewed in Fabian and Sonenberg 2012).

1.2.2 Biogenesis of miRNAs

Following transcription of the miRNA gene, the pri-miRNA is processed by the action of the Drosha enzyme in the nucleus and the resulting pre-miRNA exported to the cytoplasm. The pre-miRNA is then cleaved again by Dicer removing the terminal loop, to produce the mature miRNA (Figure 1.1). At this point, the mature miRNA molecule is produced. However, the miRNA molecule has to become bound by the Argonaute protein, in a process termed 'Argonaute loading'[6] (reviewed in Kawamata and Tomari 2010). The Argonaute loading process can be considered the final step of miRNA biogenesis.
A current model of Argonaute loading, starting with small RNA duplex is the following. In the first step, the Argonaute binds a small RNA duplex, an ATP-dependent process proposed to be mediated by the action of the HSP90 chaperone (Iwasaki *et al.*, 2010; Miyoshi *et al.*, 2010). Next, the duplex is unwinded in a process that does not involve Argonaute-mediated cleavage of the passenger strand of the miRNA-miRNA* duplex, because in general, mismatches in duplexes of this kind disallow cleavage of the miRNA passenger (miRNA*) molecule. Instead, miRNA-miRNA* mistmatches seem to facilitate the separation of the passenger molecule by the Argonaute protein itself (reviewed in Kawamata and Tomari 2010). This chaperone-dependent Argonaute loading is sustained by a wealth of biochemical evidence, however reports of HSP90 inhibition have pointed towards a role of this chaperone in mediating the proper localization and stability of Argonaute, particularly in its unloaded state (Johnston *et al.*, 2010; Suzuki *et al.*, 2009). Additional *in vivo* evidence of the necessity of HSP90 for Argonaute loading with miRNA would strengthen this model. In flies and mammals, chaperone-mediated Argonaute loading with miRNAs does not need the action of Dicer, since its presence or absence does not affect the kinetics of small RNA duplexes loading into Argonautes (Betancur and Tomari, 2012). Moreover, Dicer knockout cells can sustain siRNA-mediated gene silencing (Kanellopoulou *et al.*, 2005; Murchison *et al.*, 2005) achieved with exogenously supplied small RNA duplexes. Interestingly, there is precedence for the involvement of Dicer in Argonaute loading with small RNAs. In particular, the siRNA loading process of the fly Argonaute Ago2 requires a complex containing Dicer-2. Also, pre-miRNA processing by Dicer and the following miRNA loading into Argonaute should be expected to be coupled to a certain extent. Under the assumption that Dicer could release the small RNA molecules into the cytoplasm away from the Argonaute protein, these RNAs would likely be subject to degradation by nucleases. A physical interaction between Dicer and Argonautes has been reported

6. The term 'Argonaute loading' is preferred over 'miRISC loading'.

(Tahbaz *et al.*, 2004; Duchaine *et al.*, 2006; Wang *et al.*, 2009) and some studies have addressed their functional interaction (MacRae *et al.*, 2008).

Failure of miRNA to be incorporated into the Argonaute, will impair its accumulation, presumably because when not bound, the small RNA is rapidly degraded by the action of cellular nucleases. As a consequence, Argonautes are necessary for miRNA stability and subsequently as part of miRISC for effector functions. The catalytic activity of Argonautes has been proposed to play a role in the process of miRNA biogenesis, as evidenced by the presence of altered precursor forms in the absence of catalytically competent Argonautes (Bouasker and Simard, 2012).

1.2.3 Mechanisms of miRNA action

Mechanisms of mRNA repression

In general, miRNAs regulate genes post-transcriptionally to elicit gene silencing. This silencing occurs via interference with translation or degradation of the mRNA. However, the physiological settings where these two effects take place, preferentially or not, and how they relate to each other are issues that have been the subject of considerable scientific debate. The mechanism through which miRNAs can lead to mRNA degradation has been more detailed. In a current model, the miRISC targets mRNAs and is bound by the GW182 proteins, GW182 then recruits the deadenylation complexes CCR4-NOT1 and PAN2-PAN3 to degrade the mRNA. (reviewed in Fabian and Sonenberg 2012). Although addressed in multiple studies, several proposed mechanisms of translational inhibition are more controversial and less understood (see below).

Recent studies have embarked on measuring the relative contribution of mRNA translational inhibition compared to mRNA destabilization (*i.e.* decapping, deadenylation and degradation) during gene silencing upon miRNA activity. A current method of choice for doing these measurements is high throughput ribosome profiling, where the fraction of mRNA being actively translated, and the individual position of each ribosome on the mRNA can be determined (Ingolia *et al.*, 2009). Applying this method in mammalian cells, with a steady-state condition of miRNA abundance, it has been proposed that the miRNA-mediated effect on translational inhibition can be accounted for by reduced mRNA levels as a consequence of its degradation (Guo *et al.*, 2010). A second set of studies has demostrated an effect on translational inhibition that cannot be accounted for by mRNA degradation, but rather precedes it (Bazzini *et al.*, 2012; Bethune *et al.*, 2012). In these last studies, a non-steady state situation of miRNA is addressed, suggesting that the predominant mechanism of miRNA action varies according to its state (steady or not). It is of note that these findings do not directly address the mechanism(s) involved during miRNA action, but have contributed to the comprehension of how the mRNA

destabilization and translational inhibition quantitatively relate to each other during miRNA activity in different experimental situations. A similar study of the miRNA-mediated effects on its targets (at the protein and mRNA level) during *C. elegans* development has used high-throughput ribosome profiling and mRNA and protein quantification. This study has shown that miRNA activity induces a drastic decrease in protein levels that is stronger than expected from the concurrently observed decrease on mRNA abundance. Moreover, for some miRNA targets, mRNA levels remained unaltered while protein levels were lowered (Stadler *et al.*, 2012).

Many other studies have addressed the operating mechanisms that mediate the translational inhibitory effects induced by miRNAs. Different proposed models suggest that miRNA affect translation initiation (*e.g.* Djuranovic *et al.* (2012)), elongation, ribosome assembly, and ribosome drop-off (reviewed in Fabian *et al.* 2010). The various models also differ on whether there is a proposed effect on mRNA degradation (*e.g.* Hendrickson *et al.* (2009)) or not (*e.g.* Jovanovic *et al.* (2012)). However, judging from the high-throughput ribosome profiling analysis, miRNA have been found to induce a reduction in the fraction of mRNAs that are loaded with ribosomes, but do not alter the distribution of the individual ribosomes on the mRNA. This fact favors the model of translation initiation block (Guo *et al.*, 2010; Stadler *et al.*, 2012; Bethune *et al.*, 2012). Finally, in a different approach to the study of the mechanisms of translational inhibition mediated by miRNAs, several studies have proposed models based on interactions of the miRISC or its components. For examples, Argonautes have been proposed to interact with translation initiation factors (Kiriakidou *et al.*, 2007), and the 40S ribosomal subunit RACK-1 protein (Jannot *et al.*, 2011a).

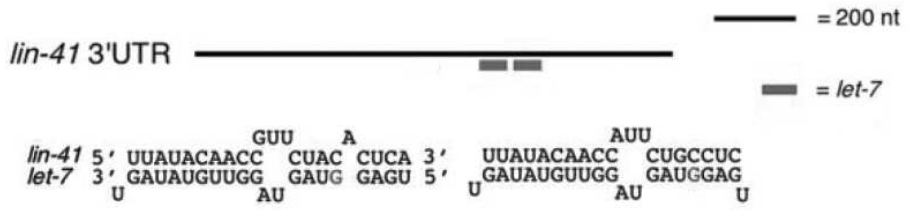

Figure 1.5: **The miRNA binding sites in the *C. elegans lin-41* mRNA.** The *lin-41* 3'UTR is illustrated, it contains two binding sites for the *let-7* miRNA (grey bars). The sequence base pairing between the sites and the *let-7* miRNA is only partially complementary. Following the seed sequence (5'UGAGGUAG) there is a bulge in the pairing which hinders Argonaute-mediated cleavage of the mRNA. Figure reproduced with permission from Reinhart *et al.* (2000).

miRNA recycling

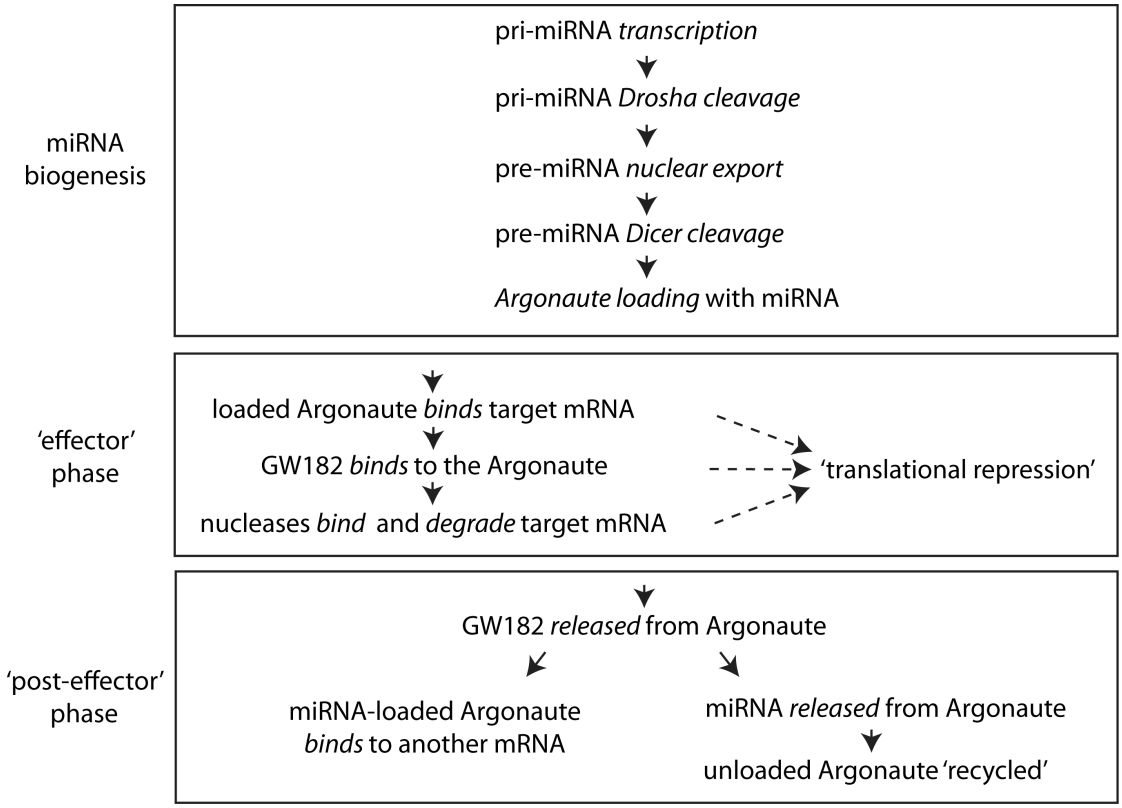

Figure 1.6: **Schematic flow of the miRNA pathway phases and processes.** This diagram summarizes the canonical form of processes (in italics) of the miRNA pathway. The 'miRNA biogenesis' and 'effector' phases have been actively studied. In contrast the 'post-effector' processes remain hypothetical and additional mechanistic alternatives could be possible.

Another aspect of microRNA action relates to the capacity of a single miRNA molecule to negatively regulate more than one mRNA. This capacity to repress multiple targets has been evidenced in a condition of perfect sequence complementarity between the target mRNA and the miRNA molecules for the AGO2 Argonaute (Hutvagner and Zamore, 2002). In this case, the Argonaute can induce cleavage of multiple targeted mRNAs[7]. However, the incomplete sequence complementarity of miRNA to its target mRNAs prevents cleavage by the Argonaute protein in animal cells (Figure 1.5). The study by Baccarini *et al.* (2011) in cultured cells brought evidence that miRNA regulate multiple mRNAs, because a fixed number of miRNAs can regulate a higher number of targeted mRNAs. Then, a given miRNA molecule is expected to be used more than once, but whether this is happening at the miRNA level or at the miRISC level can not be presently inferred. Therefore, I refer *sensu lato* to this process as

7. This cleavage-dependent mode of Argonaute action is seen with siRNAs and endows AGO2 a 'catalytic turnover' property. For miRNAs there is no Argonaute-mediated cleavage.

'miRNA recycling'. To date, the mechanism by which miRNA recycling takes place is largely unknown.

An hypothetical description of some of the posibilities for miRNA recycling and other related processes is adequate at this point, because models of the action of proteins affecting the miRNA pathway (*e.g.* vesicular trafficking components), described further in the present thesis refer to these aspects. A summary of the distinct processes of the miRNA pathway partitioned into three phases is shown in the figure 1.6. Following the effector phase of target repression by the miRISC, a number of processes should follow. As an ultimate result of repression, the miRNA-targeted mRNA is expected to be decapped, deadenylated and degraded. However, the following fate of the miRNA, Argonaute and GW182 are unknown. We can hypothesize, regarding these unknown processes, that after the miRISC has engaged a repressed mRNA to the nucleolityc degradation path, the miRISC should 'disassemble', and this could start with the separation of the Argonaute protein from the GW182 protein (referred to as 'GW182 release'). Two hypothetical scenarios can be envisioned regarding the miRNA and Argonaute at this point: 1) An 'unbound Argonaute recycling' model, in which the miRNA would be separated from the Argonaute and possibly degraded, likely allowing the unloaded Argonaute to participate in a further round of loading with miRNA (referred to as 'Argonaute reloading'). 2) A 'bound Argonaute recycling' scenario, in which the miRNA would be retained inside the Argonaute and this bi-molecular core miRISC released to participate in a new round of target mRNA repression (Figure 1.6). Future research in the miRNA field is likely to provide experimental support to clarify these different scenarios.

Finally, all miRISC components would be subjected to degradation. A number of investigations have addressed the machinery responsible for miRNA degradation. Multiple nucleases have been proposed to degrade miRNAs, including XRN1, XRN2 and the exosome complex (reviewed in Ruegger and Grosshans 2012). However, the issues of specificity for miRNA compared to other RNAs and physical interaction with the miRISC remain to be addressed. Notably, it has been observed that non-templated modifications of miRNA, *i.e.* the addition of terminal nucleotides to the miRNA molecule, are induced in a target dependent manner. The proportion of the modified miRNA compared with the total miRNA amount increases upon transcriptional shutdown, suggesting that this kind of modification is linked to its stability (Baccarini *et al.*, 2011).

1.3 The miRNA pathway and cancer

A very selective briefing of the actively explored relationship between miRNAs and cancer is provided in this section. It focuses on the miRNA expression profiles in cancerous cells, the consequence of absence of core miRNA pathway components and the cancer related role

of some particular miRNAs. The role of miRNAs in relation with cancer is explored in the reviews by (Ventura and Jacks, 2009; Chen *et al.*, 2012a).

The profiling of miRNAs in diverse cancers has shown that, on a global scale, miRNA are expressed at lower levels compared to normal tissue (Lu *et al.*, 2005). The underlying mechanisms for this global down-regulation are however unclear. It is possible that negative effects on core pathway components is one mechanism that leads to widespread reduction of miRNA expression. In addition, mechanisms that reduce or alter the differentiation state of cancer cells may convey to patterns of miRNA abundance that resemble multipotent cells, the latter of which have a smaller number of expressed miRNA compared to differentiated cells (reviewed in Lujambio and Lowe 2012). Multiple factors that operate in cancer cells can induce either miRNA upregulation or downregulation, modifying the overall cancerous miRNA profile. These factors include genomic instability (genomic duplications and deletions), epigenetic silencing (*e.g.* DNA methylation) and control of miRNA expression by transcription factors (either repressors or activators). Due to these factors cancer cells have disturbed miRNA profiles (*e.g.* Git *et al.* (2008)) as opposed to uniformly downregulated miRNA expression. An operating example of the above arguments can be found for lung cancer. Cigarette smoke, a causal agent of lung cancer, induces very prominent miRNA downregulation (reviewed in Russ and Slack 2012) by unclear mechanism(s). This negatively trending miRNA profile is in agreement with independent studies of miRNA expression in lung cancer showing the preponderance of reduced miRNA abundance (Yanaihara *et al.*, 2006).

The genetic investigation of miRNA pathway core components has unveiled stark negative effects on cell survival upon loss of this pathway. Absence of Dicer leads to a strong impairment of cellular growth, but does not preclude tumor formation in a sarcoma model (Ravi *et al.*, 2012). Along the same line, in a model of Myc-induced lymphoma, tumors were experimentally induced with success only with cells containing one or two functional copies of Dicer, but no tumor was formed by cells lacking this enzyme (Arrate *et al.*, 2010). Altogether, these studies give evidence that miRNAs are not essential for tumor formation, but complete loss of this pathway may be an event avoided by cancer cells due to the negative consequences it imposes on growth. Importantly, patient's cancer cells missing Dicer have not yet been reported. Similarly, the specific miRNAs and underlying mechanisms of this strong negative effect on growth are not yet established.

The 3' UTR region of any mRNA can be subjected *a priori* to miRNA regulation, and as consequence miRNA could in principle regulate any pathway, including those involved in cancer. At the miRNA level, a plethora of genes with tumor promoting and suppressive functions have been reported to be regulated by miRNAs (reviewed in Garzon *et al.* (2010)). For instance, the let-7 miRNA has been shown to negatively regulate the expression of the Ras oncogene. In addition to the regulation of tumor suppressor and oncogenes, miRNAs have been found to regulate genes involved in the processes of metastasis and angiogenesis (reviewed in

Wang and Wang 2012).

Certain miRNAs have been found to be activated by transcription factors of high relevance in cancer. As an example, the miR-34 miRNA family can be induced by p53 (He *et al.*, 2007). However, the mouse knockout of miR-34 (with its two paralogs) does not display changes in the p53 response to replicative senescence, irradiation-induced apoptosis or oncogenic RAS-induced transformation. Therefore, the physiological consequences of the p53-mediated regulation of miR-34 seem to be subtle. Indeed, loss of the miR-34 family of miRNAs has shown mild effects on cellular transformation induced by combination of oncogenic RAS and the E1A protein (an inhibitor of the retinoblastoma protein) and led to a minor increase of *in vitro* cell proliferation (Concepcion *et al.*, 2012).

1.4 The miRNA pathway in *C. elegans*

1.4.1 Generalities

The miRNA pathway in *C. elegans* has many similarities to that in other animals. The pathway is composed of single Dicer, Drosha and Pasha genes, two Argonautes and two GW182 protein homologs (Table 1.1). It is to be remarked that a difference occurs at the Argonaute level. While in the fly (*D. melanogaster*) and mammals some of the Argonaute proteins involved in miRNA function also functionally bind to siRNA, these roles are completely separated in worms. The *C. elegans* microRNA-specific ALG-1 and ALG-2 Argonautes neither bind to siRNAs nor participate in siRNA-mediated processes (Grishok *et al.*, 2001; Steiner *et al.*, 2007; Jannot *et al.*, 2008). Several distinct pathways have evolved in worms to mediate siRNA function, including the RDE pathway (Tabara *et al.*, 1999) and the endo-siRNA pathway (Simmer *et al.*, 2002; Kennedy *et al.*, 2004; Pavelec *et al.*, 2009). The ALG-1 and ALG-2 Argonautes are highly similar (Figure 2.1) and are described in the section 2.4.1.

At the miRNA level, the existence of 119 miRNAs has been well supported by a miRNA validation study (Warf *et al.*, 2011). Using high-throughput sequencing, in order to the confidently validate miRNAs, investigators evaluated as criteria the presence of sequencing reads for the mature miRNA, miRNA* and pre-miRNA terminal loop among other features. Likely, a few additional miRNAs remain to be confirmed by complementary approaches. The genetically characterized miRNA *lsy-6* (Johnston and Hobert, 2003) is expressed in only a pair of neurons and due to its very low abundance it was missed by the mentioned validation study. The miRNA repertoire of *C. elegans* can be cataloged in 23 miRNA 'seed' families (two or more members), that comprise a total of 76 miRNAs (Alvarez-Saavedra and Horvitz, 2010).

1.4.2 Genetics

The miRNA pathway fulfills essential functions during development in animals. In *C. elegans* multiple essential processes are controlled by miRNAs, including embryonic and larval development, gonadal maintenance and gametogenesis. The phenotypes exhibited by mutants of the different core components of the miRNA pathway vary, reflecting the life-cycle steps in which they first become limiting and also their differential involvement in the miRNA pathway and other pathways (*e.g. dcr-1*). The *C. elegans* mutants of dicer(*dcr-1*), drosha(*drsh-1*) and pasha(*pash-1*) display sterility (Grishok *et al.*, 2001; Knight and Bass, 2001; Denli *et al.*, 2004). The knockdown (using RNAi) against *alg-1* in the *alg-2* mutant background produces embryonic lethality and larval arrest (Grishok *et al.*, 2001). An essential role has been associated with the worm GW182 homologues, *ain-1* and *ain-2*. A combination of loss-of-function mutants of both genes[8], has been reported as viable (Zhang *et al.*, 2007), although the reported mutants may not correspond to null alleles. Indeed, applying RNAi against *ain-2* to this double mutant the authors reportedly induced an uncharacterized lethal phenotype (Zhang *et al.*, 2007). In addition to the core miRNA protein components, deletions of most *C. elegans* miRNAs have been investigated. The absence of most miRNA do not grossly alter development or affect viability (Miska *et al.*, 2007). Considering that miRNAs belonging to the same 'seed' family can potentially provide redundant regulatory function, mutants lacking entire miRNA seed families have also been investigated. The majority of compound mutants missing the entire members of a given family (referred to as 'miRNA family mutants') are viable and develop without gross abnormalities (Alvarez-Saavedra and Horvitz, 2010). Among fifteen miRNA family mutants studied, the loss of four of them led to prominent defects: The *mir-35* and *mir-51* miRNA families control essential aspects of embryonic development, whereas the *mir-58* family controls somatic growth, and the *let-7* family controls developmental transitions during the larval stages, which when misregulated can be of lethal consequence (Reinhart *et al.*, 2000). The absence of conspicuous defects during development for the other miRNA family mutants does not preclude that miRNA are acting to control developmental processes, but rather suggest that they may control subtle developmental aspects not easily evidenced. In addition, miRNAs have been proposed to act in the regulation of physiological responses, conferring 'buffering' responses to external environmental perturbations, such as stress conditions (reviewed in Mendell and Olson 2012; Ebert and Sharp 2012).

1.4.3 Developmental roles

The miRNA pathway controls multiple developmental processes in worms. Loss of *dcr-1* and *drsh-1* leads to sterility and similarly, loss of *alg-1/2*[9] impacts germ-line maintenance and ga-

8. The strain *ain-1(ku322)*; *ain-2(tm1863)*
9. the *alg-1* and *alg-2* genes are referred to as *alg-1/2*

metogenesis (Bukhari *et al.*, 2012). The identity of the pathways responsible for the regulation of these reproductive functions is unknown, but the miRNA regulation of germ-line function seems to occur, at least partially, in a non-autonomous cell manner. As an example, reestablishing Argonaute expression in the somatic gonadal tissues, namely the distal tip cells (DTCs) restores the defects of meiotic entry found in argonaute mutants (Bukhari *et al.*, 2012). Regarding the cell-autonomous miRNA activity in germ-line and gametes, some miRNAs are present in these cells, but their mode of function is unclear (reviewed in Suh and Blelloch 2011). For example, in the mouse ovocyte, the pathway has been proposed to be inactive (Suh *et al.*, 2010; Ma *et al.*, 2010).

During the *C. elegans* embryonic development, most of the somatic cells that constitute a worm are produced and patterned into different organs. The phases and processes that occur during this developmental period are briefly accounted in the appendix A and will be referred to in the following chapter. The roles of miRNAs during embryogenesis are evidenced by the loss of the argonautes *alg-1/2*. While single mutants of the *alg-1* and *alg-2* are viable, the double *alg-1; alg-2* mutants arrest during the morphogenetic process of elongation, with frequent attachment failures between the worm hypodermis and the subjacent muscle, further described in the chapter 2. The specific miRNAs and targeted pathways involved in this morphogenetic process are unknown. Knockout of the pasha (*pash-1*) gene leads to sterile worms, but a temperature sensitive (TS) mutant allele of this gene has been used to uncover the requirement of the miRNA pathway for normal lifespan and development (Lehrbach *et al.*, 2012). A completely penetrant embryonic lethality can observed upon switching the *pash-1* TS mutant to the restrictive temperature, confirming that miRNA activity is necessary for embryonic development. To date, the complete loss of two miRNA families has evidenced roles in the worm embryos. Loss of the *mir-35* miRNA family leads to embryonic lethality (Alvarez-Saavedra and Horvitz, 2010). Similarly, loss of the *mir-51* miRNA family affects late stage embryos, the regulation conferred by these miRNAs is necessary for the proper attachment of the pharynx to the buccal cavity (Shaw *et al.*, 2010).

The miRNAs control multiple processes during the *C. elegans* post-embryonic development. In the nervous system, the miRNA *lsy-6* controls the development of a neuronal asymmetry (Johnston and Hobert, 2003; Chang *et al.*, 2004; Sarin *et al.*, 2007), the *lin-4* miRNA plays a role in axon guidance (Zou *et al.*, 2012) and *mir-48* regulation of its target *hbl-1* mediates synaptic remodelling (Thompson-Peer *et al.*, 2012). In addition to development, miRNAs have been involved in the regulation of physiological processes, such as aging (reviewed in Kenyon 2010). Particularly well studied is the development of the seam cells, two lateral rows of epidermal cells that follow a developmental program controlled by miRNAs and their targets. The seam cells are born during embryonic development and follow a specific division program during each of the four larval stages (L1 to L4) (Sulston and Horvitz, 1977). Lastly, at the transition to adult, the seam cells differentiate to their terminal fate, exit from the cell cy-

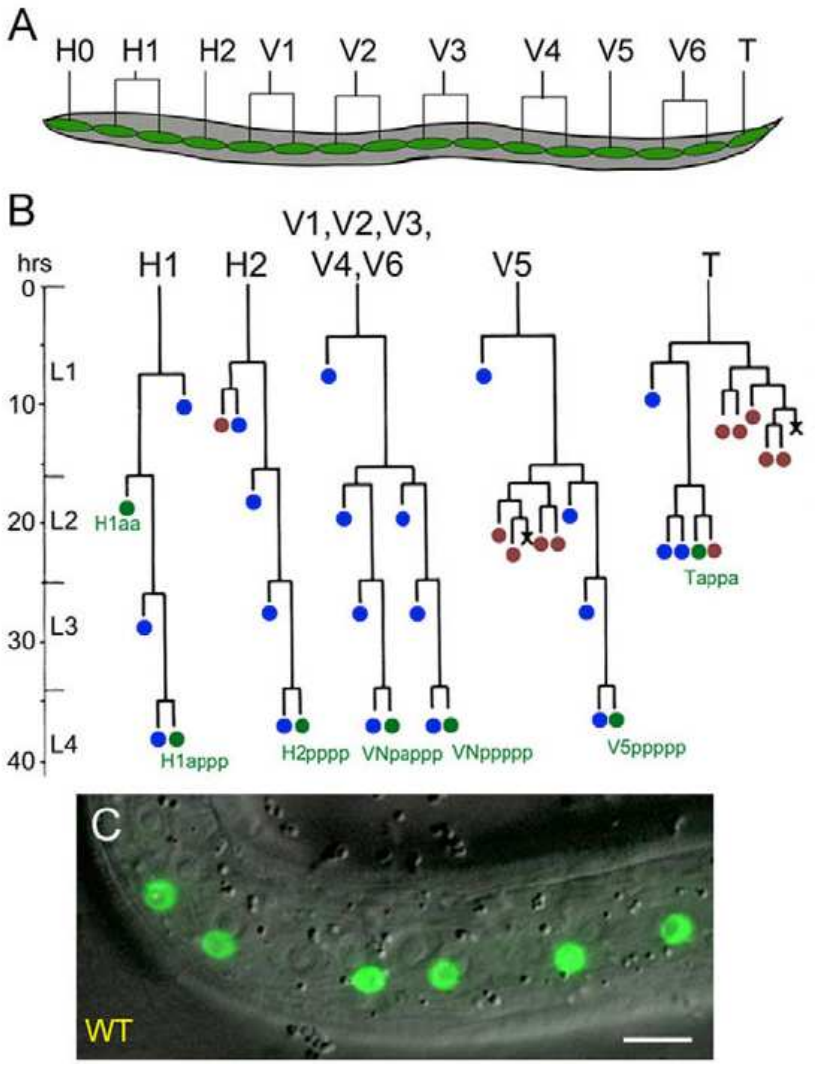

Figure 1.7: **Development of the seam cells in *C. elegans*. A)** The seam cells (indicated in green) are a lateral row of epidermal cells, comprising the cells named H0, H1, H2, V1 to V6 and T. **B)** The post-embryonic lineage of the above mentioned seam cells is shown. Developmental cell fate is indicated by circle color. blue: cell fusion to the hypodermis, green: seam cell, red: neuronal cell, cross: cell undergoes apoptosis. **C)** GFP marker indicating the seam cells in the worm epidermis. Figure reproduced with permission from Wildwater *et al.* (2011).

cle, and undergo cell fusion between them, halt the molting process and secrete a cuticular structure, the alae (Figure 1.7). The larval division program of the seam cells consists mostly of 'asymmetric divisions' that produce one daughter cell that fuses to the surrounding hypodermal syncitium (Hyp7 cell) and another daughter that continues to the next larval stage (Figure 1.7). At the L2 stage, a distinct 'symmetrical division' takes place for a set of seam cells (*i.e.* V1 to V6 cells) that leads to an increase in the number of seam cells.

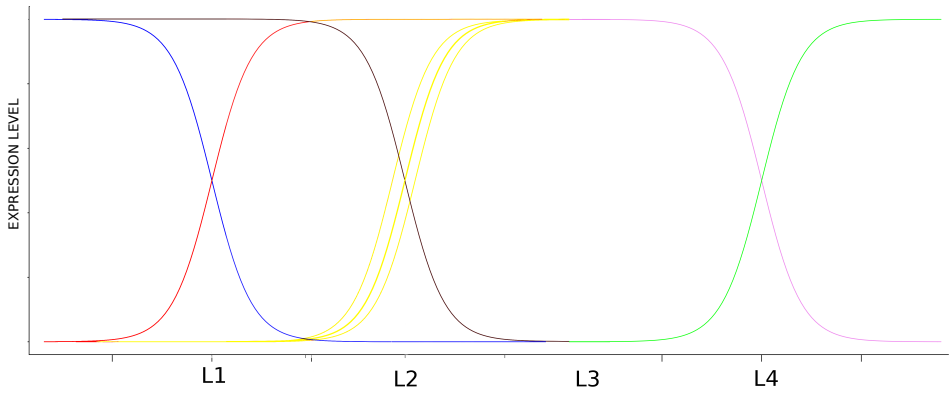

Figure 1.8: **Scheme of developmental course of miRNA action during *C. elegans* larval development.** The expression of miRNAs and their targets is inversely correlated during the four larval stages (L1 to L4). Expression of the mature miRNA lin-4 (red line) decreases that of LIN-14 (blue line) during the L1 stage. Expression of the mature miRNAs miR-48, miR-84 and miR-241 (yellow lines) decreases expression of their common target HBL-1 (brown line) during the L2 stage. During the L4 stage, expression of the mature miRNA let-7 (green line) decreases the abundance of LIN-41 (purple line). Note that during this developmental mode of action, miRNAs are temporally expressed to decrease their targets and then maintain their expression level.

A number of genes control the temporal execution of the seam cell division program. The downregulation of the *lin-14* gene regulates entry into the L2 division program. In its absence the seam cells reiterate the L1 division program. The *lin-14* gene is negatively regulated by the *lin-4* miRNA (Wightman *et al.*, 1993; Lee *et al.*, 1993) that starts to be expressed at the L1 stage (Figure 1.8). During the L2 larval stage the *mir-48*, *mir-84* and *mir-241* miRNAs, three members of the *let-7* miRNA, family downregulate the expression of the *hbl-1* gene (Abbott *et al.*, 2005; Abrahante *et al.*, 2003). Failure to downregulate *hbl-1* leads to reiteration of the L2 symmetric division program. Lastly, at the L4 to adult transition, downregulation of another miRNA target, the *lin-41* gene, allows the expression of a master terminal differentiation factor of the seam cells (*i.e* the *lin-29* transcription factor). *lin-41* is downregulated by the action of the *let-7* miRNA (Slack *et al.*, 2000; Reinhart *et al.*, 2000). The failure to downregulate *lin-41*, caused by loss of the miRNA *let-7*, abolishes the expression of the adult program and is lethal for hermaphrodites due to bursting through the vulva (Reinhart *et al.*, 2000).

1.5 Cellular aspects of microRNA function

1.5.1 Generalities

Biochemical, structural and genetical studies are complemented with those that address the cellular aspects of protein function. The localization of proteins to the nucleus, cytoplasm, to different organelles, and even down to smaller scales of spatial organization, such as membrane domains, chromatin regions and supramolecular assemblies inform about the function of proteins, accounting for their natural context inside the cells. Subcellular associations of proteins can be unveiled by experiments of co-localization of components inside the cells, biochemical fractionation of subcellular compartments and genetic studies. In the case of the miRNA pathway, miRNA biogenesis starts in the nucleus and finishes with the assembly of miRISC in the cytoplasm, the main site of miRNA action where the miRISC targets mRNAs. Protein components of this pathway display a diffuse cytoplasmic localization but have also been found associated with foci termed 'RNA granules' (Leung *et al.*, 2006). Moreover, miRISC components have been found associated with membranes of the Golgi complex (Cikaluk *et al.*, 1999; Tahbaz *et al.*, 2001), the multivesicular bodies (MVB) and endosomes (Gibbings *et al.*, 2009). The miRNAs have been also reported inside MVB-produced vesicles (named exosomes).

1.5.2 Association to RNA granules

RNA granules are non-membrane bound supramolecular assemblies that form in the cytoplasm as a result of the capability of certain proteins to bind others with high valency, forming aggregates, if not constitutively, at least under certain conditions such as diverse stresses. One kind of RNA granule contains components of the miRNA pathway: Argonautes, miRNAs and GW182 proteins. These granules, termed 'Processing bodies' (P-bodies) [10], also harbour additional components, like mRNAs and mRNA deadenylation and degradation complexes, and have been proposed to function as active sites of mRNA degradation (reviewed in Thomas *et al.* 2011). The miRISC components distribute mostly diffusively in the cytoplasm and only a fraction of them are located in P-bodies. For the Argonautes this fraction is estimated at around 1% (Leung *et al.*, 2006). For the GW182 proteins a more non-homogeneous distribution inside the cells is observed. The localization of P-bodies may not be random in the cytoplasm, and could be due to their transient association with vesicles with which they interact (Gibbings *et al.*, 2012a).

Different roles for the P-bodies have been proposed. They may function to transiently store mRNAs and may also be sites where mRNA deadenylation and degradation processes preferentially take place (reviewed in Anderson and Kedersha 2009). Impairing the formation of

10. P-bodies are also known as GW-bodies, these last named after the punctated GW182 distribution.

these granules has been shown not to affect miRNA repression, suggesting that their formation is not necessary for the miRNA activity (Eulalio *et al.*, 2007). Therefore, P-bodies may be structures formed in response to certain conditions of gene silencing, but do not constitute a necessary structure for miRNA-mediated silencing (Eulalio *et al.*, 2007). In addition to P-bodies, similar cytoplasmic RNA-containing supramolecular assemblies can form in response to stress conditions, which are named 'stress granules'. Transient shutdown of the translational machinery, that inactivates the translation initiation factors, leads to accumulation of mRNA contained within incomplete ribosomes in stress granules (reviewed in Thomas *et al.* 2011). Argonaute proteins can also be recruited to these granules in a miRNA-dependent manner (Pare *et al.*, 2011).

1.5.3 Association with biological membranes

It may be considered that processes expected to occur freely in the cytoplasm and not directly related to vesicular trafficking or membrane dynamics, have no *a priori* reason to have an association with membranes. Intriguingly, diverse links between RNA-related and membrane processes have been found (reviewed in Gibbings and Voinnet 2010).

Different lines of experimental evidence have found that various components of the miRNA pathway are associated with membranes, particularly of the endo-lysosomal system and the Golgi complex. These evidences of membrane association can be divided in three kinds: First, analyses through subcellular fractionation have shown that Argonautes and GW182 proteins are present in endosomal/MVB fractions (Tahbaz *et al.*, 2004; Gibbings *et al.*, 2009; Lee *et al.*, 2009). Second, colocalization studies provide strength to an *in vivo* association, given that AGO and GW182 colocalize with MVBs and endosomes (Gibbings *et al.*, 2009). Also, in renal and pancreatic acinar cells cells AGO2 was found to be primarily localized to the Golgi complex (Cikaluk *et al.*, 1999; Tahbaz *et al.*, 2001). Finally, genetic analysis have shown that impairment of different vesicular trafficking complexes leads to misregulation of the miRNA pathway (Lee *et al.*, 2009; Gibbings *et al.*, 2009).

It should be noted that the protein constituents of the miRNA pathway are located to the nucleus (Drosha, Pasha) and cytoplasm (Dicer and the Argonautes), and a connection to any subcellular organelles or cellular membrane is not explained by the currently known structural features of miRNA pathway components. The miRNA pathway components do not contain transmembrane spanning regions or have described post-translational modifications endowing them with membrane binding capabilities, like lipid-anchoring modifications. It is possible that additional miRNA pathway interacting proteins mediate this association with membranes, and indeed such a role has been proposed for the membrane-spanning human prion protein PRNP (also known as PrPc) (Gibbings *et al.*, 2012a).

The association to membranes of the miRNA pathway is still to be explained in terms of its biological relevance. The miRNAs are found in extracellular fluids to a certain extent and the existence of miRNA components, particularly GW182 and certain miRNAs, inside secreted vesicles (exosomes) has led to suggestions of the existence of intercellular communication mediated by miRNAs (reviewed in Chen *et al.* 2012b). This would make necessary a mechanism of generation and could justify the existence of a system to sort the miRNAs destinated for secretion. Experimental support for this idea, including mechanism and biological role is rather scarce at present. A second hypothesis suggests that the association to membranes fulfills a role in facilitating transitions of the miRISC activity (reviewed in Gibbings and Voinnet 2010). Processes proposed to be facilitated by membranes are those of 'Argonaute loading', 'miRNA recycling', and post-effector steps important for miRISC 'disassembly' (separation of GW182, Argonaute and miRNA).

1.5.4 Aspects of vesicular trafficking

This section presents a brief summary of the research papers that provide compelling evidence of membrane associations of the miRNA pathway. A primer on some of the basics of vesicular trafficking is given in the appendix B, focusing on the aspects of relevance for the present thesis.

The study by Gibbings *et al.* (2009) showed that impairment of endosomal sorting processes negatively affects miRNA activity. The ESCRT complex (named after Endosomal Sorting Complex Required for Transport) plays a role in the sorting and recycling of proteins at multivesicular bodies (MVBs). Knockdown of ESCRT complex components, vps36, Hrs and Alix in monocytes and HeLa cells, inhibited the action of the let-7 miRNA and increased the GW182 protein abundance. Of note, these cells secrete exosomes that contain GW182, miRNAs and also AGO2 protein at low levels. This study brought biochemical and subcellular localization evidence for the membrane association of miRNA pathway components. Using subcellular density gradient fractionation, it was reported that AGO2, GW182 and miRNAs cofractionate with endosomes and MVBs and also colocalize with these membrane compartments.

In a follow up of the previous study, Gibbings *et al.* (2012a) investigated in glioblastoma cells one of the proteins co-fractionating with AGO2 and GW182 proteins, the human prion protein PRNP. PRNP is a transmembrane protein normally found at the plasma membrane. However, a fraction of it associates with endomembranes in a configuration that exposes its amino terminal part to the cytoplasm. This part contains a GW/WG motif that mediates its physical interaction with the Argonaute AGO2 (Gibbings *et al.*, 2012a). In PRNP knockdown cells, less AGO2 co-immunoprecipitates with GW182, and in density gradients AGO2 is shifted towards the denser Dicer fractions. In conclusion, the authors propose that PRNP promotes miRISC recognition of target mRNA or otherwise enhance the association between Argonaute

and the GW182 protein. Importantly, PRNP is so far the sole effector that establishes an easily describable (*i.e.* a transmembrane protein with an Argonaute binding motif) direct physical link between the cytoplasmic side of vesicles and the miRNA pathway components.

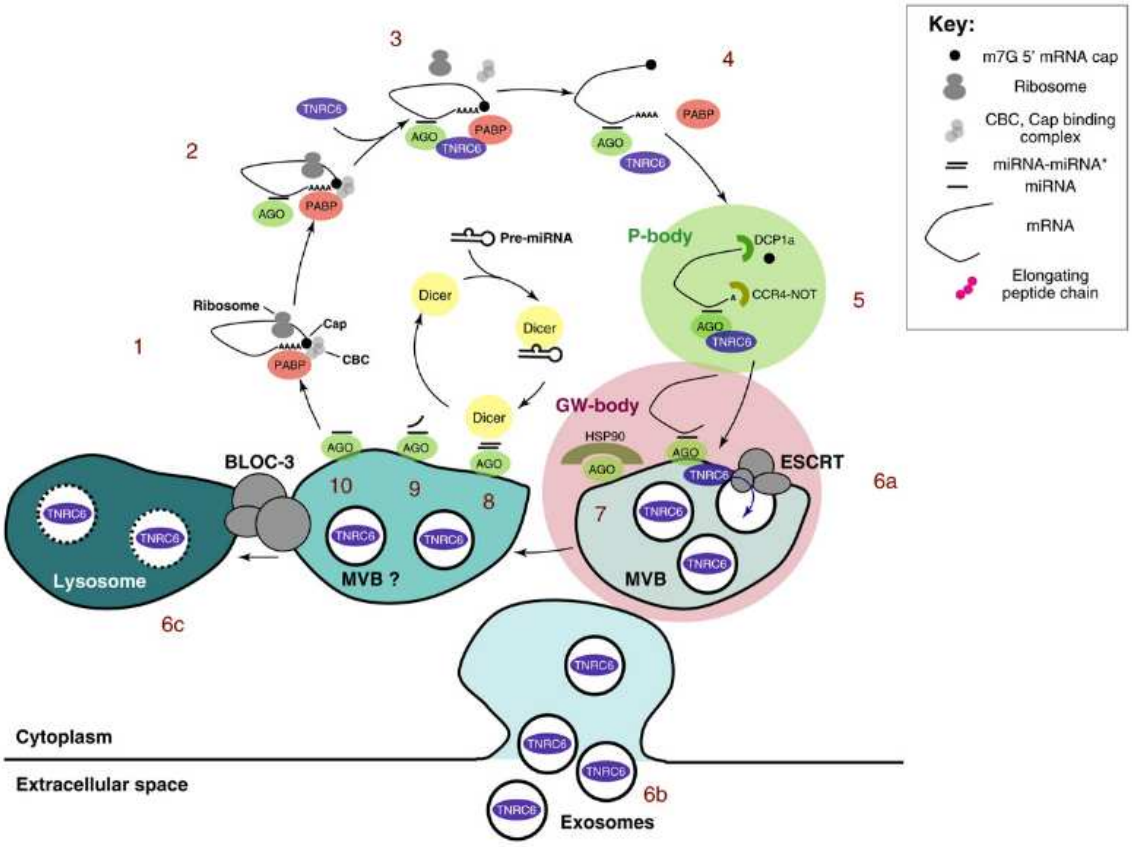

Figure 1.9: **Model of miRNA processes affected by the ESCRT and BLOC-3 complexes.** This model summarizes the findings of Gibbings *et al.* (2009); Lee *et al.* (2009). The process of Argonaute-loading could be facilitated by the association of Argonaute protein (AGO) to membranes. Most of the effector phase of miRISC-mediated repression (steps 1 to 5) would occur freely in the cytoplasm. At the 'post-effector' phase of the pathway, the separation of GW182 (TNRC6) protein from the miRISC and the stabilization of unloaded Argonaute (AGO) by the chaperone HSP90 (step 6a-7) would be processes facilitated in mebranous 'platforms' associated with P/GW bodies. Acting at this step, the ESCRT complex would participate in the separation in the separation and sorting of TNRC6 into exosomes. Following Argonaute unloading (step 7), Argonaute reloading could be also facilitated by the AGO to membranes (steps 8-10). The BLOC-3 complex could function in a process linking the MVB to the lysosomes (step 6c). Figure reproduced with permission from Gibbings and Voinnet (2010).

A genetic study in the fly *D. melanogaster* by (Lee *et al.*, 2009), found another protein involved in the trafficking of vesicles that affects the miRNA pathway. Using a genetic screen for enhancers of small RNA mediated silencing, the authors find that the loss of the HPS4 protein,

enhances silencing mediated by miRNAs and siRNAs. HPS4 encodes a subunit of the BLOC-3 complex (named after Biogenesis of Lysosome-related Organelles Complex 3) that plays a role in the biogenesis of lysosome-related organelles. Particularly, the BLOC-3 facilitates the GDP to GTP exhange of specific Rab proteins (Gerondopoulos *et al.*, 2012). Mutants of HPS4 have no effect on the activity of Dicer, but increased the Argonaute loading judging from *in vitro* loading assays, and increased the level of Argonaute-bound miRNAs. These results suggest that BLOC-3 negatively regulates miRNA pathway activity. A model of the findings of Gibbings *et al.* (2009); Lee *et al.* (2009) is presented in the figure 1.9, where the ESCRT and BLOC-3 complexes are proposed to act in the processes of Argonaute loading and post-effector release of GW182 from the miRISC.

Two recent reports, in *Arabidopsis thaliana* (Brodersen *et al.*, 2012) and the nematode *C. elegans* (Shi and Ruvkun, 2012) have shown that impairment of the mevalonate pathway, a biosynthetic route that produces lipidic intermediates important for sterol biosynthesis and protein prenylation, results in loss of miRNA activity. In both papers derepression of miRNA reporters is observed without decreases in the abundance of Argonaute proteins or miRNAs. Based on these observations, the authors proposed that the effector functions of miRISC are affected. Moreover, in the *C. elegans* report, the authors found that in addition to the mevalonate pathway, disruption of enzymes involved in N-linked glycosylation[11] derepress miRNA activity, and hypothesized that some miRNA pathway components may be glycosylated. However, this proposed post-translational modification has not yet been reported for any miRNA pathway component, although two nematode glycoproteome survey studies have been performed (Zielinska *et al.*, 2012; Kaji *et al.*, 2007).

A recent study by (Gibbings *et al.*, 2012b) has established that the abundance of the Dicer and Argonaute proteins in mammalian cells is regulated by the process of authophagy, and this regulation can negatively impinge on miRNA activity. In HeLa and epidermal cancer cells, the inhibition of authophagy by lysosome acidification inhibitors or knockdown of the autophagy involved genes ATG5-7 and NDP52, augmented DICER, AGO1 and AGO2 protein abundance. Conversely, inducing autophagy by serum starvation or via mTOR inhibition with the drugs rapamycin and pp242 decreased the abundance of these proteins. The authors reported a novel association of the DICER and AGO2 proteins (but not GW182 protein) with autophagosomes, determined by density gradient co-fractionation, co-localization, and physical association via co-immunoprecipitations. The short-term inhibition of autophagy did not reduce miRNA abundace suggesting that the AGO2 protein is targeted to autophagosomes in the unloaded state. However, inhibition of autophaghy for longer term led to decreased miRNA levels, as result of impaired Argonaute loading.

Altogether, the studies on the roles of the ESCRT complex, the PRNP protein and the mevalonate pathway, suggest that impairment of miRNA activity can occur upon disruption of

11. The addition of sugar molecules to a nitrogen atom of an aminoacid residue.

several processes of vesicular trafficking and membrane dynamics, implicating them as factors that positively regulate miRNA-mediated silencing. The impairment of miRNA activity in these cases is not correlated with reduced miRNA or Argonaute protein abundance. Of note, a role for the ESCRT complex in regulating the levels and, likely, the sorting of GW182 is proposed by Gibbings *et al.* (2009). Also in common, the processes upstream of the Argonaute loading process are not hypothesized to be altered, but rather the downstream processes would be changed, including: 1) The association of GW182 with the loaded Argonaute or the dissociation of GW182 from the miRISC; 2) The processes involved in miRNA recycling occurring in the miRISC or its components; 3) The process of Argonaute loading (particularly reloading) with miRNA.

From the above described summary of the microRNA pathway, it should be noted that this pathway represents a gene regulatory systems that touches largely different processes, during embryonic and postembryonic development, from the physiological process of aging to cancer. The understanding of the biological processes regulated by miRNAs and the mechanisms of miRNA action progress actively but it is far from complete.

1.6 Doctoral research objectives

The premise driving the presented doctoral research is that, by means of exploring the genetic interactions of the miRNA-specific Argonautes in the model organism *Caenorhabditis elegans*, it is possible to uncover both developmental processes controlled by miRNAs and cellular functions important for miRNA activity. In particular, this present work constitutes a study of the function and genetic interactions of the *Caenorhabditis elegans* argonaute genes *alg-1* and *alg-2*, in order to understand in detail their role in the miRNA pathway. The main approach taken in order to fulfill this goal has been the genetic analysis of these argonautes and a direct characterization of these genes. In a similar manner, a forward genetic screen was used to identify a new argonaute interactor followed by its characterization and the study of its relationship with the miRNA pathway.

The main objectives of my doctoral work are as follows:

- Firstly, to characterize the *Caenorhabditis elegans alg-1* and *alg-2* genes with respect to their expression, localization, and mutant phenotypes in order to gain insights into their different redundant and non-redundant functions and their essential role in developmental processes during embryogenesis.
- Secondly, to elucidate new genetic interactors of the *Caenorhabditis elegans* argonaute genes by means of a forward genetics approach, and define their role and relationship with the Argonautes and miRNA pathway.

Following the present introductory chapter, the reader will find the development of these two goals in the main chapters 2 and 3 of this thesis, followed by the final conclusions and remarks (chapter 4).

Chapter 2

Developmental characterization of the microRNA-specific *C. elegans* Argonautes *alg-1* and *alg-2*

Foreword

The present chapter is constituted by an article recently published in the journal PLoS ONE (Vasquez-Rifo *et al.*, 2012). I performed most of the experiments presented in the paper, Syed Irfan Ahmad Bukhari did the ALG-1 immunostaining of worms, Evelyne L. Rondeau performed preliminary immunoprecipitation experiments, the immunoprecipitation of Argonaute proteins was conducted by Guillaume Jannot, their associated small RNAs were hybridized to microarrays by Javier Armisen from the laboratory of Eric A. Miska. Michel Labouesse performed the immunostaining of muscle and hemidesmosomes in embryos.

Developmental Characterization of the microRNA-specific *C. elegans* Argonautes *alg-1* and *alg-2*.

Alejandro Vasquez-Rifo, Guillaume Jannot, Javier Armisen[1,2], Michel Labouesse[3], Syed Irfan Ahmad Bukhari, Evelyne L. Rondeau , Eric A. Miska[1,2] and Martin J. Simard.

Laval University Cancer Research Centre, Hôtel-Dieu de Québec (CHUQ), Quebec City, Québec G1R 2J6, Canada

[1]Wellcome Trust Cancer Research UK Gurdon Institute, University of Cambridge, The Henry Wellcome Building of Cancer and Developmental Biology, Cambridge, UK.
[2]Department of Biochemistry, University of Cambridge, Cambridge, UK.
[3]Development and Stem Cells Program, IGBMC, CNRS (UMR7104), INSERM (U964), Université de Strasbourg, 1 rue Laurent Fries, BP10142, 67400 Illkirch, France.

Corresponding Author:

Email: Martin.Simard@crhdq.ulaval.ca

Keywords: Argonaute, microRNA, *C. elegans*, embryonic development

2.1 Résumé

Les gènes *alg-1* et *alg-2* (appelé *alg-1/2*) codent pour les protéines Argonautes affiliées spécifiquement à la voie des microARNs (miARN) chez *C. elegans*. Leurs associations avec les microARNs forment des complexes effecteurs responsables de la répression génique post-transcriptionnelle. Nous avons caractérisé aspects spécifiques de ces gènes au cours du développement larvaire, afin de définir certains caractéristiques biologiques importantes pour la compréhension du mode d'action de ces protéines Argonautes. Plus particulièrement, nous avons établi que *alg-1/2* affichent un profil d'expression spatio-temporel semblable et s'associent à un ensemble commun de miARNs. Cependant dans certaines cellules, une expression différentielle est observée avec une association relative augmentée pour certains miARNs. Malgré l'observation de cette redondance et indépendamment de drastiques différences post-embryonnaires observées dans les mutants de ces gènes, seule la perte des deux gènes conduit à une létalité embryonnaire. Le développement des embryons sans expression zygotique de *alg-1/2* s'arrête principalement au cours du processus de l'allongement avec des défauts d'attachement entre l' épiderme et la structure musculaire. Nos résultats mettent en évidence des similitudes et des spécificités de *alg-1/2* susceptibles d'être expliqués à différents niveaux cellulaires et moléculaires.

2.2 Abstract

The genes *alg-1* and *alg-2* (referred to as "*alg-1/2*") encode the Argonaute proteins affiliated to the microRNA (miRNA) pathway in *C. elegans*. Bound to miRNAs they form the effector complex that effects post-transcriptional gene silencing. In order to define biological features important to understand the mode of action of these Argonautes, we characterize aspects of these genes during development. We establish that *alg-1/2* display an overlapping spatio-temporal expression profile and shared association to a miRNAs set, but with gene-specific predominant expression in various cells and increased relative association to defined miRNAs. Congruent with their spatio-temporal coincidence and regardless of *alg-1/2* drastic post-embryonic differences, only loss of both genes leads to embryonic lethality. Embryos without zygotic *alg-1/2* predominantly arrest during the morphogenetic process of elongation with defects in the epidermal-muscle attachment structures. Altogether our results highlight similarities and specificities of the *alg-1/2* likely to be explained at different cellular and molecular levels.

2.3 Introduction

Argonaute family proteins are defined by the presence of the PAZ domain which contributes to the binding of small (21-32 nucleotide long) RNA molecules and the PIWI domain that confers the endonuclease enzymatic activity present in some members of the Argonautes family (Hutvagner and Simard, 2008). This protein family is conserved from archaea to eukarya, and largely expanded in some plants and animals. Distinct kinds of small RNAs are bound by Argonautes which participate in viral defence (Ding and Voinnet, 2007), post-transcriptional gene regulation (Fabian *et al.*, 2010) and transposon silencing (Siomi *et al.*, 2008; Klattenhoff and Theurkauf, 2008), processes which in turn affect somatic and germ-line development.

In the nematode *C. elegans*, the Argonaute family comprises 24 genes and 2 pseudogenes, which partition into three groups, the Argonaute-like (AGO-like), the Piwi-like and a nematode-specific clade (Hutvagner and Simard, 2008). The genes *alg-1* and *alg-2* (hereafter, both referred to as "*alg-1/2*") belong to the conserved AGO-like clade, which includes the fly *D. melanogaster* Ago1 and Ago2, and four mammalian Argonautes, AGO1-4. *Alg-1/2* have been shown to be required for the miRNA pathway but not for exo-RNAi (Grishok *et al.*, 2001), while the fly and mammalian AGOs are differentially required for both RNAi and the miRNA pathway (Liu *et al.*, 2004; Su *et al.*, 2009; Forstemann *et al.*, 2007). Two additional *C. elegans* Argonautes in the same clade, *alg-3* and *alg-4*, are required for the accumulation of 26-nt long endogenous RNAs and affiliate to a separate endo-RNAi pathway (Conine *et al.*, 2010).

The canonical miRNA pathway involves the processing of a primary RNA molecule by the RNase III enzyme Drosha, to produce a stem-loop precursor molecule which is next cleaved by the Dicer enzyme to release a small double-stranded RNA moiety (21-23nt). One of strands from this small duplex will then be loaded into the Argonaute protein, forming the core complex that targets the 3' untranslated region (UTR) of mRNAs with sequence specificity to elicit post-transcriptional gene silencing (Fabian *et al.*, 2010).

In distinct organisms, multiple Argonautes are involved in the miRNA pathway. In mammals, ectopic expression of the AGO1-4 Argonautes is able to provide miRNA function in cells (Su *et al.*, 2009), while fly Ago1 is typically loaded with most miRNAs, some specific ones are bound by Ago2 (Forstemann *et al.*, 2007; Iwasaki *et al.*, 2009). The presence of several Argonautes in the miRNA pathway implies possible redundant and specialized functions, an aspect still incompletely understood. In this report, we describe the expression and embryonic phenotypes of *C. elegans alg-1/2* along with their post-embryonic miRNA interaction profiles with the purpose of providing insights into the shared and the non-redundant functions of the Argonautes of the miRNA pathway.

2.4 Results

2.4.1 Structural features of ALG-1 and ALG-2

The *C. elegans* genes *alg-1* and *alg-2* encode two Argonaute proteins with high amino acid sequence similarity (81%; Fig. 2.1A). The PAZ, PIWI and C-terminal regions of the ALG-1/2 are highly conserved, while the N-terminal region is constituted of amino acids specific to each Argonaute, especially prominent in ALG-1. The N-terminus is involved in protein interactions which confer specificity to ALG-1 (Jannot *et al.*, 2011a).

The highly conserved orthologs of both genes that are readily identified in other *Caenorhabditis* species (Fig. 2.1B) along with the high *alg-1* and *alg-2* DNA sequence similarity, indicates that these genes most probably arose by recent gene duplication as previously suggested by Grishok and collaborators (Grishok *et al.*, 2001).

2.4.2 Expression pattern of ALG-1 and ALG-2

In order to investigate functional differences between *alg-1* and *alg-2*, we first examined their expression pattern using functional translational reporters containing both ALG-1 and ALG-2 tagged with GFP or RFP, preserving their endogenous promoters and UTRs in the respective mutant backgrounds. For simplicity, we refer to the GFP::ALG-2 and RFP::ALG-1 reporters as ALG-2 and ALG-1, respectively. Both Argonautes were found to be broadly expressed in most tissues, but their expression patterns were not completely overlapping. Subsets of neurons in the head ganglia expressed predominantly ALG-2, while the pharynx more prominently expressed ALG-1 (Fig. 2.3). Cells in the tail also displayed specific expression. Nonetheless, both Argonautes are expressed together in tissues including the vulva, seam cells, ventral nerve chord and somatic gonad (Fig. 2.3, Table 2.1, Fig. 2.6 and Fig. 2.7). Identical ALG-1 expression was also observed for the common tissues examined by Chan and Slack using similar translational reporter (Chan and Slack, 2009). To confirm that the expression pattern observed with chromosomal arrays reflects the expression of endogenous protein, we performed a whole-worm immunostainings using a polyclonal antibody raised against the ALG-1 specific N-terminus region (ALG-2 specific antibody is not yet available). The endogenous ALG-1 expression was confirmed for the pharynx and head neurons (Fig. 2.2) further supporting the expression pattern observed with transgenic lines.

We next examined the ALG-1/2 expression in distinct *C. elegans* stages. Examination of the ALG-1/2 expression during larval development did not reveal differences in expression during the four larval stages and adults (Fig. 2.4). However, during embryogenesis the onset of zygotic expression was distinct. ALG-2 started to be expressed from pre-morphogenetic embryonic stages while ALG-1 is first detected at the beginning of the morphogenetic phase

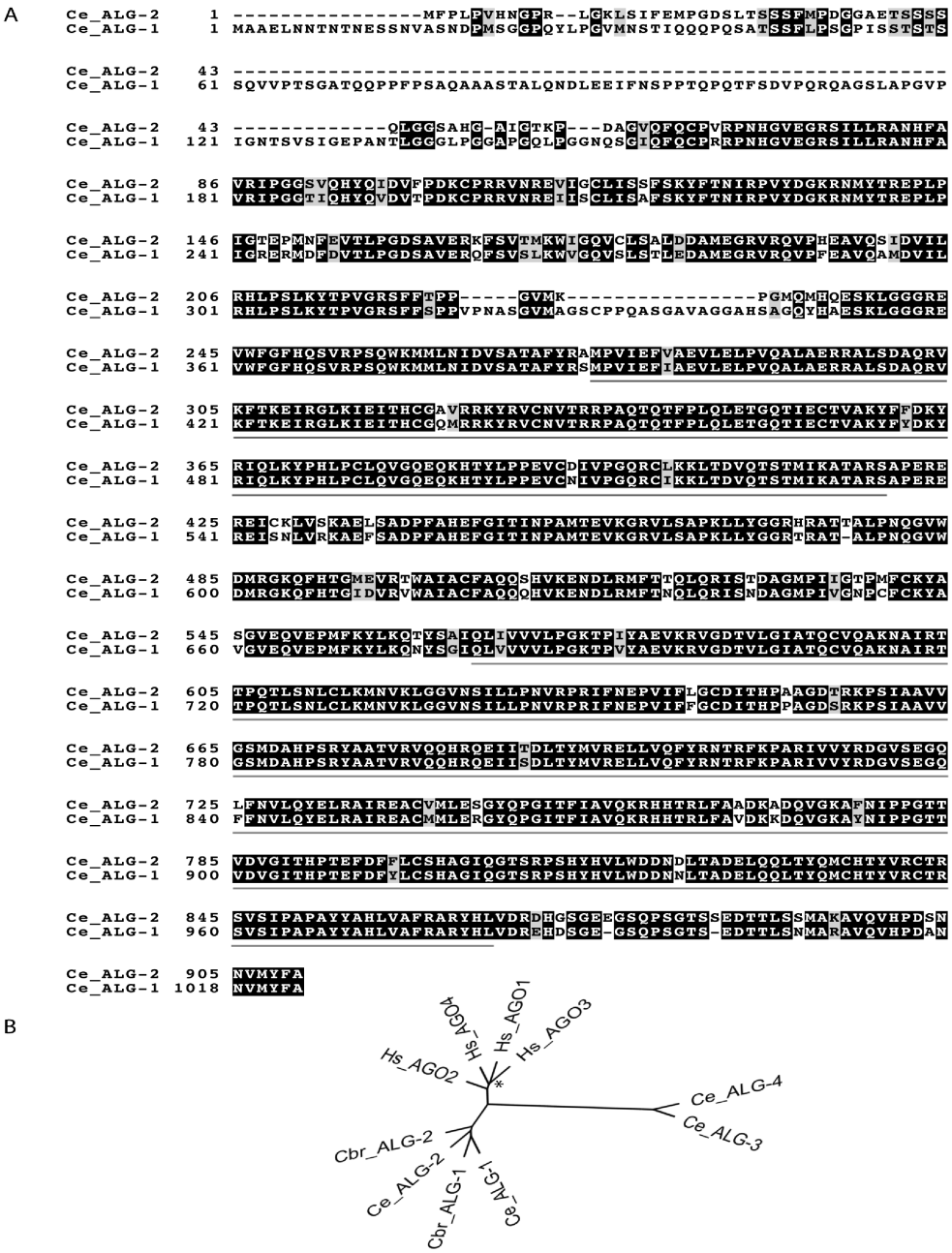

Figure 2.1: **Features of the miRNA-specific Argonautes ALG-1 and ALG-2. (A)** Amino acid sequence alignment between ALG-1 and ALG-2 proteins (77% identity and 81% similarity). Identical (black) and similar (grey) residues as well as the PAZ (pink) and PIWI (blue) signature domains are indicated. **(B)** Neighbor joining tree of nematodes and human AGO-clade Argonautes based on the conserved sites from an alignment of full length protein sequences. With the exception of human AGO1 and AGO3 (*), all the subtrees are robustly significant (higher than 95% bootstrap; 500 trials). Ce, *Caenorhabditis elegans*; Cb, *Caenorhabditis briggsae*; Hs, *Homo sapiens.*

Tissue	Abbrev.	ALG-1	ALG-2
Intestine	I	+	+
Pharynx	P	+	−
Head Hypodermis	HH	+	+
Body Hypodermis	BH	+	+
Tail Hypodermis	TH	+	+
Seam cells	SC	+	+
Excretory system	X	+	+
Spermatheca	S	+	+
Distal Tip Cells	DTC	+	+
Uterus	U	+	+
Gonadal Sheath	GS	+	+
Vulva	V	+	+
Body Neurons	BN	+	+
Head Neurons	HN	−	+
Tail Neurons	TN	+	+
Body Muscle	BM	+	+
Rectum	R	+	+

Table 2.1: **Summary of ALG-1/2 expression in different organs and tissues.** Fluorescence intensity is indicated as plus to indicate a discernible signal, and minus if signal was not clearly discernible from background fluorescence.

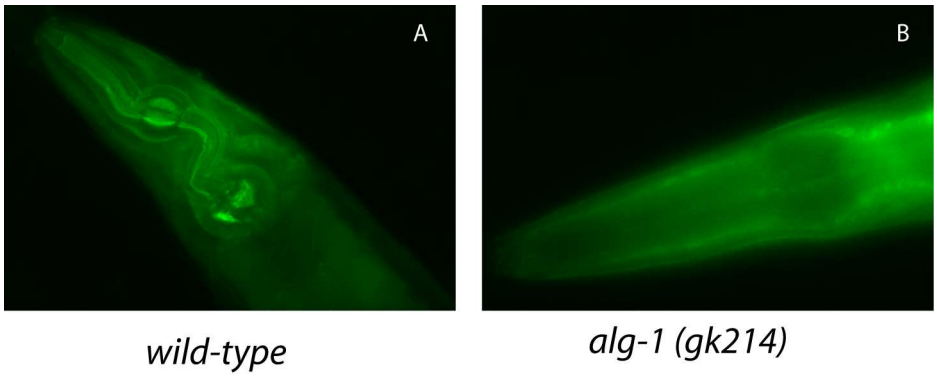

Figure 2.2: **Immunostaining of ALG-1 in adult *C. elegans* hermaphrodites.** Staining with polyclonal antibody against ALG-1 of head organs. **(A)** A specific signal is detected in the pharynx of wild-type animals. **(B)** Staining of control *alg-1(gk214)* animal.

(Fig. 2.5). Altogether, our data indicated that the ALG-1/2 expression patterns are spatially and temporally overlapping with some specific tissues where one of the Argonautes is predominantly expressed.

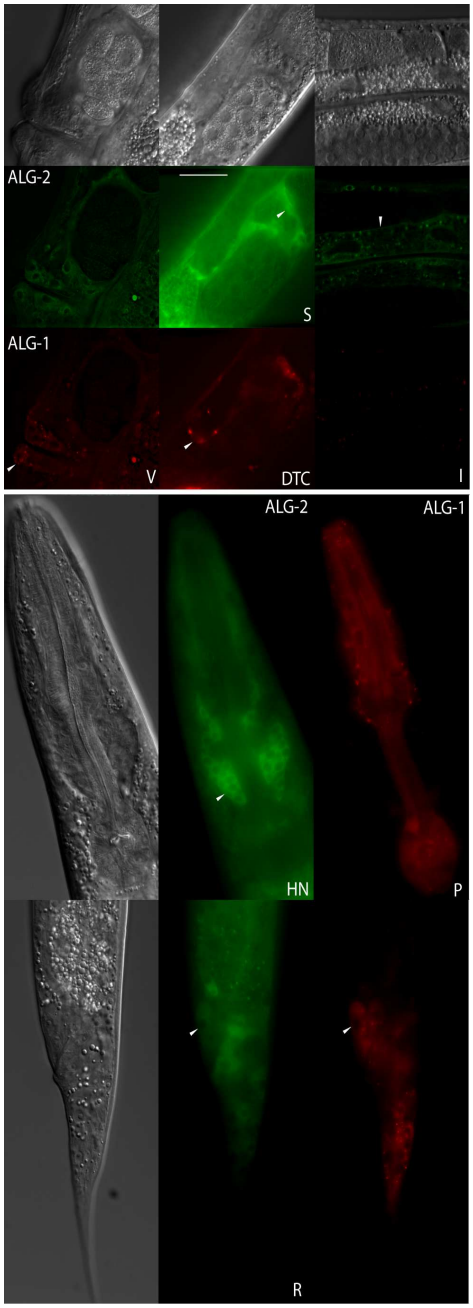

Figure 2.3: **ALG-1 and ALG-2 expression overlaps in most but not all tissues. Top panel:** GFP::ALG-2 and RFP::ALG-1 are co-expressed in most tissues including vulva (V) and spermatheca (S). **Bottom panel:** Predominant GFP::ALG-2 expression is seen in a set of head neurons (HN) and tail cells (T) while RFP::ALG-1 is strongly expressed in the pharynx (P) and some tail cells (T). Scale bar 20 μm.

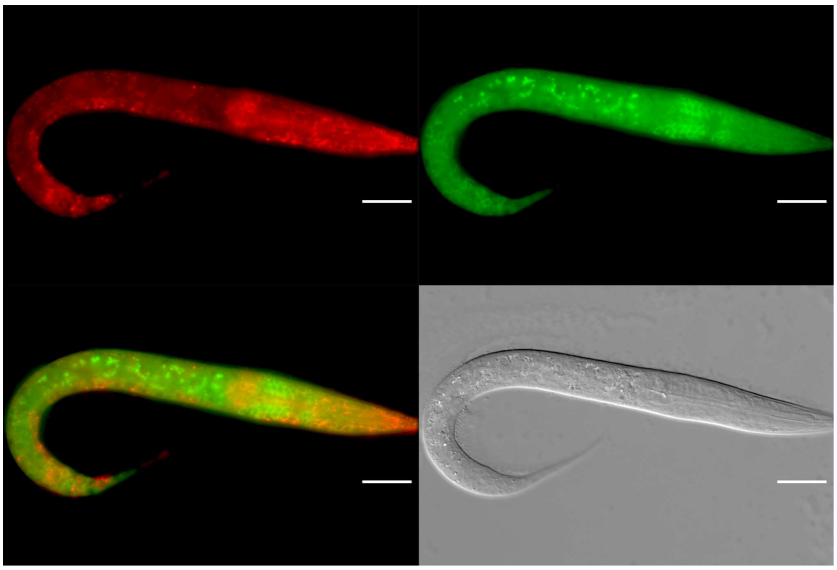

Figure 2.4: **Profile of ALG-1 and ALG-2 expression in L1 larval stage.** Expression profile of GFP::ALG-2 and RFP::ALG-1 as seen in the L1 larval stage. Subsequent larval stages (L2 to L4) and adults display the same expression profile (not shown). Scale bar 20 μm.

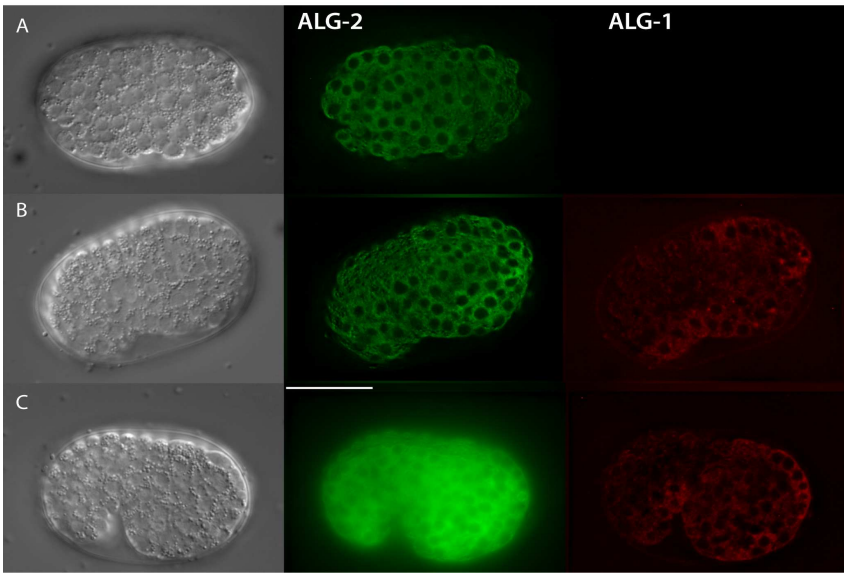

Figure 2.5: **The embryonic ALG-1 and ALG-2 expression onset differs.** The expression onset of GFP::ALG-2 and RFP::ALG-1 differs. RFP::ALG-1 fluorescence is first detected at the beginning of the morphogenetic phase (B). Scale bar 20 μm.

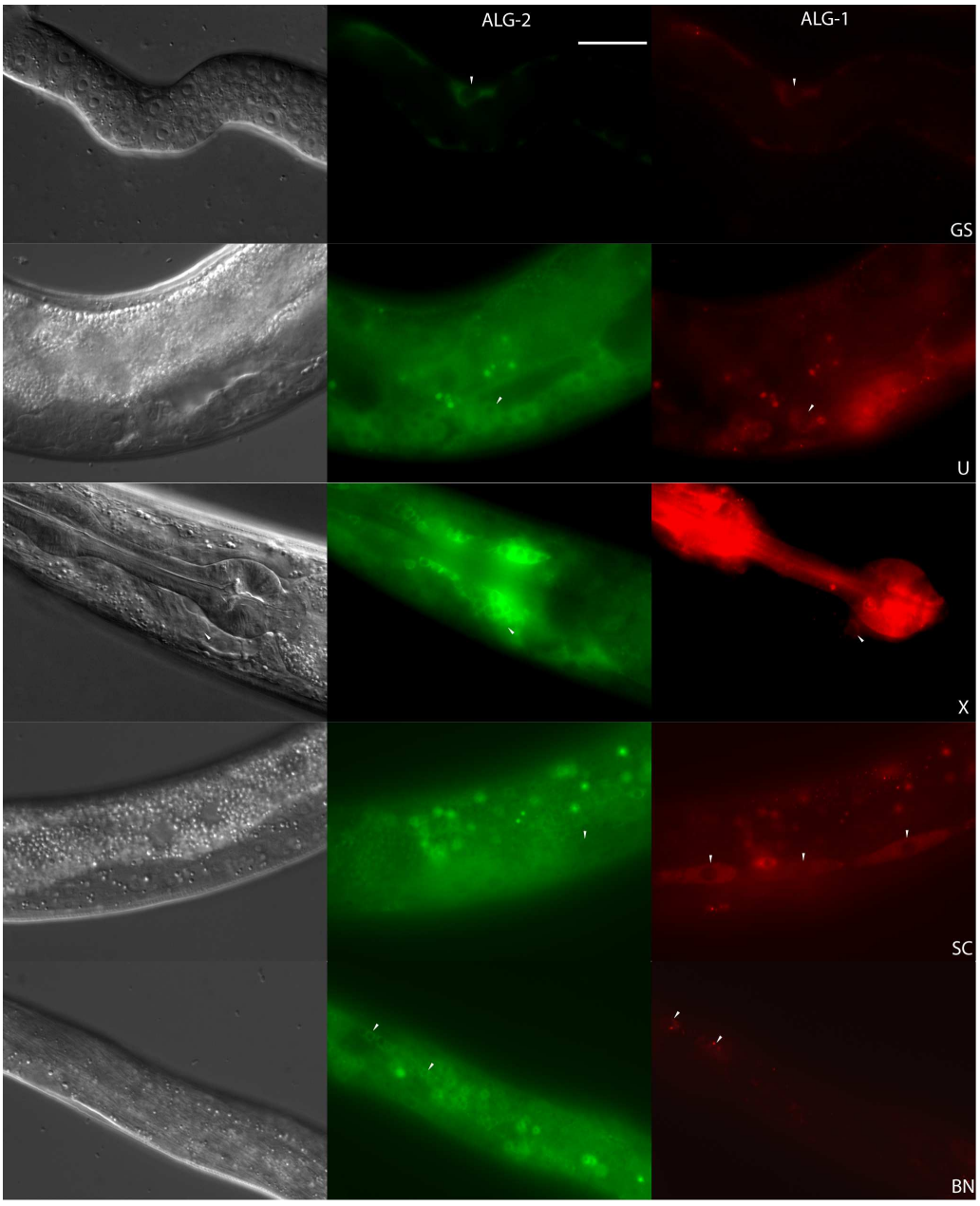

Figure 2.6: **Detailed ALG-1 and ALG-2 expression profiles in somatic gonad, seam cells and neurons.** GFP::ALG-2 and RFP::ALG-1 expression in body neurons (BN), seam cells (SC), excretory system cell (X), uterine cells lining the uterine cavity (U) and gonadal sheet cells (GS). Scale bar 20 μm

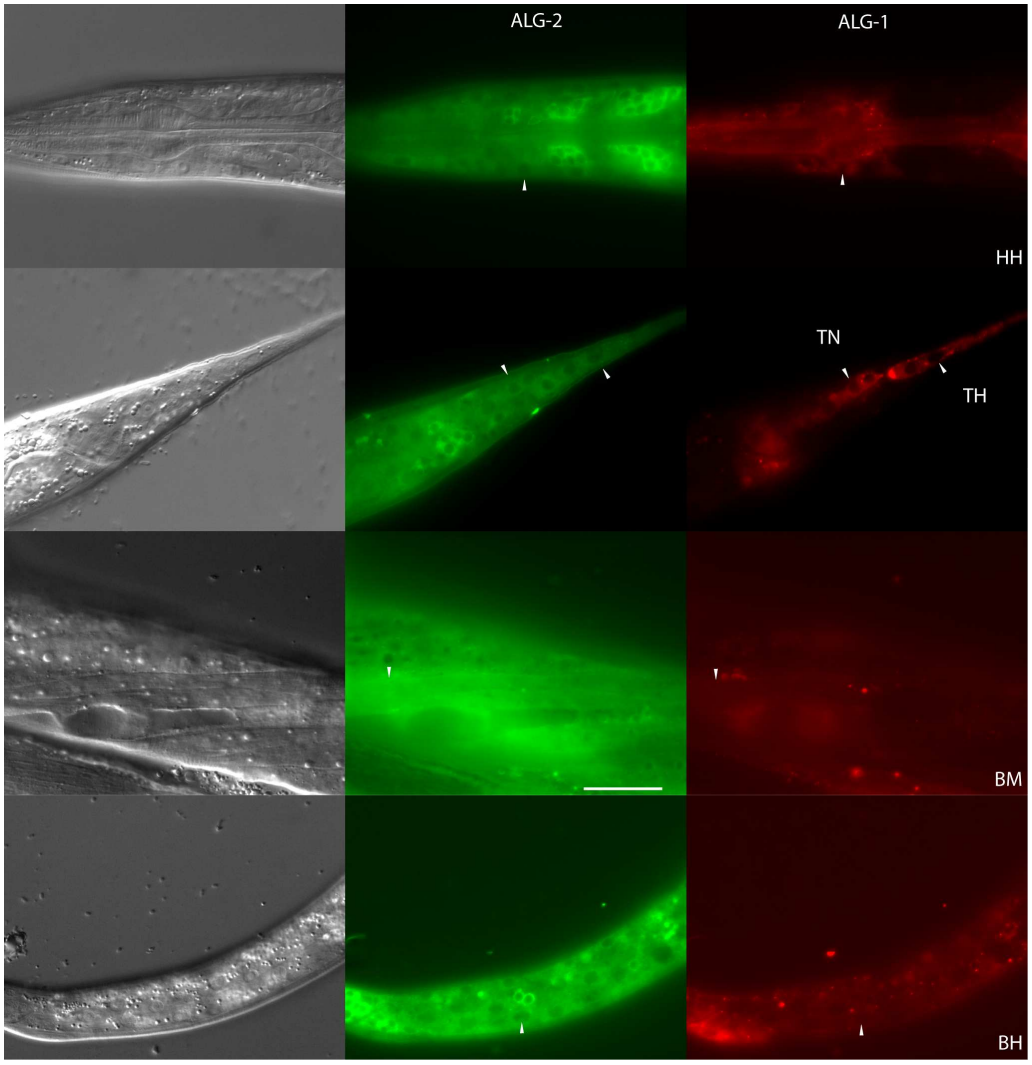

Figure 2.7: **ALG-1 and ALG-2 expression in neurons, hypodermal and muscular tissues.** GFP::ALG-2 and RFP::ALG-1 expression in head hypodermal cell (HH), tail hypodermal cells and tail neurons (TH,TN), body muscle cells (BM) and larval P cells whose lineage contribute to the neurons and body hypodermis (BH). Scale bar 20 μm

2.4.3 microRNA interactions with ALG-1 and ALG-2

To complement the ALG-1/2 expression patterns, we studied the association of a set of miRNAs with ALG-1 and ALG-2 throughout the four larval stages (L1-L4). To achieve this, we first immunoprecipitated ALG-1 and ALG-2 complexes from synchronized larval populations of transgenic worms expressing either ALG-1 or GFP::ALG-2 functional integrated transgenes (Fig. 2.8). We next purified small RNAs from ALG-1/2 complexes and determined miRNA association by microarrays. While control immunoprecipitations do not show significant difference in miRNA association (data not shown), at each stage of development, we detected a number of miRNAs associated preferentially to ALG-1 or ALG-2 and notably this preferential association was higher in the L1 and L4 stages compared to the L2/L3 stages (Fig. 2.9). The relative association of miRNAs to the Argonautes at each developmental stage followed a trend of conservation at other stages, but for some miRNAs it changed dramatically during development (*e.g.* miR-44 in L1 and L3 stages associates more with ALG-1 while at L2 and L4 it does with ALG-2, miR-253 switched its relative association from the L1/L2 stages to L3/L4). Therefore, our analysis indicates that while ALG-1/2 largely bind to the same set of miRNAs, the association of specific miRNAs to either Argonaute supports the existence of specificity at the molecular or cellular level that follows specific dynamics during development.

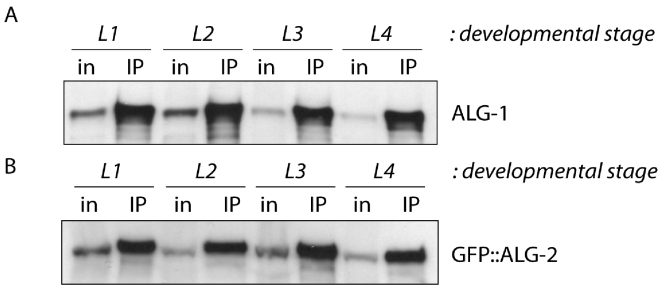

Figure 2.8: **Detection of ALG-1 and GFP::ALG-2 in purified complexes.** Detection of ALG-1 **(A)** and GFP::ALG-2 **(B)** by Western blot analysis found in the immunopurified (IP) complexes from each developmental stage (L1 to L4) used for microRNA microarrays. 50 μg of the total protein (in) were run as controls.

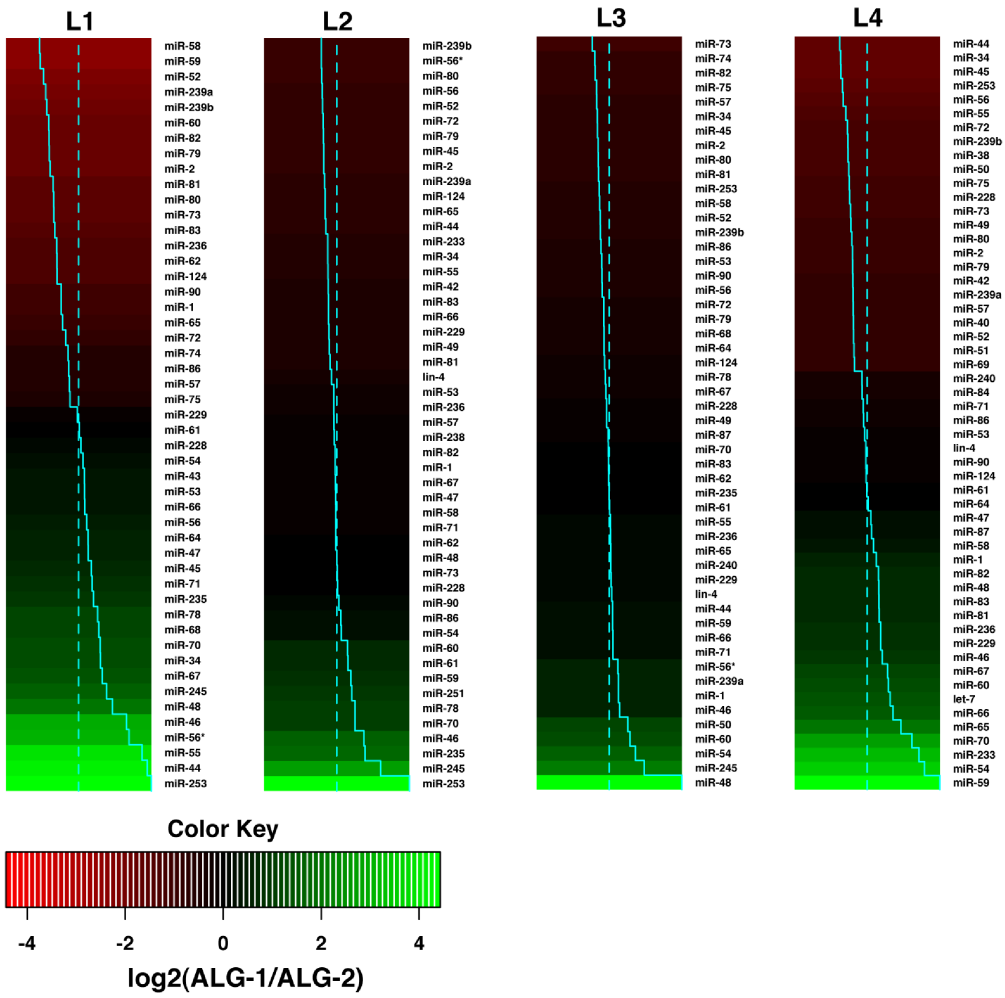

Figure 2.9: **ALG-1 and ALG-2 commonly associate with most but not all miRNA.** Heatmaps representing the ratios of ALG-1 to ALG-2 associated miRNAs at the larval stages indicated as estimated from miRNA microarrays (towards red: stronger association to ALG-2, towards green: stronger association to ALG-1). miRNA expression data were filtered for robustly expressed miRNAs. Ratios were log2 transformed, centered and normalized for each column. The distance of the solid blue line from the center of each color-cell is proportional to the ratio. Mean ratio indicated as dotted blue line.

2.4.4 ALG-1/2 are required for embryonic morphogenesis

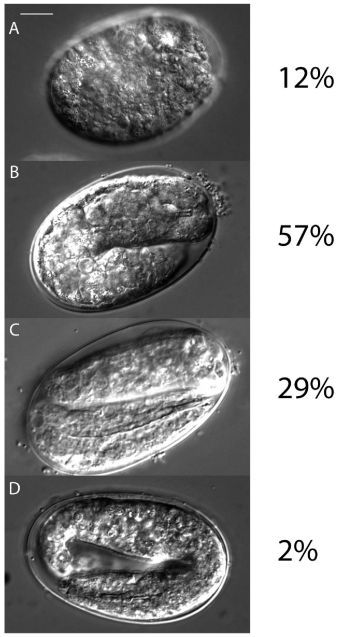

Figure 2.10: **Embryos without ALG-1 and ALG-2 arrest during embryonic development.** Statistics of embryonic arrest at 15°C (n=272). Freshly layed eggs on petri dishes were examined after a period of 12h. A major fraction of double mutant embryos arrest during the morphogenetic phase of development (**B-D**), mainly at the 2-fold stage (**B**).

Although *alg-1* and *alg-2* are highly similar at the sequence level and have mostly overlapping expression patterns, mutants of these Argonautes differ substantially in their phenotypes. Comparison of putative null alleles, reveals that *alg-1(gk214)* mutants have lesser growth and fertility compared to *alg-2(ok304)* (Bukhari *et al.*, 2012) and much more penetrant miRNA-related phenotypes like gapped alae (*alg-1* 24%, *alg-2* 0%, n=60) and bursting through the vulva (*alg-1* 27%, *alg-2* 0%, n=40). Besides these post-embryonic phenotypes, neither *alg-1(gk214)* or *alg-2(ok304)* have detectable embryonic lethality under standard growth conditions. To further precise the two Argonautes embryonic phenotypes, a balanced strain with deletion alleles of both genes was constructed (*alg-2(ok304)*; *alg-1(gk214)* / *unc-84(e1410)*). The strain segregated the expected genotypes but no homozygous *alg-2(ok304)*; *alg-1(gk214)* double mutants (hereafter referred to as double mutants) were ever found as viable worms. Indeed, homozygous double mutants arrested as embryos, consistent with the phenotype observed in simultaneous RNAi knockdown of *alg- 1* and *alg-2* (Grishok *et al.*, 2001).

The embryonic arrest of the double mutant indicates that at least one of the two Argonautes has to be zygotically expressed in the embryo to allow complete development. The double mutant predominantly arrested at the 2-fold stage of development at 15 and 25°C (Fig.2.10 and data not shown). This stage is part of the morphogenetic phase of development, which

follows after most embryonic cell divisions have taken place and comprises major shape changes and completion of organogenesis. The fraction of embryos that arrested either after complete elongation or before morphogenesis is possibly due to incomplete penetrance and variation of the maternally contributed ALG-1 and ALG-2.

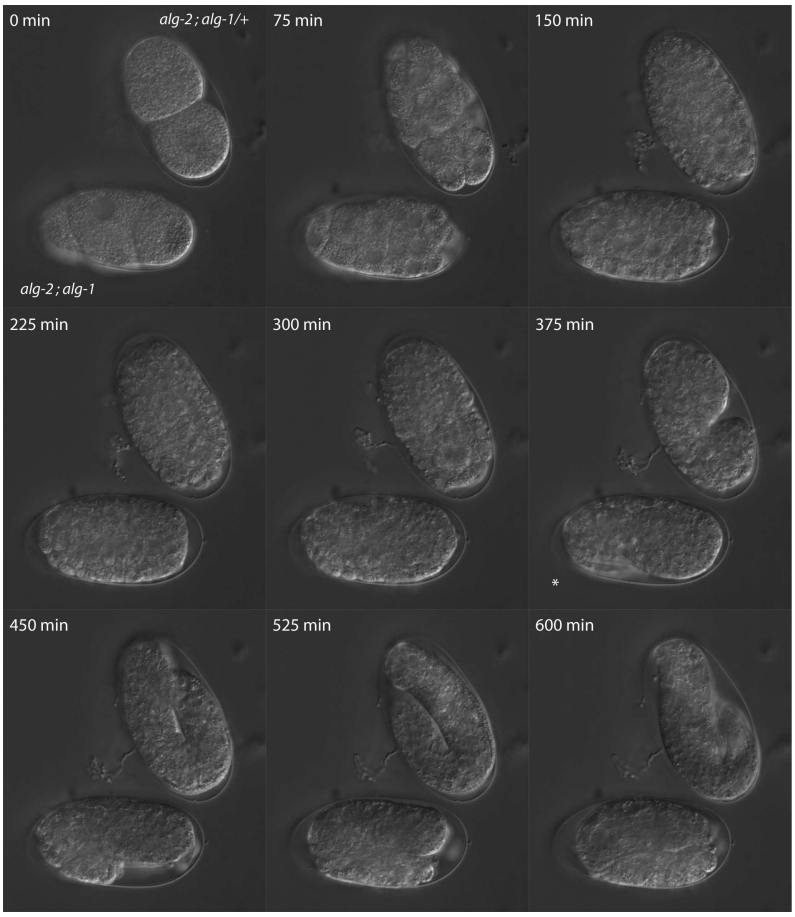

Figure 2.11: **Developmental timing is not affected in the double *alg-1/2* mutant.** Time-lapse microscopy of *C. elegans* embryos. Both embryos proceed through development at similar rates until the morphogenetic phase (375 min) were the *alg-2(ok304); alg-1(gk214)* double mutant arrest (asterisk). Viable siblings were able to proceed development normally. The double mutant embryos are not paralyzed and are able to twitch (see supplementary movie).

To further characterize the embryonic requirement of *alg-1/2*, time-lapse microscopic recordings were conducted. We did not detect developmental defects in the double mutants before the 2-fold stage, and the recordings revealed no evident difference in developmental timing between the double mutant embryos and their viable siblings prior to the 2-fold stage were arrest occurred (Fig. 2.11 and Movie S1). This supports that the 2-fold arrest is likely caused by the disruption of one or various morphogenetic processes taking place and not the consequence of an earlier embryonic defect.

2.4.5 ALG-1 and ALG-2 requirement in epidermal cytoskeleton and muscle development

The observed embryonic arrest may reflect an impairment of one or several of the process taking place during the morphogenetic phase of development, namely epidermal migration, ventral enclosure and elongation (Chisholm and Hardin, 2005). During this phase, the epidermal cells, initially located in the embryonic dorsal part, intercalate and extend around the embryo towards the ventral side and fully enclose it. Upon completion of epidermal enclosure, embryos continue to elongate anteroposteriorly, a process whereby epidermal and muscle cells actively drive the constriction of the embryo along its cross-section. Examination of the epidermal adherens junctions, as judged by staining with the junction-specific monoclonal antibody MH27, did not reveal any apparent epithelial polarity defect and revealed a minor epidermal cell shape defect commonly found in embryos with partial or severe muscle defects (data not shown). Consistent with DIC pictures (Fig. 2.10), embryos could not elongate much beyond the two-fold stage resulting in slightly deformed embryos (Fig. 2.12B). Thus, proper epidermal specification, dorsal intercalation and ventral enclosure are achieved in the double mutant embryos with very few exceptions.

The elongation process depends on the concerted epidermal and muscle function, and both tissues connect through specialized junctions containing hemidesmosomes and intermediate filaments (known as fibrous organelles) (Zhang and Labouesse, 2010). To investigate their integrity, we co-stained embryos from *alg-2(ok304)*; *alg-1(gk214) / unc-84(e1410)* parents with a hemidesmosome marker (antibodies against VAB-10A protein) and a monoclonal antibody against a muscle marker (NE8/4C6). We observed that fibrous organelles were interrupted, and that muscles appeared to detach from the body wall in those areas in most putative *alg-2(ok304)*; *alg-1(gk214)* embryos: out of 80 embryos laid by heterozygous parents, 21 had elongation defects (putative double mutants), 18 of which also showed fibrous organelle and/or muscle defects (Fig. 2.12). However, fibrous organelle defects were not as severe as in very strong fibrous organelle mutants such as *vab-10* and *vab-19*, or in *vab-10(e698); eel-1(ok1575)* double mutants (Zahreddine *et al.*, 2010). The muscle NE8/4C6 staining pattern was also less severe than in the most severe *pat* mutants which disrupt the attachment of myofibers to the muscle plasma membrane (Hresko *et al.*, 1994).

Altogether our immunofluorescence data are consistent with the time-lapse analysis and suggest that defective embryonic morphogenesis is the primary cause of lethality of the double mutant. The penetrant fibrous organelle defect is compatible with either disruption of a fibrous organelle component, or of a muscle component.

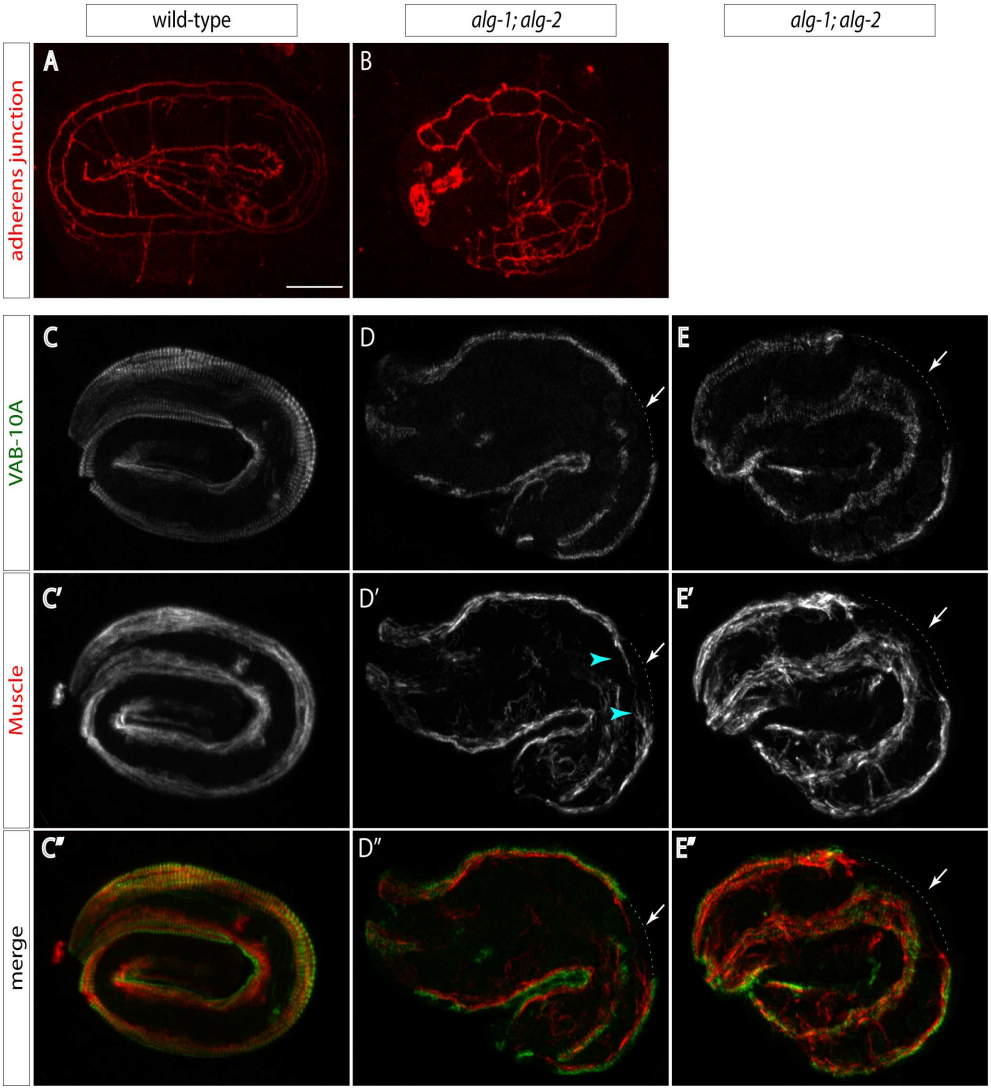

Figure 2.12: **ALG-1/2 function is required to maintain attachment between muscle and the epidermis. (A-B)** Embryos collected between 6-8 hours post egg-laying at 25°C and stained with the antibodies MH27 (adherens junction). The *alg-1; alg-2* mutant embryo did not progress beyond the two-fold stage, yet has grossly normal junctions. **(C-E)** Embryos collected between 6-8 hours post egg-laying at 25°C and stained with the antibodies 4F2 (VAB-10A; C-E) and NE8/4C6 (muscle; C'-E'); merge picture (C''-E''). Arrow, are where the fibrous organelle (D-E) and muscle (D'-E') pattern is partially interrupted; in addition, muscles do not closely follow the body wall in this area (they should be closer to the blue dotted line; see blue arrowheads). Embryos did not elongate beyond the two-fold stage.

2.5 Discussion

Our study indicates that the Argonaute encoding *alg-1* and *alg-2* genes have remarkable similarities that do not preclude major functional differences. Multiple resemblances include high sequence homology, overlapping expression patterns, partially coincident sets of bound miRNAs, and their redundant requirement for embryonic development. However, single mutant of these genes lead to very distinct phenotypes and effects on the miRNA pathway during worm post-embryonic stages. The more penetrant defects seen in *alg-1* mutants do not correlate with differences in the relative abundance of ALG-1/2, as judged by western analysis using antibody against the conserved region of ALG-1/2 ((Wu *et al.*, 2010); unpublished observations).

The detailed analysis of the expression pattern of *alg-1* and *alg-2* demonstrates that ALG-1/2 proteins are overlapping in many tissues, but a specific expression pattern is observed in a subset of head neurons, pharynx and specific cells in the tail. The embryonic onset of expression differs and leads to a pattern that remained constant from the first larval stage to adults. The differences in the *alg-1/2* expression patterns may result in part from transcriptional differences. Genome-wide analysis of the transcription factor PHA-4 has found that it binds to the *alg-1* promoter, while no significant binding is detected in the promoter (2kb upstream from start site) of *alg-2* (Zhong *et al.*, 2010). Thus, PHA-4 and additional transcription factors may contribute to the specificity of the *alg-1/2* expression in certain tissues.

In agreement with the observed expression overlap, miRNA profiling during the worm larval stages showed that ALG-1/2 bind the studied set of miRNAs coincidently although a preferential association is detected for some miRNAs. Similar associations between miRNA and Argonaute proteins have also been observed for the human Argonautes in cultured cells (Azuma-Mukai *et al.*, 2008). This preferential association could arise in two ways, differential co-expression of Argonaute and miRNA in certain cells, or as result of molecular Argonaute-miRNA specificity. It should be noticed that observed preferential association of some miRNAs to ALG-1/2, does not constitute an exclusive association that would make specific miRNAs completely dependent on the presence of either ALG-1 or ALG-2.

In a first scenario, the co-expression of a specific Argonaute and miRNA could increase their relative association. The expression of many *C. elegans* miRNAs has been described (Martinez *et al.*, 2008; Isik *et al.*, 2010; Johnston and Hobert, 2003) and ranges from highly specialized (*i.e. lsy-6*) to widely expressed. The presence of specific tissues where one of the *alg-1/2* is predominantly expressed, and the specialized expression seen in some miRNAs could dictate specific miRNA-ALG-1/2 interactions in certain cells or tissues. The correlation of miRNA and ALG-1/2 expression is subject to confounding effects given that the relative association we measured reflects the contribution of all the tissues were the miRNA is expressed. In few cases a correlation is straightforward, ALG-2 is predominantly expressed in neurons of the head ganglia, and it associates preferentially with the miR-72 miRNA that is

expressed only in the head neurons (Martinez *et al.*, 2008).

Alternatively, molecular specificity may explain preferential miRNA-Argonaute association. The identity of the 5' terminal nucleotide confers affinity on small RNAs for different plant Argonautes (Mi *et al.*, 2008), and duplex mismatches sort out siRNA and miRNA in flies and *C. elegans* (Steiner *et al.*, 2007; Jannot *et al.*, 2008; Tomari *et al.*, 2007). However, it is yet unknown what could determine the specificity of Argonaute proteins for particular miRNAs. The sequence and structure of miRNAs and their precursor molecules as well as Argonaute interactions with additional factors could potentially confer this specificity. These kinds of features may potentially explain the relative association observed among ubiquitously expressed miRNAs such as miR-52 and miR-71 that are associated preferentially with ALG-2 and ALG-1, respectively.

Our observations also demonstrate that genetically, *alg-1/2* share functions during embryonic development. The embryonic lethality of the *alg-1/2* double mutant is not observed in single mutants of Dicer and Drosha, due to the fact that the maternal contribution of these enzymes of the microRNA pathway allows homozygous mutants to complete all developmental stages and become sterile adults (Knight and Bass, 2001; Denli *et al.*, 2004). In contrast, the embryonic lethality of the double mutant reveals that *alg-1/2* maternal contribution is insufficient to complete development, and thus zygotic expression is required. The *alg-1/2* maternal contribution (Tops *et al.*, 2006) present in the double mutant, disallowed the examination of the ALG-1/2 role during early development. An early developmental role for specific miRNAs and associated Argonautes in the degradation of maternal transcripts at the maternal to zygotic transition has been documented in zebrafish (Giraldez *et al.*, 2006) and the *X. laevis* (Lund *et al.*, 2009), and could be explored in *C. elegans* by using RNAi. Considering that *alg-1/2* function in the miRNA pathway and that most miRNAs are not essential for development (Miska *et al.*, 2007; Alvarez-Saavedra and Horvitz, 2010), the observed embryonic arrest may be the result of the combined loss of a specific set of miRNAs. To date, the absence of the complete *mir-35* and *mir-52* families has been reported as embryonic lethal. The loss of miR-35 family results in a slower development and arrest at the 2-fold to 3-fold stage (Alvarez-Saavedra and Horvitz, 2010), while the miR-52 family mutant displays detachment of the pharynx at a late stage of embryonic development (Shaw *et al.*, 2010). Identification of the miRNAs and targeted genes involved in the embryonic arrest remains open for future work.

Beside *C. elegans*, mutants of the miRNA Argonautes in mammals and *Drosophila* also display embryonic lethality. Ago2 knockout mice display early mesoderm defects (Morita *et al.*, 2007; Alisch *et al.*, 2007), as well as mid-gestational death due to placental defects (Liu *et al.*, 2004; Cheloufi *et al.*, 2010). Similarly, ago1 and ago2 are together essential for the establishment of segment polarity in flies (Meyer *et al.*, 2006). Some of these essential developmental roles of the miRNA pathway during animal development may reflect a common requirement of the

pathway for the proper differentiation and function of certain tissues. Along this line, our data demonstrate the requirement of *alg-1/2* during the morphogenetic phase of embryonic development, manifested through the predominant arrest at the 2-fold stage, where worms are unable to complete the elongation process. For the most part, the epidermal and muscle tissues of the double mutant embryos are properly specified and epidermal adherens junctions are presumably normal. In contrast, the epidermal-muscle attachment structures are mildly but frequently affected. The defects most likely stem from epidermal fibrous organelle or muscle defects. Since both the elongation defects and fibrous organelle staining defects were less severe than those observed in core fibrous organelle mutants, we do not think that ALG-1 and ALG-2, hence that miRNAs, are essential for the production of a core fibrous organelle component. We recently established that muscle contractions are required to pattern hemidesmosomes and promote epidermal morphogenesis (Zhang *et al.*, 2011). Hence, one or more miRNAs might contribute either to some aspect of muscle differentiation and/or contractility, or within the epidermis to relay the muscle-to-epidermis mechanical signal, possibly in a feedback loop. Future experiments should help clarify among these possibilities.

2.6 Materials and Methods

Culture conditions and general methods

Worms were cultured in standard conditions (Brenner, 1974). All experiments were performed at 20°C unless otherwise noted.

Transgenic strains

The following transgenic strains were generated by microinjecting a mix of plasmids and UV integrated as described in (Mello and Fire, 1995; Mello *et al.*, 1991):

- MJS13: *alg-1 (gk214)* In[*alg-1p::rfp::alg-1::alg-1 3'UTR* ; *alg-2p::gfp::alg-2::alg-2 3'UTR* ; pRF4]
- MJS18: *alg-2 (ok304)* In[*alg-1p::gfp::alg-1::alg-1 3'UTR* ; *alg-2p::rfp::alg-2::alg-2 3'UTR* ; pRF4]
- MJS46: *alg-1 (gk214)* In[*alg-1p::alg-::alg-1 3'UTR* ; pRF4]
- MJS26: *alg-2 (ok304)* In[*alg-2p::gfp::alg-2::alg-2 3'UTR* ; pRF4]

Microscopy

Worms were examined mounted on agar pads using a Zeiss axioimager M1 microscope.

Time-lapse recordings were done using the AxioVision (Release 4.8) software at 1 minute interval during 600 minutes.

Immunostainings

For embryo stainings, heterozygous *alg-2(ok304); alg-1(gk214) / unc-84(e1410)* mothers were propagated at 25°C (non-permissive for *unc-84*) and allowed to lay eggs for 2-hour intervals. Embryos were collected, fixed and immuno-stained with mAb MH27 (DSHB, University of Iowa; recognizing AJM-1) and polyclonal LIN-26 antibodies (epidermal nuclei; Labouesse *et al*, 1996), or with the mAb NE8-4C6 (muscle marker; Schnabel, 1995) and polyclonal 4F2 antibodies (against VAB-10A; Bosher *et al.* , 2003) as described elsewhere (Bosher *et al.*, 2003). The NE8/4C6 monoclonal antibody was provided by the Medical Research Council. Stacks of images every 0.3 µm were captured using a confocal microscope (Leica SP2 AOBS RS); generally 10 confocal sections were projected using ImageJ and then processed using Adobe Photoshop.

For whole worm staining, mix-staged worms were collected and washed extensively several times with M9 buffer and staining was performed as by (Bettinger *et al.*, 1996). Fixed and permeabilized animals were incubated overnight at 4°C with purified rabbit anti-ALG-1 antibody (1:100)[1] and probed with Alexa Fluor 488 anti-rabbit (1:500) (Molecular Probes) as secondary antibody for 4 hours at room temperature. Images were captured using Zeiss motorized Axioplan 2 microscope at 630X with an AxioCam MRm camera and AxioVision acquisition software.

MicroRNA array profiling in ALG-1 and ALG-2 complexes

The transgenic animals expressing integrated arrays of either ALG-1 or GFP::ALG-2 tagged protein were harvested at specific development stages corresponding to four different larval transitions and total protein lysates were prepared as described previously (Jannot *et al.*, 2011a). Protein lysates prepared from *alg-1(gk214)* and for wild-type N2 animals were used as controls for ALG-1 and GFP::ALG-2, respectively. Immunoprecipitations were performed by preclearing 4 mg of total protein with 20 µl of protein-G magnetic beads (invitrogen) for 1h at 4°C. The cleared lysates were then incubated for 2h at 4°C with 20 µL of protein-G magnetic beads conjugated with either 5 µg of affinity-purified polyclonal anti-ALG-1 antibody (Bukhari *et al.*, 2012) or with the monoclonal antibody anti-AFP 3E6 (QBiogene). The beads were then washed three times with ice-cold lysis buffer containing 1% of Superasin (Roche). 90 % of the purified beads were used for total RNA extraction performed as described in (Hutvagner *et al.*, 2004). The remaining 10% of beads were boiled in SDS loading buffer and protein resolved by SDS-PAGE on an 8% gel. To detect ALG-1 and GFP-tagged ALG-2, the membranes were incubated overnight at 4°C with either affinity-purified polyclonal anti-ALG-1 diluted 1:5000 or a mouse monoclonal anti-GFP (Roche) diluted 1:2000 in TBST-milk solution, incubated 1 h at room temperature with either anti-rabbit (ALG-1) or anti-mouse (GFP-ALG-2) HRP-conjugated secondary antibody and then visualized by Western Lightening ECL Kit

1. The specificity of the anti-ALG-1 antibody is reported by Bukhari *et al.* (2012).

(Perkin Elmer).

RNA molecules extracted from ALG-1 and ALG-2 complexes were then subjected to size selection and purified small RNAs were used for miRNA array profilings as performed in (Miska *et al.*, 2004). All miRNA expression data have been submitted to the Gene Expression Omnibus (GEO) with accession number GSE35505 and GPL15181 (for microarray platform used).

Acknowledgements

We would like to thank members of our laboratories for comments on the manuscript. We also like to thank Eric Paquet for bioinformatics advice, the DNA microarray platform of the Infectious Disease Research Centre (CHUL/CHUQ) as well as Dr Barbara Papadopoulou and Marie-Jeanne Fiola for their help and advice in making the arrays. Some nematode strains were provided by the *Caenorhabditis* Genetics Center, which is funded by the NIH National Center for Research Resources (NCRR).

Chapter 3

Implication of the GARP complex in the *let-7* microRNA family function in *C. elegans*

Foreword

The present chapter is constituted by a manuscript submitted for publication in the journal 'Proceedings of the National Academy of Sciences of the United States of America'. I performed most of the experiments presented in the manuscript. Derrick Gibbings from the laboratory of Olivier Voinnet carried to completion the experiments in mammalian cells. Gabriel Bossé contributed to the mutant identification and performed Northern blotting analyses. Evelyne L. Rondeau performed the random mutagenesis screen.

Implication of the GARP complex in the *let-7* microRNA family function in *C. elegans*

Alejandro Vasquez-Rifo[1], Derrick Gibbings[2,3], Gabriel D. Bossé[1], Evelyne L. Rondeau[1], Olivier Voinnet[2] and Martin J. Simard[1].

[1]Laval University Cancer Research Centre, Hôtel-Dieu de Québec (CHU de Québec), Quebec City, Québec, Canada
[2] Swiss Federal Institute of Technology (ETH-Z), Department of Biology, Zurich, Switzerland
[3] University of Ottawa, Department of Cellular and Molecular Medicine, Ottawa, Canada

Corresponding Author:

Email: Martin.Simard@crhdq.ulaval.ca

Short Title: The GARP complex modulates miRNA activity

Keywords: *Caenorhabditis elegans*, microRNA, GARP complex, Argonaute, GW182

3.1 Résumé

De nombreux composants de base de la voie des microARNs (miARN) ont été élucidés et la connaissance de leurs mécanismes d'action progresse activement. En revanche, les facteurs qui jouent un rôle modulateur dans cette voie commencent seulement à être identifiés. À l'aide d'un crible génétique chez le nématode *C. elegans*, nous avons identifié le gène *vps-52*, un composant du complexe GARP (Golgi Associated Retrograde Protein), comme un nouveau partenaire génétique du gène codant pour la protéine ALG-1. En effet, nous avons démontré que la perte de fonction de *vps-52* aggravent les défauts prolifératifs des cellules souches épidermiques retrouvés dans les mutants *alg-1* ainsi que du miARN miR-48. Nous avons également montré que la perte de fonction de *vps-52* se rapport à une baisse significative des niveaux des microARNs de la famille let-7 (miR-48/miR-241) et des protéines GW182. En outre, la perte de VPS-52 augmente la létalité de l' allèle hypomorphe *let-7(n2853)* de façon dépendante de *lin-41*. L'effet de *vps-52* sur l'activité des miARN semble être conservée dans les cellules de mammifères, où VPS52 co-fractionne avec des composants du miRISC. Sur la base de notre analyse, nous proposons que par l'intermédiaire de GARP et par un processus membranaire relié au transport rétrograde, VPS-52 joue un rôle modulateur positif sur la fonction des miARNs.

3.2 Abstract

Many core components of the microRNA pathway have been elucidated and knowledge of their mechanisms of action is continuously progressing. In contrast, factors with modulatory effects on the pathway are just starting to become known and understood. Using a genetic screen in *C. elegans*, we identify a component of the GARP (Golgi Associated Retrograde Protein) complex, *vps-52*, as a novel genetic interactor of the miRNA pathway. The alteration of *vps-52* enhances seam cell defects in *alg-1* and the *mir-48* microRNA mutant animals. In addition, the loss of GARP exacerbates the lethality of a *let-7* hypomorph in a *lin-41* dependent manner and suppresses the heterochronic seam cell defects of a *hbl-1* mutant. Interestingly, we noticed that the GARP component co-fractionates with the miRISC, and underpinning the observed genetic interactions, we found that VPS-52 regulates the abundance of the GW182 protein, AIN-1 as well as the *let-7* family microRNAs miR-48 and miR-241. Altogether, we demonstrate that the GARP complex fulfills a positive modulatory role on microRNA function and postulate that acting through GARP, *vps-52* participates in a membrane-related process of the microRNA pathway.

3.3 Introduction

The miRNA pathway is a gene regulatory system that uses small non-coding RNAs to target messenger RNAs (mRNAs) for post-transcriptional regulation. In the canonical form of miRNA biogenesis, miRNA-containing transcripts are processed through sequential cleavage mediated by the Drosha and Dicer enzymes into mature miRNA species (21-23 nucleotides long) that associate with an Argonaute protein (reviewed in Krol *et al.* 2010). In its effector phase, the miRNA-loaded Argonaute, as part of the core miRNA-induced silencing complex (miRISC), regulates target mRNAs through binding sites in their 3'UTRs. The most detailed repressive effector function of this complex is mediated by its association with GW182 proteins (TNRC6A-C in mammals) (reviewed in Fabian and Sonenberg 2012). The miRISC-mediated effector phase of target regulation, may involve the repression of multiple target molecules by each single miRNA through the process of 'miRNA recycling', and this mRNA regulation affects miRNA stability (Baccarini *et al.*, 2011; Gibbings *et al.*, 2009; Gibbings and Voinnet, 2010; Ameres *et al.*, 2010; Chatterjee *et al.*, 2011). Finally, all miRISC components would be subjected to degradation, as nucleases have been proposed to degrade miRNAs (reviewed in Ruegger and Grosshans 2012), and autophagy mediates the degradation of miRNA-free Argonaute and Dicer (Gibbings *et al.*, 2012b).

In the nematode *Caenorhabditis elegans (C. elegans)*, the miRNA pathway comprises over 120 miRNAs (Warf *et al.*, 2011), two GW182 homologues (the genes *ain-1* and *ain-2*) (Ding *et al.*, 2005; Zhang *et al.*, 2007), the Argonautes genes *alg-1* and *alg-2* (both referred to as *alg-1/2*) (Grishok *et al.*, 2001) and single genes for Dicer (*dcr-1*) (Knight and Bass, 2001; Grishok *et al.*, 2001) and Drosha (*drsh-1*) (Denli *et al.*, 2004). In worms, as in other animals, the miRNA pathway is essential for development and reproduction. Animals mutant for *dcr-1* or *drsh-1* genes are sterile (Knight and Bass, 2001; Grishok *et al.*, 2001; Denli *et al.*, 2004), while at the Argonaute level, the loss of both *alg-1/2* results in embryonic arrest (Vasquez-Rifo *et al.*, 2012; Grishok *et al.*, 2001). In contrast, single mutants of *alg-1* or *alg-2* display differentially penetrant post-embryonic, somatic and germ line defects (Bukhari *et al.*, 2012). As exemplified here, the existence of these two gene paralogs, with specialized and partially redundant functions provides an opportunity to study the miRNA pathway in a sensitized genetic condition where miRNA activity is reduced albeit not completely abolished, by screening for genetic enhancers of the partial loss-of-miRNA condition.

In the present study, we identify the *vps-52* gene, which encodes a component of the GARP complex, as a genetic interactor of the miRNA-specific *alg-1* Argonaute, and establish that this complex fulfills a positive modulatory role in regulating the activity of the *let-7* family miRNAs. Based on our data, we propose that the GARP complex facilitates a transition of the miRISC occurring at endomembranes.

3.4 Results

3.4.1 The gene *vps-52* is a genetic interactor of the microRNA pathway

In order to identify new components and modulators of the miRNA pathway, we conducted a forward genetic screen for interactors of the *alg-1/2* Argonautes, based on a design that allows the recovery of gene enhancers, including synthetic lethal gene pairs. In brief, we subjected to mutagenesis worms carrying a partially inheritable extrachromosomal array containing a functional GFP-tagged *alg-2* gene expressed in the *alg-2(ok304)* mutant (referred to as *alg-2* mutant) background. F2 clones were scored and selected as candidate interactors if their progeny was uniformly transgenic (*i.e.* there was no segregation of viable worms lacking the extrachromosomal array in the population), indicative of a possible genetic interaction of an unknown mutated factor, in the transgenic setting, with the *alg-2(ok304)* background. Upon removal of the screening background (array and *alg-2* mutation), a strain with increased growth and fertility defects in *alg-1/2(RNAi)* was selected, mapped and mutations identified by whole-genome sequencing. We transgenically rescued the growth and fertility defects of the mutant strain, confirming the identity of the genetic interactor as *vps-52* (Fig. 3.2). In addition to the single allele *vps-52(qbc4)* retrieved from the screen, an available deletion allele, *vps-52(ok853)* was studied and found to display similar phenotypes (Fig. 3.1). As expected, *vps-52* behaved genetically as an enhancer, but interestingly double mutants of *vps-52* with either *alg-2* or *alg-1* were obtained as viable strains, and the loss of *vps-52* induced a visible phenotypic enhancement in combination with the loss-of-function *alg-1(gk214)* mutant (referred to as *alg-1(0)*), but not with *alg-2(ok304)* as reported below. The mutant strain initially isolated from the screen does not sustain the segregation of viable animals without the extrachromosomal array, which could be accounted for by array-mediated overexpression effects of the GFP::ALG-2 fusion protein or additional secondary background mutations; its segregation was not further investigated.

The *vps-52* gene encodes a conserved structural protein (Fig. 3.2A), that functions in the traffic of vesicles to the *trans*-Golgi network (TGN). It forms part of a conserved TGN-localized multimeric complex, known as the GARP (Golgi Associated Retrograde Protein) complex (Conibear and Stevens, 2000; Liewen *et al.*, 2005), which comprises in *C. elegans* the genes *vps-51*, *vps-52*, *vps-53* and *vps-54* (Luo *et al.*, 2011). Expressing fluorescently tagged VPS-52 from a single copy genomic insert controlled by endogenous gene regulatory elements (referred to as *Si[vps-52]*), we detected widespread VPS-52::mCherry expression in cytoplasmic puncta of many somatic tissues including the hypodermis (Fig.3.2B-C), consistent with a previous report (Luo *et al.*, 2011).

A

Genotype	Cuticular alae (%) gapped	complete	n
Wild type	0	100	59
vps-52(ok853); Si[vps-52]	0	100	60
vps-52(qbc4); Si[vps-52]	0	100	60
vps-52(qbc4)	5	95	60
vps-52(ok853)	2	98	51
vps-53(ok2864)	5	95	42
vps-53(ok2864); vps-52(qbc4)	4	96	52
alg-2(ok304)	0	100	47
vps-52(qbc4); alg-2(ok304)	0	100	45
alg-1(0)	23	77	45
vps-52(qbc4) alg-1(0)	58	42	48
vps-52(ok853) alg-1(0)	73	27	33
vps-53(ok2864); alg-1(0)	68	32	22
vps-52(ok853) alg-1(0); Si[vps-52]	40	60	60

B

Genotype	mean seam cell number	range	n
Wild type	16	16	20
vps-52(qbc4)	17.6	16-20	25
alg-1(0)	18.1	16-23	21
vps-52(qbc4) alg-1(0)	25	23-26	11

C

Figure 3.1: **Seam cell-related phenotypes of the GARP mutants. A)** Percentage of young adult worms with defective cuticular alae. Young adult hermaphrodites from synchronized populations were mounted and analyzed under Nomarski optics. The continuity of the cuticular alae was scored and categorized as gapped (one or more interruptions) or complete (no gaps present). Strains above the black line were scored at 20° C, those below that line (starting with *alg-2(ok304)*) were grown and scored at 15° C. **B)** Average and range of seam cells number at adulthood. The indicated strains were crossed with a strain expressing GFP in the seam cells (*scm::GFP*) and the number of seam cells scored in young adult hermaphrodites grown at 15° C. The mean value and range covered by the individual counts are indicated. **C)** Representative average of the seam cells at adulthood scored in B. The pictures correspond to DIC and GFP fluorescence, the number of seam cell nuclei is indicated within parentheses.

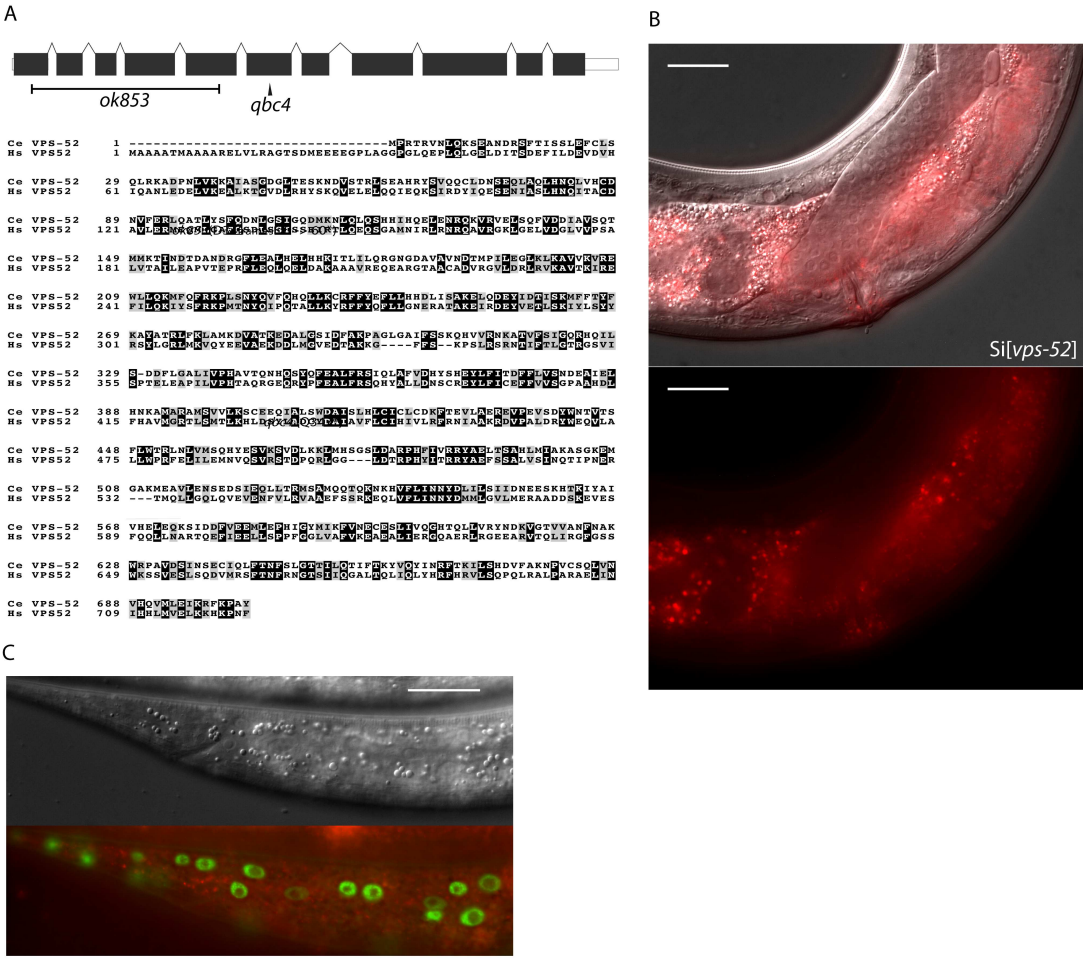

Figure 3.2: **Features and mutants of the *vps-52* gene. A)** (top) Schematic representation of the intron-exon structure of the *C. elegans vps-52* gene. The two studied alleles are indicated (the allele *qbc4* is a non-sense mutation and the allele *ok853* is a frameshift deletion). VPS-52 contains predicted coiled coils stretches, but no distinct protein domains have been identified. (bottom) *vps-52* is conserved from worms to humans. ClustalW alignment of human (*Hs*) and *C. elegans* (*Ce*) VPS-52 orthologs, the proteins share a 56 % of sequence similarity. The amino acid changes introduced by the two alleles are indicated. **B)** Expression of a single copy insertion of *Pvps-52*::*vps-52*::*mCherry*::*vps-52* 3'UTR (referred to as Si[*vps-52*]). Top panel: micrograph of merged Nomarski with mCherry fluorescence pictures. Bottom panel: micrograph of mCherry fluorescence. Scale bar measures 20 µm. The gene is widely expressed in somatic tissues starting from very early development. It localizes to the cytoplasm puntacted foci. **C)** Expression of VPS-52::mCherry in the hypodermal cells. Micrographs of Nomarski (top) and merged GFP and mCherry fluorescence (bottom). VPS-52 (in red) is expressed in the cytoplasm around the seam cells nuclei (in green, GFP tagged).

3.4.2 GARP mutants enhance the miRNA-related defects of the animals lacking the Argonaute *alg-1*

To address whether the phenotypes of *vps-52* mutants reflect an impairment of the GARP complex activity, we included in our study a strain defective for another subunit of this complex, the *vps-53(ok2864)* mutant. To analyze the function of *vps-52* and *vps-53* in the miRNA pathway, we first studied the development of seam cells. These lateral rows of hypodermal cells have a postembryonic developmental program, consisting of patterned rounds of division during each larval stage (L1 to L4), ended by terminal differentiation encompassing exit from the cell cycle, cell fusion and production of a cuticular structure (named alae) at the larva to adult transition. The seam cell developmental program is controlled at different larval stages by the miRNA lin-4 (Ambros and Horvitz, 1984) and those of the let-7 family (miR-48, miR-84, miR-241 and let-7) (Reinhart *et al.*, 2000; Abbott *et al.*, 2005) and their targets *lin-14, lin-28, hbl-1, daf-12* and *lin-41* (Lee *et al.*, 1993; Wightman *et al.*, 1993; Moss *et al.*, 1997; Reinhart *et al.*, 2000; Slack *et al.*, 2000; Abrahante *et al.*, 2003; Abbott *et al.*, 2005; Grosshans *et al.*, 2005). The repetition of the symmetrical seam cell division program that normally occurs once at the L2 stage is a frequently observed defect in mutants of core components of the miRNA pathway, such as *alg-1/2*, *dcr-1* and *ain-1/2* (Grishok *et al.*, 2001; Zhang *et al.*, 2007). Similarly to these mutants, other pathway modulators and components also display distinctive seam cell defects (Hammell *et al.*, 2009; Jannot *et al.*, 2011a). Discontinuities in the cuticular alae (*i.e.* gaps) arise from inappropriate terminal differentiation, and are an indicator of possible alterations in the development timing of seam cell division or terminal differentiation. We analyzed the *vps-52* and *vps-53* mutants and noticed mildly penetrant defects in the alae structures (Fig. 3.1A) that were not exacerbated in the *vps-52; vps-53* double mutant, demonstrating epistasis consistent with both gene belonging to a common complex.

We then proceeded to analyze the defects of the *vps-52* and *vps-53* mutants (referred to as GARP mutants) in the absence of functional *alg-1/2* Argonautes. Given that defects of the *alg-1* null mutant are milder at lower temperatures (data not shown), we conducted the following quantification of alae and seam cell counts under more permissive condition (15º C) to allow for better phenotypic enhancement. No enhancement of alae defects was observed in *vps-52(qbc4); alg-2* double mutant animals (Fig. 3.1A). However, combining either *vps-52* or *vps-53* with the *alg-1* null mutant caused a very prominent increase in alae defects, which were partially rescued by transgenic *vps-52* expression (Fig. 3.1A). The enhancement of the *alg-1(0)* alae defects was correlated with an increase in the number of seam cells. While single GARP mutants showed minor deviations from the wild-type lineage (16 seam cells at adulthood), the mean number of seam cells in *alg-1* mutant at 15º C (18 cells), reached 25 in *vps-52(qbc4) alg-1(0)* (Fig. 3.1B-C). This increase in seam cells was not observed in the L1 larval stage (data not shown), indicating that it likely results from the reiteration of the L2 stage proliferative division of the seam cells.

Genotype	Gapped (%)	Complete (%)	n
Wild type	0	100	30
rab-6.2(ok2254)	0	100	21
Wild type*; alg-1(RNAi)*	27	73	20
vps-52(qbc4); control(RNAi)	5	95	22
vps-52(qbc4); alg-1(RNAi)	41	59	20
rab-6.2(ok2254); control(RNAi)	0	100	21
rab-6.2(ok2254); alg-1(RNAi)	100	0	20

Table 3.1: **Alae defects of vesicular trafficking mutants.** L1 animals of the indicated strains were fed with bacteria expressing either control (*control(RNAi)*) or *alg-1* targeting (*alg-1(RNAi)*) dsRNA. The worms were grown at 15° C and scored under Nomarski optics for alae defects (gapped or complete) at young adult stage. The percentage of animals with complete or gapped alae is indicated (n = total number of animals).

To address whether the effects of *vps-52* mutant on the seam cell phenotype of *alg-1(0)* worms were recapitulated with other mutants of vesicle trafficking processes, we tested the effect of disrupted Golgi trafficking by impairing the action of the worm small GTPase *rab-6.2*, whose gene product physically interacts with the GARP complex (Luo *et al.*, 2011). While single mutants of the putative null *rab-6.2(ok2254)* did not display any gapped alae, the exposure of *rab-6.2(ok2254)* to *alg-1(RNAi)* caused a strong interruption in the continuity of alae (Table 3.1). Moreover, this disruption was much stronger than that obtained for *vps-52(qbc4)* assayed under the same experimental conditions (Table 3.1). We conclude that the loss of *vps-52* or *vps-53* function does not prominently affect seam cell development, but effectively synergizes in the absence of ALG-1 to induce the reiteration of the L2 stage seam cell division program. Our observations of similar synergy for the mutant of *rab-6.2* suggest therefore, some specificity between Golgi-associated functions and miRNA-controlled development of the seam cells.

3.4.3 GARP mutants enhance the defects of the let-7 miRNA family in a target-dependent manner

The let-7 family members miR-48, miR-84 and miR-241 redundantly regulate the expression of their target gene *hbl-1* at the L2 to L3 larval stage transition (Abrahante *et al.*, 2003; Abbott *et al.*, 2005). Abolishing completely the function of these three miRNAs causes seam cells to reiterate their L2 developmental program (Abbott *et al.*, 2005). Loss of singleton or pairs of these genes leads to seam cell defects of varied penetrance, thereby constituting useful sensitized genetic backgrounds where the action of pathway modulators can be unveiled, as previously exemplified for the *nhl-2* modulator (Hammell *et al.*, 2009). It was therefore possible that the altered seam cell development observed in *alg-1* mutant and enhanced by loss of *vps-52* resulted from impaired miR-48, miR-84 and miR-241 miRNAs function. Consequently, we evaluated whether GARP mutants would alter seam cell development in the absence of

Genotype	Early L4 alae synthesis (%)			Adult alae (%)			
	no alae	alae	n	no alae	gapped	complete	n
Wild type	100	0	20	0	0	100	20
vps-52(qbc4)	100	0	20	0	5	95	60
mir-48(n4097)	-	-	-	0	0	100	20
vps-52(qbc4); mir-48(n4097)	-	-	-	4	22	74	23
hbl-1(ve18)	10	90	20	-	-	-	-
hbl-1(ve18) vps-52(qbc4)	45	55	20	-	-	-	-

Table 3.2: **Alae defects for the *vps-52, hbl-1* and *mir-48* mutant animals.** The indicated strains were grown at 20° C and scored under Nomarski optics for alae synthesis and defects (gapped, complete or absent) at early L4 and young adult stages. The percentage of animals with complete, absent or gapped alae is indicated (n = total number of animals).

miR-48, with the *mir-48(n4097)* mutant allele (referred to as *mir-48(0)*). Although loss of this miRNA did not induce seam cells defects on its own, concomitant loss of *vps-52* did lead to increased alae defects (Table 3.2). We next investigated the genetic interaction of *vps-52* with *hbl-1*, a main target of the *let-7* miRNA family. Reduced *hbl-1* function results in the precocious terminal differentiation of the seam cells at the third larval molt evidenced by the production of alae (Abrahante *et al.*, 2003; Hammell *et al.*, 2009). The combination of the reduced-function allele, *hbl-1(ve18)*, with a *vps-52* mutant resulted in the partial suppression of the *hbl-1(ve18)* precocious phenotype (Table 3.2 and Fig. 3.3). Similarly, suppression of this *hbl-1* mutant phenotype has been reported upon concomitant loss of the let-7 miRNA family (Hammell *et al.*, 2009). Altogether, the loss of *vps-52* diminishes the activity of let-7 family miRNAs. This negative effect likely underpins the enhanced defects in the L2 stage developmental program of the seam cells.

We next extended our analysis to the let-7 miRNA, which regulates developmental programs at the L4 to adult transition. The complete loss of the *let-7* miRNA gene produces a highly penetrant phenotype of bursting through the vulva (Reinhart *et al.*, 2000) that is classically used in phenotypic assessments of miRNA functions (*e.g.* Parry *et al.* 2007). In this respect, we did not observe any bursting phenotype in the GARP mutants (Table 3.3). In addition, the bursting of the GARP mutant in combination with *alg-1(0)* was not overtly different from that of single *alg-1* mutant (data not shown). We then investigated if there was any effect on sensitized *let-7* genetic backgrounds. We used, to that aim, the hypomorphic *let-7* mutation, the*n2853* allele, that carries a point mutation in the miRNA seed region, which leads to a reduction of mature let-7 miRNA level (23, 33) and to temperature-sensitive reduction in the activity of this miRNA (23). Remarkably, the GARP mutants strongly enhanced the *let-7(n2853)* bursting phenotype at permissive temperature (Table 3.3). The let-7 miRNA represses expression of *lin-41*, one of its major target genes; reduced *lin-41* function suppresses the bursting phenotype of *let-7* mutants (Reinhart *et al.*, 2000; Slack *et al.*, 2000; Vella *et al.*,

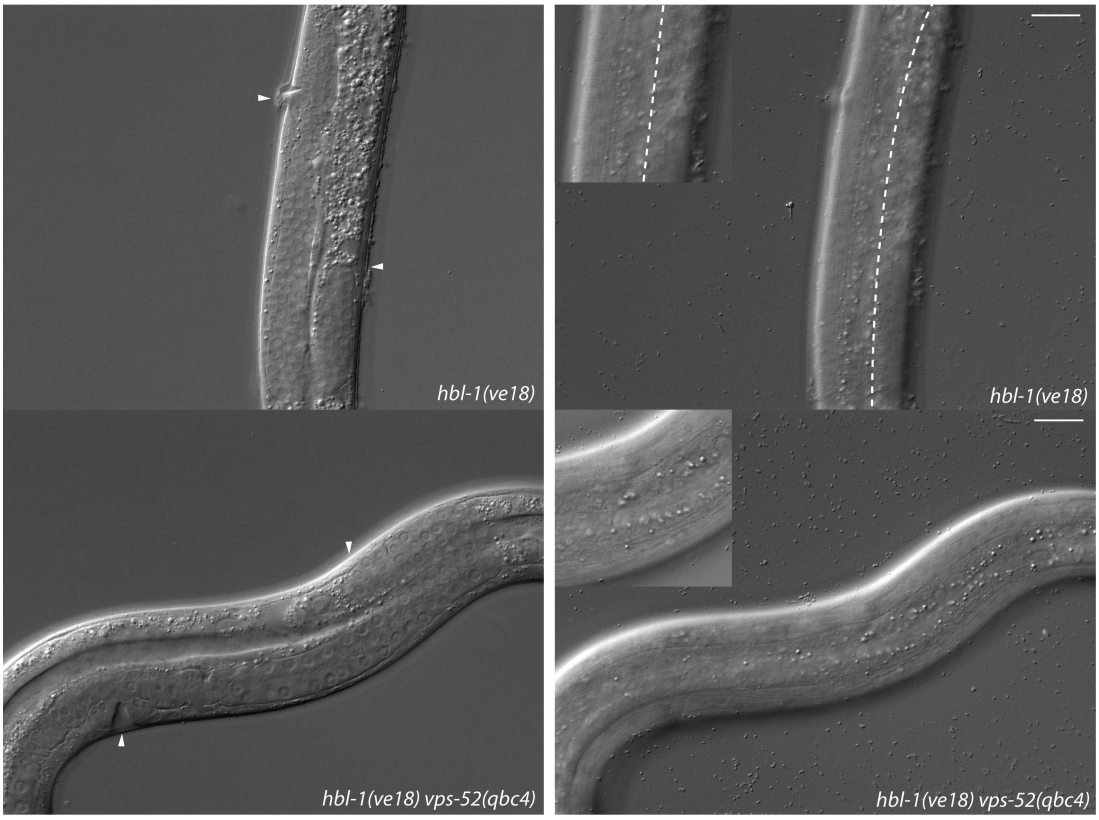

Figure 3.3: **Analysis of precocious alae synthesis.** Representative Nomarski micrographs of *hbl-1(ve18)* and suppressed *hbl-1(ve18) vps-52(qbc4)* worms at the early L4 stage. Left panel: The early L4 vulva and gonad developmental stages (arrowheads) are indicated. The vulva lineage is abnormal in *hbl-1(ve18)* mutants (24). Right panel: The corresponding worm cuticules are shown (enlarged in the insets). Precocious alae of *hbl-1(ve18)* are indicated by the dotted lines.

2004). We therefore decided to verify whether the *lin-41* impairment could suppress the penetrant bursting of the double *vps-52(qbc4) let-7(n2853)* mutant. The combination of the *lin-41(ma104)* hypomorph with *vps-52(qbc4) let-7(n2853)* resulted in a viable triple mutant and the complete loss of bursting (Table 3.3). Thus, the effect of *vps-52* on the sensitized *let-7* background is dependent on its target.

Our phenotypic analysis indicates that *vps-52* and *vps-53* mutants display weakly penetrant miRNA-related defects, but synergize with the *alg-1* and *mir-48* null mutants in enhancing seam cell developmental defects as well as enhancing the bursting phenotype of the *let-7(n2853)* allele, in a miRNA target-dependent manner. In addition, the *vps-52* mutant partially suppresses an heterochronic *hbl-1(ve18)* phenotype, suggestive of a reduced inhibitory action of let-7 family miRNAs on its targeted gene. These collective results, obtained in the context of multiple miRNA-dependent phenotypes in sensitized genetic backgrounds, suggest a positive role for the GARP complex in worm miRNA function.

Genotype	Lethality (% of bursters)	n	Temp
Wild type	0	60	20° C
alg-1(0)	3	60	"
vps-53(ok2864)	0	60	"
vps-52(qbc4)	0	60	"
let-7(n2853)	29	42	15° C
let-7(n2853); vps-53(ok2864)	75	20	"
let-7(n2853); vps-52(qbc4)	100	20	"
let-7(n2853); vps-52(qbc4); lin-41(ma104)	0	31	"
let-7(n2853); control(RNAi)	21	47	"
let-7(n2853); alg-1(RNAi)	82	33	"

Table 3.3: **Lethal vulva bursting phenotype observed in different mutant backgrounds.** The indicated strains (grown at 15° C or 20° C, as indicated) were scored for bursting through the vulva at the developmental transition to the adult stage. The percentage of bursted animals is shown (n = total number of animals). The value for *let-7(n2853) vps-52(qbc4)* was determined from individually genotyped progeny of *let-7(n2853) vps-52(qbc4)/+* mothers. The same procedure was used for *let-7(n2853); vps-53(ok2864)* mutant. Animals were fed bacteria expressing either control (*control(RNAi)*) or *alg-1* targeting (*alg-1(RNAi)*) dsRNA, as indicated.

3.4.4 GARP subunit co-fractionates with miRISC components and its loss reduces the abundance of GW182 and miR-48/miR-241

In order to gain insights into the steps at which *vps-52* regulate miRNA activity, we investigated the physical association of VPS-52 with components of the microRNA pathway in *C. elegans*. Using immunoprecipitation, we did not observe physical interaction between VPS-52 and the miRISC components AIN-1 or ALG-1 (data not shown). Nonetheless, considering that in human cultured cells components of the miRNA pathway, TNRC6 and AGO2, associate with endomembranes, particularly with multi-vesicular bodies (MVB) (Gibbings *et al.*, 2009, 2012a), we decided to further test whether GARP components associate with miRISC taking advantage of this cellular system. Firstly, we explored the functional role of VPS52 in human cells. The VPS52 siRNA knockdown had no effect on a reporter of miRNA activity, under the control of endogenous let-7a (Fig. 3.4A). Thus, as observed in *C. elegans*, impairment of VPS52 function alone does not overtly affect miRNA activity in human cells. We then tested a condition analogous to the sensitized background used with worms; concomitant knockdown of VPS52 and TNRC6A impeded the miRNA activity beyond levels achieved by knocking down TNRC6A alone (Fig. 3.4A), supporting that VPS52 may regulate miRNA activity in sensitized conditions. We then proceeded with a subcellular gradient fractionation analysis. Consistent with previous reports (Gibbings *et al.*, 2009, 2012a), AGO2 and TNRC6 partitioned with an MVB marker (PrP^c) (Fig. 3.4B). Remarkably, VPS52 fractionated in pattern that partially overlapped with the miRISC components in MVBs (fraction 11; Fig. 3.4B). Altogether, these

results suggest a close, possibly functional, association of VPS52 with miRISC components at endomembranes.

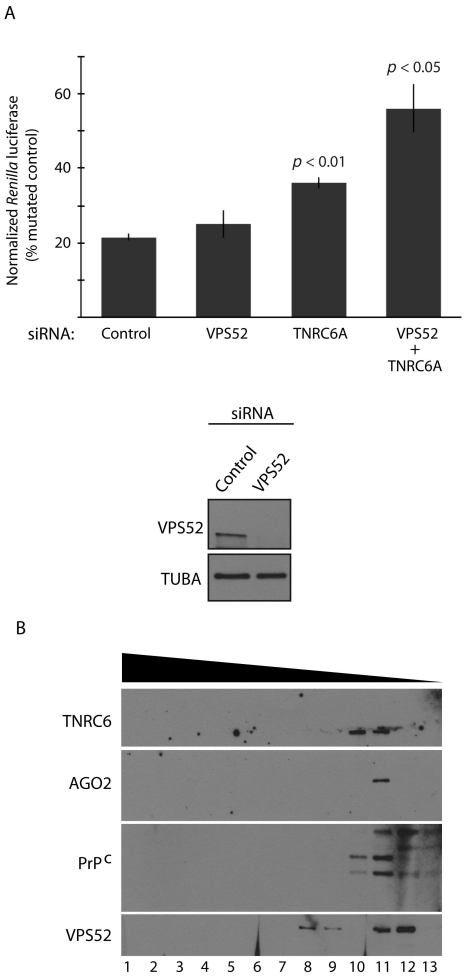

Figure 3.4: **Fractionation of VPS52 with the miRISC components in human cells. A)** (Top) Dual luciferase assays reporting the activity of endogenous let-7a miRNA in HeLa cells treated with control siRNA (10 nM), VPS52 (5 nM + 5 nM control siRNA), TNRC6A (5 nM + 5 nM control siRNA), or TNRC6A + VPS52 (5 nM + 5 nM respectively). Represented values from three independent experiments correspond to the remaining mRNA translation after miRNA repression and are calculated as follows for the let-7a reporter: (Renilla luciferase / Firefly luciferase) of miRNA-targeted reporter / (Renilla luciferase / Firefly luciferase) of control reporter with mutated let-7a miRNA sites. The error bars represent the standard error of the mean (SEM) and significance was analyzed with a Student t-test. (Bottom) Western blot analysis of HeLa cells treated with control siRNA or siRNA targeting VPS52. Similar results were obtained with a second independent siRNA (data not shown). Alpha-tubulin (TUBA) serves as a loading control. **B)** Continuous density gradient analysis (iodixanol, 5-25%) of HeLa cells. The fraction numbers (from heavier to lighter) are indicated.

To gather further insights on how the miRNA pathway is affected by the impairment of the GARP complex, we investigated if the GARP mutations affected the abundance of key miRNA pathway proteins in *C. elegans*. While we did not detect any effect on the DCR-1 or ALG-1/2 protein levels in all genetic combination of the GARP mutants tested (Fig. 3.5A), the abundance of the GW182 AIN-1 protein was reduced in both *vps-52* and *vps-52 alg-1* mutants (Fig. 3.6A) and this without affecting the expression at the mRNA level of the *ain-1* gene (Fig. 3.5B). These results support that the GARP complex may regulate the abundance of the GW182 AIN-1 protein.

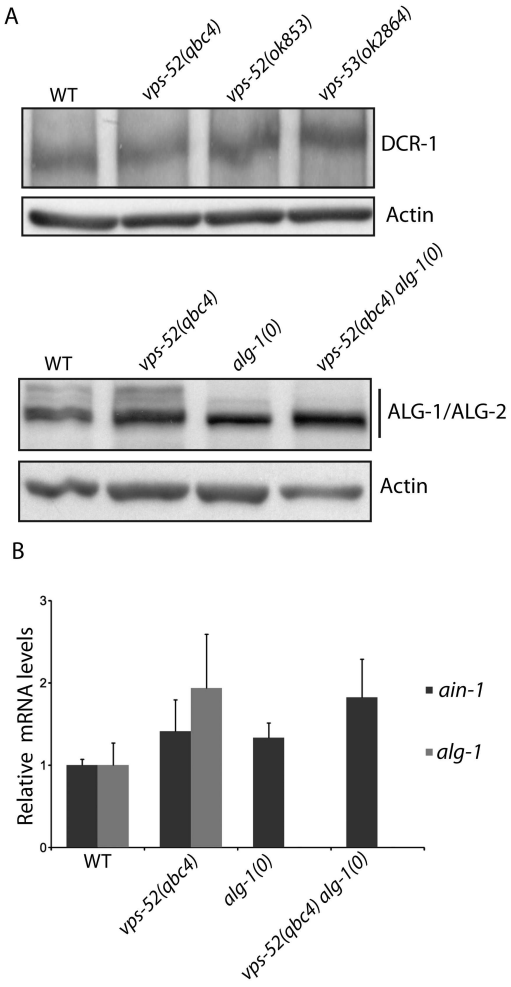

Figure 3.5: **Effect of the loss of *vps-52* on the level of components of the miRNA pathway. A)** Abundance of the DCR-1 and ALG-1/2 proteins, determined by western blotting of adult worm samples. Actin level was used as loading control. **B)** The *alg-1* and *ain-1* mRNA levels were measured by real-time quantitative PCR in adult animals and compared with the level found in wild type worms (WT: 1). The *tba-1* mRNA was used as control RNA. The error bars represent SD of three independent experiments. No statistical difference was found (Student *t*-test).

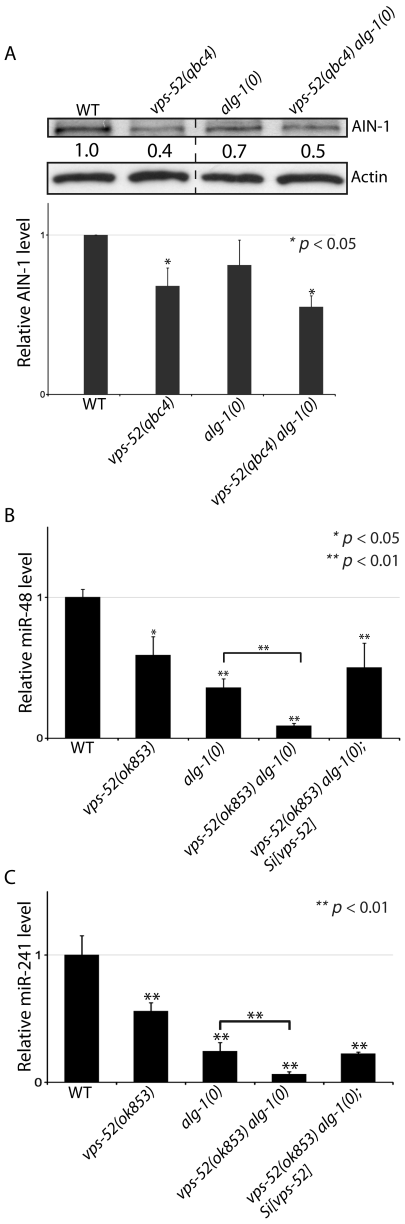

Figure 3.6: **Effect of *vps-52* on miRISC components. A)** Abundance of the AIN-1 protein. (top) Western blot of synchronized adult worms samples. Actin served as loading control. (bottom) Quantification of the AIN-1 signal compared with the level found in wild type worms (WT: 1). The error bars represent standard deviation (SD) from three independent experiments. p values were obtained using a two-sided Student's test. **B-C)** The abundance of the miR-48 and miR-241 miRNA was measured by quantitative real-time PCR (TaqMan assay) in mid-L3 synchronized mutant animals and compared with the level found in wild type worms (WT: 1). The small nucleolar RNAs sn2841 was used as the normalization control. The error bars represent the standard deviation of three independent experiments and p values were obtained using a two-sided Student t-test.

Next, we determined the effects of the alteration of *vps-52* on miRNA levels. While in the single *vps-52* mutant, we observed a significant decrease of the let-7 family miRNA members miR-48 and miR-241, their levels were further reduced in *vps-52 alg-1(0)* double mutant (Fig. 3.6B-C). Moreover, this reduced miR-48 and miR-241 abundance was rescued to the levels found in the single *alg-1(0)* mutant upon expression of a *vps-52* transgene (Fig. 3.6B-C). The level of primary and precursors miRNA molecules remained intact (Fig. 3.7), supporting that the decreased miRNA abundance is not due to diminished transcription or biogenesis of these miRNA. We conclude that the GARP-mediated increase of *alg-1(0)* defects is likely underpinned by the reduced AIN-1 and miR-48 and miR-241 abundance, resulting in the misregulated L2 proliferative seam cell division controlled by the let-7 family of miRNAs.

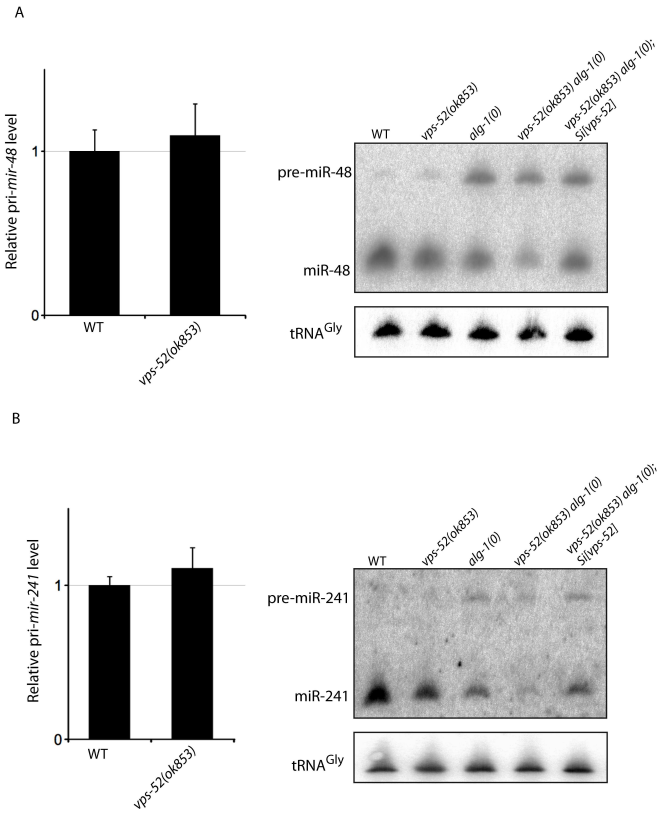

Figure 3.7: **Detection of the primary and precursor miRNA forms of let-7 family miRNAs.** The precursor and primary forms of miR-241 **(A)** and miR-48 **(B)** were investigated by Northern blot (tRNA Gly was used as loading control) and real-time quantitative PCR in mid-L3 synchronized animals. The levels of the primary forms were compared with that found in wild type worms (WT: 1). The *tba-1* mRNA was used as control RNA. The error bars represent standard deviation of three independent experiments.

3.5 Discussion

Employing a genetic screen for *alg-1/2* Argonaute interactors, we have identified the gene *vps-52*, encoding a component of the GARP complex, as a genetic enhancer of miRNA pathway activity in *C. elegans*. The *vps-52* mutants displayed weakly penetrant miRNA defects at the seam cells, and correspondingly mild molecular alterations of the pathway. However, upon *vps-52* loss, a positive role was uncovered by the genetic interactions observed in sensitized backgrounds for Argonautes, miRNAs and their targets. The phenotypes we observed for *vps-52*, postulate it as a modulator of miRNA activity rather than a core pathway component.

Throughout our analysis similar phenotypes were encountered for the mutants of *vps-52* and *vps-53*. Given that this two genes encode components of the GARP complex, it is likely that the regulation of miRNA activity conferred by theses genes corresponds to the impairment of a GARP complex function, rather than other putative additional role(s) of these genes. The GARP complex is involved in the tethering of endosome-derived vesicles reaching the TGN, in a recycling pathway known as 'retrograde transport' (reviewed in Bonifacino and Hierro 2011). This pathway allows the recycling of proteins such as the cation-independent mannose 6-phosphate receptors in mammalian cells, and its impairment in both mammals and yeast leads to protein missorting (Conibear and Stevens, 2000; Perez-Victoria *et al.*, 2008). In addition, absence of GARP function can also secondarily impinge on the endo-lysosomal system (Siniossoglou and Pelham, 2002; Luo *et al.*, 2011; Perez-Victoria *et al.*, 2010). Consequently, we hypothesize that the mechanism underlying the observed regulation of miRNA activity is related to the known function of the GARP complex in tethering endosome-derived vesicles at the TGN and the consequences of it. Noteworthy, a different sensitized *let-7* background was previously employed in a genome-wide screen for regulators of the miRNA pathway (Parry *et al.*, 2007). Among the top hits identified were components of the COG (Conserved Oligomeric Golgi) complex, a vesicle-tethering complex, exemplifying again the link between Golgi trafficking functions and miRNA activity.

Numerous studies have reported on several endomembrane-related aspects of the miRNA pathway in diverse organisms: 1) The presence of Argonaute at the Golgi of certain cultured cells (Cikaluk *et al.*, 1999; Tahbaz *et al.*, 2001); 2) The co-fractionation of pathway components with MVBs and the negative effects of disrupting components of this compartment (Gibbings *et al.*, 2009); 3) The miRNA regulatory effects of the BLOC-3 complex (Lee *et al.*, 2009); 4) those of disrupting the isoprenoid producing enzymes of the mevalonate pathway (Shi and Ruvkun, 2012; Brodersen *et al.*, 2012); and 5) The selective degradation of miRNA-free Dicer and Argonaute through autophagy (Gibbings *et al.*, 2012b). Although all these findings may be underpinned by different mechanisms, they highlight the importance of membrane-regulated aspects on the function of the miRNA pathway.

An interesting possibility regarding the membrane association of the miRNA pathway is that it

relates to the sorting and secretion of miRNAs in MVB-derived exosomes. Indeed, circulating miRNAs have been detected in diverse body fluids and, tentatively proposed to be involved in some form of intercellular communication (reviewed in Chen *et al.* 2012b). Similarly, if miRNA secretion were eventually used to alter gene expression in other cells, it should be expected to alter the cell autonomy of miRNA action to certain extent. In *C. elegans* this aspect has been only studied for *lin-4* in the seam cells, where this miRNA functions cell autonomously (Zhang and Fire, 2010). Nonetheless, the sorting of the miRNA and pathway components in exosomes, their putative secretion as well as their role in intercellular communication in *C. elegans* and other organisms are research topics that require further exploration.

An alternative and non-mutually exclusive possibility with that of miRNA secretion, is that the membrane association of the miRNA pathway could be part of a process that facilitates certain transitions occuring during the course of miRNA action (Gibbings and Voinnet, 2010). This process being facilitating rather than necessarily required, its absence would only impair, but not completely abolish, miRNA-mediated gene regulation. Based on this idea, an interpretative model of our findings is proposed (Fig. 3.8). In this model, the miRISC would be associated with membranes of MVBs to facilitate its transition possibly including, the recycling of miRISC components, its assembly or disassembly. In this context, impairing the GARP function in retrieving endosomal vesicles carrying miRISC components or other factors required for proper miRISC activity would have two foreseeable consequences: i) missorting of miRISC components, such as the GW182 proteins and; ii) a 'block' of the miRISC at membranes. As a result, the affected complexes would be disallowed from engaging in further repression of target mRNAs, and also from participating in the accumulation of new miRNAs (Fig. 3.8). Although a role for GW182 in regulating miRNA stability has been recently proposed in mammalian cells (Yao *et al.*, 2012), other reports indicated that the abundance of miRNAs is not affected by the absence of the GW182 proteins (Zhang *et al.*, 2007; Jiang *et al.*, 2012), suggesting that miRNA abundance and GW182 accumulation can be uncoupled.

In addition to the processes of miRNA biogenesis and core effector functions, the understanding of subsequent phase(s) of the microRNA pathway will likely unveil the existence of new components that facilitate miRNA activity and regulate its recycling and turnover. The present trends of discoveries suggest that these facets may be, at least in part, dependent on processes occurring at the interface of endomembranes. Future studies will be required to establish whether or not the GARP regulation of miRNA activity does generally apply for all or to a restricted set of miRNAs. In order to do so, additional genetic backgrounds sensitized for miRNA function and their correspondent activity readouts will be needed. Similarly, further research will be helpful to better understand the mechanisms by which membrane-based processes regulate the activity of miRNAs.

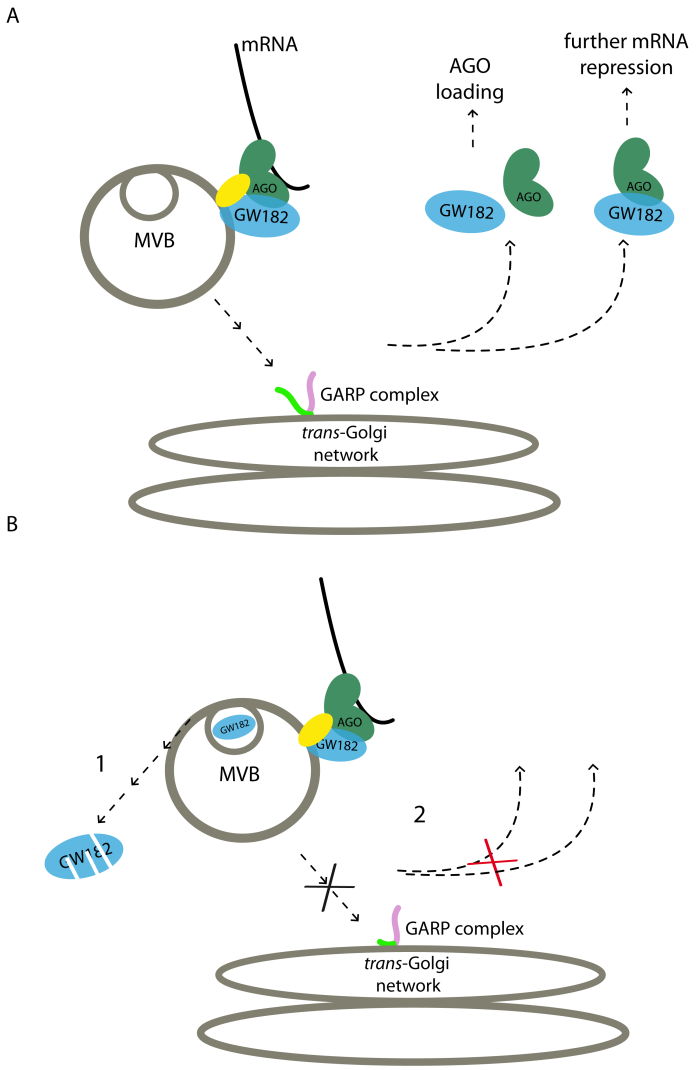

Figure 3.8: **Interpretative model of GARP-mediated effects on miRNA activity. A)** A pool of the miRISC associates with Multivesicular body (MVB) membranes, in a process that facilitates a transition of complex function (such as assembly, diassembly or recycling). Vesicles carrying unknown components important for miRISC function(s) are transported back from the MVBs to the *trans*-Golgi network by the GARP complex. **B)** Impairing the function of GARP leads to: 1) missorting of pathway components (such as GW182) with consequent mislocalization and degradation. 2) 'block' of miRISC residing at MVB disallowing its participation in further mRNA repression and miRNA loading (red crosses).

3.6 Materials and Methods

Culture conditions and general methods

Worms were cultured in standard conditions (Brenner, 1974). All experiments were performed at 20°C unless otherwise noted. The strains used in the present study were outcrossed four

times before analysis. The RNAi by feeding was performed on nematode growth media (NGM) plates containing 1mM IPTG (Isopropyl b-D-1-thiogalactopyranoside) after overnight induction (25º C) of the bacterial culture. The *alg-1/2*(RNAi) was performed as described in (Grishok *et al.*, 2001). The *alg-1*(RNAi) was performed with a construct targeting the *alg-1*-specific N-terminal gene region (Jannot *et al.*, 2011a).

Genetic screen and mutant identification

The genetic screen followed a design to isolate enhancers of the queried gene (including synthetic lethal interactors) previously used in *C. elegans* (Fay *et al.*, 2002). EMS (ethyl methane sulfonate) was used to mutagenize *alg-2(ok304)* worms carrying an extrachromosomal array containing *alg-2::GFP* copies (strain MJS11). From a pool of 1,000 mutagenized fluorescent F1, F2 clones where the non-integrated array becomes necessary for worm survival, evidenced by a homogeneous population of GFP expressing animals were kept and further investigated. Next, single mutant strains (with neither transgenic array nor *alg-2(ok304)*) were obtained and tested as follows. Upon outcrossing with wild type N2 males, a random set of F2 worms (chosen to be GFP negative, without the *alg-2(ok304)* deletion), was fed with *alg-1/2(RNAi)* and mendelian segregation of a discernible phenotype in the RNAi condition was assessed. One single mutant strain displaying increased defects upon *alg-1/2*(RNAi) with the expected segregation frequency was selected for further characterization. Using *alg-1/2(RNAi)* the mutant locus was SNP mapped to the X chromosome in the genetic interval (-2.9, -0.76 cM). Mutations inside the interval were unveiled by whole genome sequencing (in collaboration with Dr Don Moerman from the British Columbia Cancer Agency). Only a single nonsense mutation inside the interval (in the F08C6.3 gene) was found. A transgenic strain carrying the wild-type *vps-52* gene (named *qbcSi01*), rescued all the visible defects of the mutant strain. To note, the obtained *vps-52(qbc4)* mutant is sensitive to both germline and somatic RNAi (data not shown).

Plasmids

The Mos transposase plasmid (pJL44) and the co-injection markers, pGH8, pCFJ90, pCFJ104 were used following the MosSCI method (Frokjaer-Jensen *et al.*, 2008). To generate the *vps-52* rescue plasmid MSp166 (*Pvps-52::vps-52::mCherry::vps-52 3'UTR*, two genomic regions comprising the whole *vps-52* gene were amplified, introducing a NotI site adjacent to the stop codon and terminal restriction digestion sites (AvrII and BsiWI). Upon NotI ligation, the resulting gene fragment was introduced into double digested (AvrII, BsiWI) pCFJ151 plasmid and verified by sequencing. Using the introduced C-terminal NotI site, a mCherry NotI cassette was ligated to produce MSp166. The oligonucleotides used for plasmid construction are listed below.

Transgenic strains

A single copy transgenic line containing the promoter, coding sequence and both 5' and 3' untranslated regions of the *vps-52* gene was obtained as follows. Mutant *unc-119(ed9)* worms (strain EG4322) were injected with a mix of the MSp166 plasmid, Mos transposase and marker plasmids following the MosSCI method (Frokjaer-Jensen *et al.*, 2008). The obtained transgenic lines were processed according to the heat-shock protocol of the method. The integrity of the single copy insert was tested by PCR and sequencing. The obtained line (carrying the *qbcSi01* transgene) was then used for crosses.

Western blotting

Synchronized worm populations of the desired stage were disrupted and dissolved in Laemmli buffer. Protein bands in the immunoblots were visualized using the western lighting plus ECL kit (Perkin-Elmer). Antibodies were used at the following dilutions. Actin-HRP (1:10,000) was used as loading control. Rabbit anti-ALG-1 (1:5,000), rat anti-AIN-1 (1:10,000) (Zhang *et al.*, 2007), rabbit anti-DCR-1 (1:2,000) (Duchaine *et al.*, 2006), rabbit anti-ALG-1/2 (1:1,000) (Wu *et al.*, 2010). HeLa cells were lysed in 1% (V/V) NP-40, 10% (V/V) glycerol in PBS containing a cocktail of protease inhibitors (Roche Complete EDTA-free) for 30 minutes. Lysate was centrifuged 5 min (1,000 g) and supernatant was analyzed by western blot with the following antibodies: TNRC6 (serum 18033, a kind gift of M. Fritzler), AGO2 (clone 11A9, Sigma-Aldrich), VPS52 (Abcam), PrP^{C} (monoclonal clone SAF37, gift from P. Leblanc) and Tubulin (clone DM1A, Sigma-Aldrich), as previously described (Gibbings *et al.*, 2012b).

Northern blotting

Total RNA was separated by gel electrophoresis, transferred into a Genescreen plus membrane (Perkin-Elmer) and crosslinked using 1-ethyl-3-(3-dimethylaminopropyl) carbodiimide hydrochloride (EDC) (Sigma). DNA probes radiolabeled with the Starfire system (IDT) were hybridized to the membrane. After washing, the membrane was exposed to an image plate and scanned with the FLA-5100 phosphoimager. Image quantification was done using the ImageGauge 4.1 (Fujifilm) software. The oligonucleotide probes are listed below.

Real-time quantitative PCR

Total RNA from synchronized worm populations was prepared using Tri-Reagent (Sigma-Aldrich). Reverse transcription was performed with the high capacity cDNA reverse transcription kit (Life technologies). A 7900HT PCR system was used for quantitative real-time PCR. SYBR Green I (Invitrogen) was used to monitor pri-miRNA and mRNA levels. TaqMan small RNA assays (Life technologies) were used to measure microRNA levels (miR-48, miR-241 and let-7) following the manufacturer protocol. The *sn2841* (small nucleolar RNA) Taqman assay was used as control. The oligonucleotides used for qPCR are listed below.

Experiments with Mammalian Cells

Cells were treated with 10 nM of siRNA targeting VPS52 (Ambion Silencer Select) or a control siRNA (Ambion Silencer Select) delivered with Lipofectamine RNAiMax (Life Technologies). VPS52 siRNA (Silencer Select s12449: 5'- CGTAGCAGTCAGCTAGATAAG -3'). Continuous iodixanol (Optiprep^{TM}, 5-25%) density gradients were performed as previously described (Gibbings *et al.*, 2009) 48 h after siRNA-mediated knockdown of VPS52. Dual luciferase reporters were used as previously described 48 h after treatment of HeLa cells with siRNA (Gibbings *et al.*, 2012b).

Acknowledgements

We are grateful to Dr D Moerman from the British Columbia Cancer Agency for his help with the analysis of high-throughput sequencing data of the *vps-52(qbc4)* mutant allele; Drs T Duchaine, M Han, P Leblanc and M Fritzler for reagents. We would like to thank members of our laboratories for comments on the manuscript and for their help doing the genetic screen. Some nematode strains were provided by the *Caenorhabditis* Genetics Center, which is funded by the NIH National Center for Research Resources (NCRR). GDB is a Natural Sciences and Engineering Research Council of Canada Graham-Bell Scholar. The work has been funded by the Canadian Institutes of Health Research (CIHR) (MJS) and by a core grant from ETH-Z to OV. MJS is a Junior 2 scholar from Fonds de Recherche du Québec-Santé.

Chapter 4

Concluding remarks and perspectives

4.1 Developmental aspects of *alg-1* and *alg-2*

I provide in the first section of this chapter some remarks of the investigation presented in the chapter 2. Prior to this study the information regarding several biological aspects of *alg-1* and *alg-2* was absent, both genes were known to associate with the miRNA pathway and to display an uncharacterized embryonic lethal phenotype evidenced by gene knockdown using RNAi (Grishok *et al.*, 2001). Our characterization of these genes provides insights into the essential developmental process controlled by the miRNA-specific Argonautes, and also on other shared and unique features, evidenced by their spatio-temporal expression pattern and their association to miRNAs.

4.1.1 Expression patterns and associated miRNAs

Spatio-temporal features of protein expression are biological variables of importance to understand its function. A protein can be expressed in a temporally regulated manner, in widespread or restricted spatial manner, and these features may explain specificity of its action. In the present study, we addressed the expression pattern of the ALG-1 and ALG-2 proteins and found that their localization is not identical but overlaps in many tissues. These expression patterns were mainly obtained using transgenic lines. The strains used to address these spatio-temporal profiles were obtained by a traditional worm transgenic procedure (Mello *et al.*, 1991). In this method, upon injection of a plasmid mix into the hermaphrodite gonads, an extrachromosomal DNA array with multiple copies of the inserted plasmids is formed. The resulting plasmid array is then integrated randomly in the chromosomal DNA using UV irradiation. The transgenic animals obtained with this procedure, commonly overexpressed the inserted transgenes, *i.e.* the fusion of fluorescent proteins to the Argonautes. A caveat of this

method is that very regularly the obtained transgenic lines are subjected to germ-line silencing. Indeed, this limited our study to report ALG-1/ALG-2 expression only in somatic tissues, and future studies will be needed to report the Argonaute expression in germ cells. Also, fluorescent patterns observed with transgenic lines must be verified, via multiple independent integration lines and preferentially with immunostaining of the endogenous protein. In our case, the reported expression patterns were identical among multiple integrated lines, were not affected by switching the RFP and GFP tags between *alg-1* and *alg-2* (data not shown), and were consistent with immunostaining of the worm head tissues using an anti-ALG-1 antibody (Fig. 2.2). Furthermore, similar expression was observed with an available transcriptional reporter, a fusion of GFP to the promoter of *alg-1* (the strain BC12895, data not shown). Finally, a good overlap between our expression data and previously published ALG-1 expression profile was found (Chan and Slack, 2009). Altogether, these data strenghten the presented expression pattern of ALG-1 and ALG-2.

Different transcription factors likely contribute to explain the observed Argonaute expression domains. In addition to the transcription factor PHA-4, a recent study has reported binding sites for the transcription factor DAF-12 upstream of the *alg-2* promoter and other miRNA pathway components such as *ain-1* and *nhl-2* (Hochbaum *et al.*, 2011). It is also possible that not yet identified factors regulate the non-coding sequences of *alg-1* and *alg-2* mRNAs to influence their expression. Transcriptional factors contribute to establish transcript abundance, and consequently they can influence differences in protein levels, that can strongly contribute to differentiate the function of related genes. Consistent with the temporal expression profile, ALG-2 is likely highly abundant in early embryos. However in later stages we do not noticed a drastic difference in the overall abundance of ALG-1/2 using an antibody recognizing both proteins (data not shown). Thus, we do not support that distinct overall protein levels are determinant to explain the differences between the ALG-1 and ALG-2 Argonautes.

In order to investigate the association of ALG-1 and ALG-2 with miRNAs, we immunoprecipitated endogenous ALG-1 and GFP:ALG-2 [1] and isolated the associated miRNAs. To determine the association of miRNAs to Argonautes, we relied on custom miRNA microarrays. The majority of miRNAs associated with both ALG-1 and ALG-2, but some displayed a preferential association to a specific Argonaute (Figure 2.9). This preferential association can be due to the specific expression patterns of both miRNA and Argonaute. However, the specific association of either ALG-1 or ALG-2 to some miRNA cannot be ruled out. In plants, different Argonautes can selectively bind miRNAs according to the identity of the 5' terminal nucleotide. Further research would be necessary to explore the molecular basis of the differences in relative miRNA association to ALG-1/2.

1. Presently, there is no antibody specific for only ALG-2

4.1.2 Embryonic roles of ALG-1 and ALG-2

In order to study the role of both argonaute genes during development, I constructed the balanced strain MJS25: (*alg-2(ok304)*; *alg-1(gk214)* / *unc-84(e1410)*). This strain allowed easy maintenance and segregated the double mutant *alg-1(gk214); alg-2(ok304)* embryos that we analyzed. The terminal phenotypes of the double mutant embryos showed a majority arrested at the morphogenetic stage of development, in particular at the 2-fold stage (Figure 2.10). The microscopic recordings, done by mounting pairs of embryos in a small inverted chamber, allowed us to follow their embryonic development and establish that there is no overt timing delay between the double mutants and its viable siblings (Figure 2.11). The double mutant embryos remained mostly arrested, unable to elongate but displaying muscular twitching for some time before passing away. This indicated that disregulated development in the absence of *alg-1/2* is likely due to a disrupted morphogenetic process.

The microscopic examination of the above mentioned strain, carrying a GFP marker of apical junctions (ajm::GFP), revealed that the epithelial cells were mostly unaffected and achieved the intercalation and enclosure processes (data not shown). These observations were verified by the immunostaining of muscle and hemidesmosomes (Fig. 2.12). The interruptions in the attachment structures between the muscle and the epidermis, the fibrous organelles (FOs), are likely causative of the failure to elongate, because FO defects impair the mechanical coupling between these two tissues that is necessary for elongation. It should be noted that our analysis does not allow us to differentiate if the FO defect is due to problems in the epidermis or the muscle or both tissues. Muscular activity induces FO remodelling (see Appendix A), therefore problems in the muscular tissue can be reflected in the FOs. Alternatively, a process mediated by the Argonautes ALG-1/2 is important for the proper function of the FOs in the epidermis itself. Rescue experiments with tissue-specific Argonaute expression is a possible experimental alternative to distinguish between these possibilities.

It is interesting to remark that miRNAs have established roles in the development and function of muscular tissues. Zebrafish embryos lacking Dicer have defective sarcomeres (Mishima *et al.*, 2009), tissue specific knockdown of Dicer and Pasha affects heart development (reviewed in Boettger and Braun 2012), and multiple miRNAs have been found to promote the differentiation of the muscular cell type (reviewed in Guller and Russell 2010).

The phenotypes resulting from the loss of different miRNA components is varied (see section 1.4.2). It would be interesting to address whether the embryonic arrest of *alg-1/2* loss-of-function mutants, can be recapitulated making use of recently available temperature sensitive Pasha (*pash-1*) mutant. This mutant display an uncharacterized embryonic lethality that is fully penetrant at the restrictive temperature (Lehrbach *et al.*, 2012). Also, if the embryonic arrest of the *alg-1/2* mutant reflects a process controlled by miRNAs, it should be recapitulated by the abolishment of the miRNAs that control this process. Albeit, no miRNA mutant

has been reported to affect the elongation process, it is possible that multiple miRNAs act redundantly to control aspects of it. The study of the role(s) of miRNAs during worm morphogenesis remains open to further exploration. Interestingly, the complete loss of the *mir-52* miRNA family in worms leads to failure in the attachment of the pharynx to the buccal cavity, due to the misregulation of the cadherin gene *cdh-3* (Shaw *et al.*, 2010). Altogether with the *alg-1/2* embryonic elongation arrest, this two phenotypes highlight the importance of genes with structural functions (*e.g.* cytoskeleton, extracellular matrix) for proper worm viability and morphogenesis, and the fact that their function is controlled by miRNAs.

4.1.3 Shared and unique aspects of *alg-1* and *alg-2*

The following aspects reflect mostly similarities of the *alg-1/2* genes: 1) *alg-1/2* share a high degree of sequence homology, and the investigation by Bouasker and Simard (2012), on the activity of recombinant ALG-1/2 has not unveiled major differences between the *in vitro* properties of the two proteins. 2) Their expression is overlapping in many tissues; 3) The sets of miRNAs associated with both Argonautes, have substantial overlap as well and; 4) The described embryonic arrest during the elongation process is only observed upon loss of both argonautes. Single mutants are not close to exhibit the phenotypes of complete loss of both genes, that is, a highly penetrant embryonic and larval lethality. All these features testify for the 'partial redundancy' of *alg-1* and *alg-2* with regard to the developmental process they control. This genetic status does not imply that the two argonautes have to have the exact molecular mechanism of action, but even if they would not, the outcome of that function would be of similar consequences (*i.e.* repression of gene expression).

Aspects reflecting mostly *alg-1/2* differences are: 1) The distinct postembryonic argonaute mutant phenotypes, single mutants of *alg-1* display reduced progeny sizes, impaired growth (Bukhari *et al.*, 2012) and strong defects in the seam cells and vulva. In contrast, single mutants of *alg-2* do not display similarly penentrant phenotypes; 2) At the molecular level, *alg-1* loss of function leads to a strong and widespread reduction in the mature miRNA levels while mutant of *alg-2* does not induce similar deficits. Although it can be postulated that the preferential association of *let-7* family miRNAs to the ALG-1 Argonaute, would explain post-embryonic seam cells and vulval defects, it would not account for the widespread reduction of mature miRNA levels. The study of the involvement of ALG-1/2 in miRNA biogenesis has evidenced that the catalytic function of either Argonaute is sufficient for viability (Bouasker and Simard, 2012), pointing the explanation of *alg-1/2* differences away from this aspect.

It remains open that interactions with additional gene products are distinct between ALG-1 and ALG-2. Factors interacting with the conspicuous amino terminal ALG-1 sequence could be involved (*e.g.* Jannot *et al.* (2011a)). Also, differential post-translational modifications or

interaction with AIN-1 and AIN-2 or DCR-1 could be adduced. Exploring these aspects may shed light on the particular functions of the *C. elegans* miRNA-specific Argonautes. A precedent of differential Argonaute interactions can be found in *D. melanogaster*. The fly Ago1 protein associates mainly with miRNA and Ago2 mostly with siRNAs, but a few miRNA are bound to Ago2 (Kawamura *et al.*, 2008). Interestingly, the mechanisms by which Ago2 repress mRNA are different between these two Argonautes, and involve a differential association with GW182 (Iwasaki *et al.*, 2009; Behm-Ansmant *et al.*, 2006).

We can hypothesize that the ALG-1 and ALG-2 Argonautes fulfill different roles in distinct cells. An interesting case for future research is that of the gametes, germline and early embryo. Embryonic patterning processes in *Drosophila* and *Xenopus* are controlled by maternally deposited mRNAs that are translationally repressed and proteged from degradation by the action of specific RNA binding proteins, to be subsequently expressed only in very defined spatio-temporal domains (reviewed in Richter and Lasko 2011). A similar mode of action could be conceived for mRNAs targeted by miRNAs in the germline, gametes and very early embryo. The miRNAs are present in those cells, and they have been reported not to induce silencing in a canonical manner (miRNA action is highly dampened in ovocytes, reviewed in Suh and Blelloch 2011), opening the possibility that their presence corresponds to a distinct biological role(s) with a likely variant mode of operation. As mentioned above, the germline expression of ALG-1 and ALG-2 is not yet known. However, our data shows that ALG-2 is predominantly expressed in the early embryo, and differences in Argonaute expression would not be unexpected in germline and gametes. Further studies on germline miRNA function and miRISC complexes should shed light on these speculations.

In different experimental settings the absence of core miRNA pathway components produces defects associated with morphogenesis rather than cell-type specification. For examples, absence of dicer in zebrafish leads to late embryonic death (Wienholds *et al.*, 2003), and alters brain morphogenesis (Giraldez *et al.*, 2005). Similarly, knockout of mammalian dicer does not alter limb patterning (Harfe *et al.*, 2005), or skin specification (Yi *et al.*, 2006). These findings suggest that miRNA function during development to reinforce cell specification and differentiation rather than to establish it. It is of note that absence of core miRNA pathway components is lethal in mammals, but the effect of defects in extraembryonic tissues, that can impair the development of the embryo in a non-autonomous manner, should be considered when analyzing the observed phenotypes. A number of defects found in mutants of the miRNA pathway components derive from defective extraembryonic tissue, indeed the miRNA pathway is necessary for proper extraembryonic tissue development *e.g.* (Jiang *et al.*, 2012).

At the cellular level, the absence of the mammalian miRNA related Argonautes AGO1-4 has been found to lead the cells to apoptosis (Su *et al.*, 2009). In contrast to this essential Argonaute role, viable embryonic stem cells without dicer have been reported (Murchison *et al.*, 2005; Kanellopoulou *et al.*, 2005). Nonetheless, these knockout cells exhibit severe prolifera-

tion and differentiation defects. Additionally, a modest increase in the basal apoptotic rate of these cells has been observed, and this is strongly enhanced upon treatment with DNA damage agents (Zheng *et al.*, 2011). In mice, mutants of the group of *mir-17–mir-92* clusters, leads to embryonic death with increased apoptosis affecting the early stage B cells, the spinal cord and fetal brain (Ventura *et al.*, 2008). In several other studies of miRNA function, apoptosis has been linked to the miRNA regulation of the proapoptotic gene Bim (Ventura *et al.*, 2008; Koralov *et al.*, 2008; Spruce *et al.*, 2010). Altogether, these studies have established a molecular link suggesting that as a direct consequence of the absence of miRNA activity, the cell apoptotic machinery is activated in mammalian cells.

At this respect, we did not notice any obvious sign of increased apoptosis in the *alg-1/2* mutant embryos. It is then interesting to suggest that a direct link between loss of miRNA activity and initiation of apoptosis may not operate during the *C. elegans* embryonic development. Early apoptotic events in *C. elegans* are common, during the embryonic development of a hermaphrodite worm 131 cells undergo apoptosis, of a total of 671 that are generated (Sulston *et al.*, 1983). It should be noted that, evidence for the coupling of apoptosis to absence of miRNA activity in the worm soma is scarce. So far, only the *miR-35* dependent deadenylation of the pro-apoptotic gene *egl-1* in embryonic lysates has been reported, but the phenotypical consequences of this regulation remain unknown (Wu *et al.*, 2010). In contrast to the situation in the worm embryo, increased apoptosis is readily increased in its germ-line upon Argonaute loss (Bukhari *et al.*, 2012). Future research may shed light on the mechanisms linking apoptosis to miRNA-mediated regulation in *C. elegans*.

4.2 *vps-52*, a new genetic interactor of the *C. elegans* microRNA pathway

Following the characterization of the *alg-1* and *alg-2* argonaute paralogs (chapter 2), we addressed the interaction of these argonautes with other genes through a forward genetics approach. In this manner we identified the gene *vps-52*, encoding a component of the conserved GARP (Golgi Associated Retrograde Protein) complex as a genetic interactor of the *alg-1* gene, and established its role as a modulator of miRNA activity (chapter 3).

4.2.1 Genetic screen and mutant identification

The identification of genetic interactors of the miRNA argonautes was done using a forward genetic screen. In this approach, upon random mutagenesis, mutants worms are scored for a phenotype of interest. This is followed by the mapping and identification of the induced DNA lesion. Upon successful identification, the mutant can be characterized by genetic analysis

and other means. In our case, the performed screen followed a design intended to isolate gene enhancers, including synthetic lethal gene pairs, as described in section 3.4. Given that *alg-2(ok304)* mutant background was used for screening, it is expected that mutants of *alg-1* should show up in the recovered candidate mutant strains. So far, no mutant of *alg-1* has been identified, although a non yet mapped complementation group is linked to the chromosome X where *alg-1* is located. The small size of the screen, 1556 screened F2 clones, led to candidate mutant strains grouped into six complementation groups. At this scale it could be possible that certain interacting genes were not mutagenized or recovered during the screen. So far, only the mutations in two groups have been identified, *vps-52* and *dcs-1*[2]. The most unexpected feature of *vps-52* with regard to the screen is the absence of a visible interaction with the mutant *alg-2(ok304)*. In this respect, it should be noticed that given the redundancy between the *alg-1/2* argonautes, genes that interact with both argonautes could also be obtained from the screen, regardless of the mutant argonaute background used in the screen. Additionally, a possible genetic interaction between *vps-52* and *alg-2* should not be completely ruled out. Such interaction may be tested using supplementary phenotypic assesments of increased sensitivity, as described below.

4.2.2 Genetic interactions of *vps-52*

To genetic study of *vps-52* was based on the analysis of microRNA-related phenotypes in several genetic backgrounds. We studied two alleles of *vps-52* and one allele of *vps-53*, an additional subunit of the GARP complex. The single mutants of *vps-52* and *vps-53* showed mild or absent phenotypical defects related to the miRNA-mediated regulation of developmental processes in the seam cells or vulva, indicating that these mutants do not strongly disrupt miRNA processes. Unveiling the action of these genes was achieved by mutant combinations of *vps-52* and *vps-53* with the argonautes, miRNA genes and their targets.

Interaction with the miRNA-specific Argonautes

The genetic interaction of *vps-52* with the loss-of-function *alg-1(gk214)* argonaute mutant, was evidenced by the enhancement in the number of seam cells and the consequent increase in the gapped alae (Fig. 3.1). This seam cell phenotype is likely due to reduced activity of the *mir-48/-84/-241* family of miRNAs that control the seam cell division program at the L2 larval stage (Abbott *et al.*, 2005) as evidenced below. In contrast, the vulva bursting phenotype was not observed in neither single *vps-52* mutants nor in combination with *alg-1(gk214)*. The absence of phenotypic enhancement for the *let-7*-controlled vulva bursting phenotype suggest that the sensitized backgrounds required to observe a phenotypical enhancement differ between

2. *dcs-1* is analyzed in the study by my colleague Gabriel Bossé.

the *let-7* and *mir-48/-84/-241* miRNAs, probably reflecting differential dynamics with respect to their targets. Indeed, additional genetic analysis showed that absence of *vps-52* enhances the defects induced by the specific *let-7* miRNA mutants (see below).

Remarkably, no interaction was found between *vps-52* and *alg-2* for the seam cells and vulva phenotypes. It is likely that specific miRNA-action readouts, predominantly controlled by the ALG-2 Argonaute, are necessary to phenotypically uncover a possible interaction between these two genes. The possibility of synthetic lethality between *vps-52* and *alg-1/2* was ruled out by the obtention of viable double mutant combinations of *vps-52* with both argonautes. However, the interaction between *vps-52* and *alg-1* can be considered as 'synthetic sick', because it imposed drastic impairment of growth and reproduction (data not shown).

Interactions between *alg-1* and other trafficking mutants

The absence of the *alg-1* argonaute induces strong defects, and therefore it could be argued that the loss of additional genes with likely pleiotropic defects could led to unspecific gene interactions. A genetic approach to define the specificity of *vps-52* action is to analyze whether mutations affecting other trafficking processes lead to similar consequences with regard to miRNA action. A vesicular trafficking defect observed in *vps-52* mutant is an enlargement in the lysosomal size of coelomocytes (Luo *et al.*, 2011). This defect does not affect the capability of this organelle to degrade proteins but may rather reflect an unbalance in membrane transport. Mutations in the *ppk-3* gene, encoding for the phosphatidyl inositol 4,5 (PIP4,5) lipid kinase (PIKFYVE) also exhibit a similar lysosomal enlargement (Nicot *et al.*, 2006). The function of *ppk-3* is essential and therefore we made use of the *n2668* hypomorph allele that does not lead to developmental arrest at 15°C temperature. Additionally, we investigated the worm homologues of the rab6 small GTPase, complete absence of rab6 function, mediated in *C. elegans* by the paralogs *rab-6.1* and *rab-6.2*, has been reported as lethal (Luo *et al.*, 2011)). However, abolishing one of the two worm paralogs, namely *rab-6.2(ok2254)*, does not strongly impair viability and leads to partially impaired trafficking processes. We used RNAi to measure the effect of *alg-1* knockdown on the cuticular alae in the different vesicular trafficking mutants and found that similarly to *vps-52*, the *rab-6.2* mutant sensitizes for alae defects (Table 3.1), while *ppk-3* does not (data not shown), regardless of its common lysosomal phenotype with *vps-52*. Given that the RAB-6 protein is physical interactor of the GARP complex (Luo *et al.*, 2011), these results suggest some specificity between the Golgi process and the microRNA-controlled seam cell development. The study of the genetic interactions between mutants of vesicular trafficking processes and miRNA components, as done for *rab-6.2* and *ppk-3*, could be continued to better establish the pathway(s) that mediate their genetic interaction. In addition to the GARP complex components and *rab-6.2*, it would be interesting to unveil potential roles on regulating miRNA activity for selected SNARE proteins, that par-

ticipate in the docking of vesicles, and the ESCRT complex, that has been previously linked to miRNA pathway in mammalian cells (section 1.5.3).

Interactions with the *let-7* family miRNAs

Next, we extended the interactions observed between *vps-52* and *alg-1/2*, to the microRNA level using hypomorphic and null mutants of the *let-7* family of miRNAs[3]. The synergy observed between *alg-1* and *vps-52* was recapitulated with a *mir-48* null mutant. This *mir-48* single mutant do not display alae defects, but upon combination with *vps-52* and increase in the alae defects was observed. This result supports that the seam cells defects observed in the double *vps-52 alg-1* mutant are due to reduced activity of the *mir-48/-84/-241* miRNAs. The interaction observed with the *mir-48* mutant, could be evaluated as well for the *mir-84* and *mir-241* miRNA mutants, that act redundantly to control *hbl-1* expression.

Next, we studied the vulva bursting phenotype, characteristic of absence of *let-7* function. We used hypomorphic mutations of this miRNA to evaluate which effect would have concomitant loss of *vps-52* function. Remarkably, *vps-52* showed a drastic effect on the penetrance of vulva bursting in the *let-7(n2853)* background. The *let-7(n2853)* allele is a point mutation in the seed region of the let-7 miRNA that compromises its activity to the point of showing temperature sensitive behavior. While the penetrance of the bursting defect disallowed the propagation of *vps-52 let-7(n2853)* double mutants, we obtained a partially rescued strain upon transgenic *vps-52* expression. Moreover, we showed that the effect of *vps-52* on *let-7(n2853)* was dependent of the main *let-7* target, *lin-41*. Unfortunately, we could not investigate the *vps-52 let-7(n2853)* strain molecularly due to its lethality.

We then focused on another hypomorphic *let-7* mutant, *let-7(mg279)*, which conveys reduced let-7 levels, without affecting the nucleotide sequence of this miRNA. The *let-7(mg279)* allele leads to mild phenotypes and do not display vulva bursting at any temperature. When we combined with *let-7(mg279)* with *vps-52*, no vulva bursting phenotype was observed. However, this double mutant strain had decreased growth and fertility (data not shown), and we observed that the let-7 abundance was reduced in this double mutant combination, suggesting that *vps-52* also regulates let-7 activity in a second hypomorphic genetic background.

It would be interesting to extend the analysis of *vps-52* to other miRNAs and their targets. Genetically, the *alg-1(gk214)* background offers a widespread lowering effect on the level of many miRNAs, while partial miRNA family mutants regulating a commonly targeted gene are a second alternative for sensitized background. Mutations affecting a single miRNA similarly to the hypomorphic alleles available for *let-7* are not currently available. Future studies will address and clarify the issue of the generality of *vps-52* action on miRNA function.

3. As stated previously, this family includes the *mir-48*, *mir-84*, *mir-241* and *let-7* miRNAs.

4.2.3 Molecular basis of the *vps-52*-mediated modulation of miRNA activity

Effects on protein components

The effect of *vps-52* could be mediated by alterations of several cellular aspects, including the abundance of miRNA pathway components or their subcellular distribution. The first aspect was taken into account by quantifying immunoblots of the pathway proteins. As result, it was observed that the level of DCR-1 and ALG-1/2 are not affected but that of AIN-1 was reduced, in a post-transcriptional manner (Figure 3.6). It would be interesting to test if *vps-52* affects the abundance of other proteins likely important for Argonaute loading and stability like the HSP90 chaperone. Also, the subcellular distribution of the miRNA pathway proteins was not addressed, and future studies could analyze this aspect using either subcellular fractionation or fluorescent reporters.

Effects on miRNA abundance

In agreement with the absent or weak miRNA-related phenotypes of *vps-52* mutants, the abundance of the miRNAs of the *let-7* family was mildly altered in these mutants. However, the double mutant *vps-52 alg-1* had significantly reduced levels of miR-48 and miR-241, and this decrease was not due to a reduction in the levels of the corresponding pre-miRNA and pri-miRNAs. This miRNA reduction is consistent and likely causative of the observed increase in seam cells number and alae defects of the double mutant strain. The observed reduction in miRNA abundance could be attributed to a biogenesis defect posterior to the pri-miRNA level, like Argonaute loading. Alternative mechanisms could also be adduced, like increased miRNA degradation. A future experiment to investigate this possibility, would be to measure the miRNA decay rate after shutdown of biogenesis in the presence and absence of *vps-52*, a task that can be achieved using a recently available termosensitive pasha (*pash-1*) mutant.

Effects on mammalian cells

As observed in *C. elegans*, siRNA-mediated knockdown of VPS52 in HeLa cells did not alter miRNA activity as measured with miRNA reporters. However, in the sensitized condition of concomitant knockdown of the human GW182 protein (*i.e.* TNRC6A), a derepression of the miRNA reporters was reached, indicating that the positive activity of VPS52 on miRNA activity is conserved between worms and humans. Evidence for a close physical association between VPS52 and miRISC components was obtained using subcellular gradient fractionation. Co-fractionation of VPS52 with the Argonaute AGO2, TNRC6A protein and the prion protein PRNP was detected, suggesting that these components are located in common endomem-

branes. Moreover, VPS52 knockdown induced a shift of TNRC6A towards denser fractions (data not shown). Further support for the close association of these proteins was attained by the presence of some co-localization of TNRC6A, AGO2 with the golgi marker syntaxin-6 (data not shown). It would be interesting to perform similar density gradient fractionation and co-localization experiments in worms.

Additional molecular analysis

In *C. elegans*, we investigated if there is association of the VPS-52 protein with components of the microRNA pathway via immunoprecipitations. Using a strain carrying mCherry tagged VPS-52 (MJS21 strain, containing the Si[vps-52] transgene) we tested if VPS-52 complexes do contain miRISC components (Argonautes or GW182 proteins). No co-immunoprecipitation (co-IP) of VPS-52 with AIN-1 or ALG-1 was found under several tested conditions (Figure 4.1). Similarly, no interaction by co-IP was found in the mammalian cells (data not shown). Therefore, we do not presently support a protein-protein interaction of VPS-52 with the miRISC components. The co-fractionation of VPS52 with the miRISC likely indicates a vesicle-mediated interaction that cannot be recapitulated in the conditions used in the immunoprecipitations. Further biochemical approaches will be necessary to better dissect the observed co-fractionation of VPS52 with miRISC components.

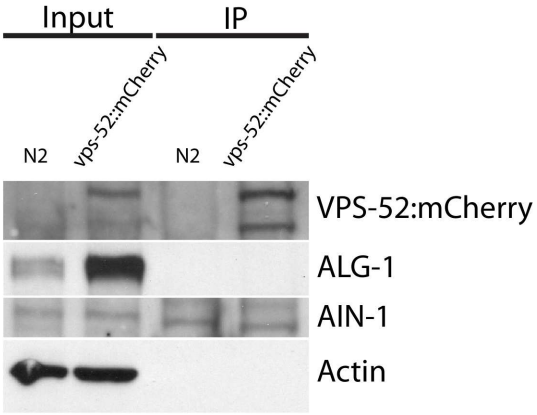

Figure 4.1: **Immunoprecipitation of VPS-52**. Synchronized adult worms (WT and MJS21 strain) were disrupted in lysis buffer (100mM potassium acetate, 30mM HEPES, 2mM Magnesium acetate, 1mM DTT, 0.5% Triton X-100 and mini EDTA-free protease inhibitor cocktail (Roche)). The crude lysate was cleared by centrifugation at 13,000g for 10 minutes at 4 °C, and protein concentration dosed. One miligram total protein was used for immunoprecipitation using protein G dynabeads (Life technologies) coupled to anti-RFP antibody for 1 hour at 4 °C. Blots of the immunoprecipitate were probed with antibodies anti-ActinHRP, anti-dsRed, anti-ALG-1 and anti-AIN-1.

We also addressed if *vps-52*, as a single mutant or in combination with the different sensitized backgrounds, exhibited amounts of Argonaute-associated miRNA distinct than those measured from total RNA samples. We measured the let-7 family miRNA levels following 2'-o-methyl pulldowns and ALG-1 immunoprecipitations, using quantitative real-time PCR. We found no evidence in any *vps-52* mutant combination of increased or reduced miRNA abundance, compared to the corresponding levels seen in the analysis of total RNA samples (data not shown). These results suggest that the miRNA abundance measured with total RNA samples correspond very closely to the amount of Argonaute-associated miRNA in the analyzed worms.

4.2.4 Function of *vps-52* in the miRNA pathway

Altogether, our phenotypic and molecular analysis allow us to conclude, that absence of *vps-52* function impairs miRNA-mediated silencing, and therefore *vps-52* has a positive role on miRNA activity. The effects of *vps-52* were mostly observed in sensitized mutant backgrounds, indicating that absence of only this gene does not grossly impairs miRNA activity and suggesting that *vps-52* fullfils a modulatory rather than necessary function with respect to miRNA activity. By the same token, VPS-52 is likely not a core component of the miRNA silencing pathway but rather part of a system that facilitates miRNA activity. Also, throughout our analysis we attested similar results for mutants of the *vps-52* and *vps-53* genes, both of which encode components of the GARP complex. Therefore, we propose that the regulatory activity these genes confer is related to the their GARP complex function, and not to other putative and yet unknown GARP-independent roles of *vps-52*.

In the molecular analysis of *vps-52* action, we observed no indication of defective miRNA transcription (no effect on the abundance of pri- and pre-miRNAs), but reduced mature miRNA abundance. In addition, we observed co-fractionation of VPS52 with the Argonautes and GW182 proteins. Additionally, effects on the abundance of GW182 protein were observed in worms and mammalian cells. Therefore, we temptatively suggest that VPS-52 is not acting upstream of the 'Argonaute loading' process but rather at or downstream of it, in close association with the miRISC and its components.

In our interpretative model of the role of VPS-52 in the miRNA pathway (Figure 3.8), this protein facilitates a 'transition' of miRISC activity at the 'post-effector' phase of the pathway (see Figure 1.6), like the release from the miRISC of GW182 or the steps involved in miRNA recycling or Argonaute reloading. In the model, the miRISC would be associated with the cytosolic side of membranes at endosomes or MVBs, and the proper activity of GARP in retrieving vesicles and cargo from these membrane-bound compartments would be required to ensure that the miRISC transition at those membranes occurs properly. Whether or not the retrogradely transported vesicles (via GARP tethering) contain miRNA pathway components is not considered in the model, but it should be noticed that Argonaute proteins have been found localized

to the Golgi in previous studies, as described earlier (section 1.5). No knowledge about the biomolecules (protein, lipids, RNA, etc.) retrogradely transported by the GARP complex in *C. elegans* is currently available. Malfunctioning of the GARP complex, would induce two consequences: 1) Missorting and erduced abundance of miRISC components, such as the GW182 protein and; 2) A 'block' of membrane-localized miRISC. Loss of miRNA-mediated repression could occur as consequence, in the condition where this membrane-localized miRISC and its components need to be recycled to engage in further target mRNA repression [4]. In such scenario, we can expect that experimental conditions that reduced miRNA abundance should sensitize miRNA-mediated processes to loss of GARP function, because such condition would likely impose a stronger need for miRNA recycling. This expectation is indeed met by our observations of phenotypic synergy upon loss of *vps-52* with the *alg-1* and miRNA mutants but no disturbance of miRNA-mediated silencing upon loss of *vps-52* alone.

Accounting for our observations of reduced miRNA abundance (*e.g.* miR-48 and miR-241), we can envision that the miRISC blocking effect can negatively affect the 'Argonaute loading' process by sequestering factor(s) important for loading [5], like the Argonaute protein themselves or the chaperone HSP90. This last protein has been shown to mediate the membrane association of Argonaute in certain cells and participates in the miRNA loading process (section 1.2.2). Finally, the reduced abundance of GW182 and miRNAs, are two outcomes that we propose are not directly linked, and we adduce no role of the GW182 protein in regulating miRNA stability in our model. Indeed, the abundance of miR-48 has been previously reported to be unchanged by the presence or absence of the worm GW182 proteins (Zhang *et al.*, 2007). Further experimentation will be required to better address the mechanisms proposed in our model and achieve a better understanding of the action of *vps-52* impinging molecularly on miRNA activity.

4.2.5 Final considerations and Perspectives

Throughout the research presented in this thesis we have explored the function and genetic interactions of the *C. elegans* argonaute genes *alg-1* and *alg-2*. We furthered the characterization of these miRNA-specific Argonautes, evidenced a new role of these proteins during the worm embryonic elongation process, and defined common and distinct features related to their expression and association with miRNAs. Clearly, further research is needed to better understand the role of miRNAs during the processes of embryonic morphogenesis. The study of essential miRNA-controlled processes can also bring us to understand some essential 'hubs' in the network of genes controlled by miRNAs in *C. elegans* and related them to the corresponding human network. For example, the cellular process activated in response to global miRNA absence (*e.g.* apoptosis) could be different between these two organism and be differentially

4. In other words, in a condition where the miRNA/miRISC is limiting with respect to the target mRNA.
5. making these factors effectively limiting.

modulated in distinct cell types. The processes involving miRNAs during development, the different cellular functions they regulate in distinct tissues by controlling multiple genes is a venue for future scientific exploration.

Another interesting topic that deserve further investigation is the mechanism(s) by which the Argonautes ALG-1 and ALG-2 fullfil not only common, but also distinct functions. These differences may relate to Argonaute-specific interactions with other components of the miRNA pathway like Dicer, the GW182 proteins or other factors. Similarly, extending our study of *alg-1* and *alg-2* function to the gonads, germline and early embryo would complement our knowledge of these genes in somatic tissues. We should expect that ALG-1 and ALG-2 display peculiarities in their action in distinct tissues, given their separate expression in specific tissues and putative gene-specific mechanistic features.

Beyond the interaction of *alg-1* with *alg-2*, our study on the genetic interactions of these miRNA-specific *C. elegans* argonautes with additional genes, led us to discover a role for *vps-52* in positively regulating miRNA activity. In particular, we evidenced this role for the *let-7* miRNA family in *C. elegans* and find evidence that the miRNA-related role of *vps-52* may be conserved in mammalian cells. Future studies shall be focused in better understanding the mechanisms by which this regulation occur, and address its generality. In a wider manner, the association of the miRNA pathway with membrane-related processes, evidenced by multiple experimental findings including our discovery of a role for the 'vesicle tethering' GARP complex, remains to be better understood in term of its biological functions, and the components and mechanisms that underpin this association.

Finally, the study of the genetic interactions of the miRNA pathway shall be continued, the processes at the effector and post-effector phases of the pathway are far from completely understood and may be biologically regulated, involving the participation of new components. The study of these genetic interactions shall be carried in genetically sensitized settings as we have done in screening for argonaute interactors.

Bibliography

A. L. Abbott, E. Alvarez-Saavedra, E. A. Miska, N. C. Lau, D. P. Bartel, H. R. Horvitz, and V. Ambros. The let-7 microrna family members *mir-48*, *mir-84*, and *mir-241* function together to regulate developmental timing in *Caenorhabditis elegans*. *Dev Cell*, 9(3):403–14, 2005.

J. E. Abrahante, A. L. Daul, M. Li, M. L. Volk, J. M. Tennessen, E. A. Miller, and A. E. Rougvie. The *Caenorhabditis elegans* hunchback-like gene *lin-57/hbl-1* controls developmental time and is regulated by microrna. *Dev Cell*, 4(5):625–37, 2003.

R. S. Alisch, P. Jin, M. Epstein, T. Caspary, and S. T. Warren. Argonaute2 is essential for mammalian gastrulation and proper mesoderm formation. *PLoS Genet*, 3(12):e227, 2007.

E. Alvarez-Saavedra and H. R. Horvitz. Many families of *C. elegans* microRNAs are not essential for development or viability. *Curr Biol*, 20(4):367–73, 2010.

V. Ambros and H. R. Horvitz. Heterochronic mutants of the nematode *Caenorhabditis elegans*. *Science*, 226(4673):409–16, 1984.

S. L. Ameres, M. D. Horwich, J. H. Hung, J. Xu, M. Ghildiyal, Z. Weng, and P. D. Zamore. Target rna-directed trimming and tailing of small silencing rnas. *Science*, 328(5985):1534–9, 2010.

P. Anderson and N. Kedersha. RNA granules: post-transcriptional and epigenetic modulators of gene expression. *Nat. Rev. Mol. Cell Biol.*, 10(6):430–436, 2009.

M. P. Arrate, T. Vincent, J. Odvody, R. Kar, S. N. Jones, and C. M. Eischen. MicroRNA biogenesis is required for Myc-induced B-cell lymphoma development and survival. *Cancer Res.*, 70(14):6083–6092, 2010.

A. Azuma-Mukai, H. Oguri, T. Mituyama, Z. R. Qian, K. Asai, H. Siomi, and M. C. Siomi. Characterization of endogenous human Argonautes and their miRNA partners in RNA silencing. *Proc Natl Acad Sci U S A*, 105(23):7964–9, 2008.

A. Baccarini, H. Chauhan, T. J. Gardner, A. D. Jayaprakash, R. Sachidanandam, and B. D. Brown. Kinetic analysis reveals the fate of a microRNA following target regulation in mammalian cells. *Curr. Biol.*, 21(5):369–376, 2011.

C. Barreau, L. Paillard, and H. B. Osborne. AU-rich elements and associated factors: are there unifying principles? *Nucleic Acids Res.*, 33(22):7138–7150, 2005.

A. A. Bazzini, M. T. Lee, and A. J. Giraldez. Ribosome profiling shows that miR-430 reduces translation before causing mRNA decay in zebrafish. *Science*, 336(6078):233–237, 2012.

I. Behm-Ansmant, J. Rehwinkel, T. Doerks, A. Stark, P. Bork, and E. Izaurralde. mRNA degradation by miRNAs and GW182 requires both CCR4:NOT deadenylase and DCP1:DCP2 decapping complexes. *Genes Dev.*, 20(14):1885–1898, 2006.

J. G. Betancur and Y. Tomari. Dicer is dispensable for asymmetric RISC loading in mammals. *RNA*, 18(1):24–30, 2012.

J. Bethune, C. G. Artus-Revel, and W. Filipowicz. Kinetic analysis reveals successive steps leading to miRNA-mediated silencing in mammalian cells. *EMBO Rep.*, 13(8):716–723, 2012.

J. C. Bettinger, K. Lee, and A. E. Rougvie. Stage-specific accumulation of the terminal differentiation factor LIN-29 during *Caenorhabditis elegans* development. *Development*, 122(8):2517–27, 1996.

M. T. Blahna and A. Hata. Smad-mediated regulation of microRNA biosynthesis. *FEBS Lett.*, 586(14):1906–1912, 2012.

T. Boettger and T. Braun. A new level of complexity: the role of microRNAs in cardiovascular development. *Circ. Res.*, 110(7):1000–1013, 2012.

M. T. Bohnsack, K. Czaplinski, and D. Gorlich. Exportin 5 is a RanGTP-dependent dsRNA-binding protein that mediates nuclear export of pre-miRNAs. *RNA*, 10(2):185–191, 2004.

J. S. Bonifacino and A. Hierro. Transport according to garp: receiving retrograde cargo at the trans-golgi network. *Trends Cell Biol*, 21(3):159–67, 2011.

S. Bouasker and M. J. Simard. The slicing activity of miRNA-specific Argonautes is essential for the miRNA pathway in *C elegans*. *Nucleic Acids Res.*, 2012.

S. Brenner. The genetics of *Caenorhabditis elegans*. *Genetics*, 77(1):71–94, 1974.

P. Brodersen, L. Sakvarelidze-Achard, H. Schaller, M. Khafif, G. Schott, A. Bendahmane, and O. Voinnet. Isoprenoid biosynthesis is required for miRNA function and affects membrane association of argonaute 1 in arabidopsis. *Proc Natl Acad Sci U S A*, 109(5):1778–83, 2012.

S. I. Bukhari, A. Vasquez-Rifo, D. Gagne, E. R. Paquet, M. Zetka, C. Robert, J. Y. Masson, and M. J. Simard. The microrna pathway controls germ cell proliferation and differentiation in *C elegans*. *Cell Res*, 22(6):1034–45, 2012.

S. P. Chan and F. J. Slack. Ribosomal protein RPS-14 modulates let-7 microRNA function in *Caenorhabditis elegans*. *Dev Biol*, 334(1):152–60, 2009.

S. Chang, R. J. Johnston, C. Frokjaer-Jensen, S. Lockery, and O. Hobert. MicroRNAs act sequentially and asymmetrically to control chemosensory laterality in the nematode. *Nature*, 430(7001):785–789, 2004.

S. Chatterjee, M. Fasler, I. Bussing, and H. Grosshans. Target-mediated protection of endogenous microRNAs in *C elegans*. *Dev. Cell*, 20(3):388–396, 2011.

S. Cheloufi, C. O. Dos Santos, M. M. Chong, and G. J. Hannon. A dicer-independent miRNA biogenesis pathway that requires Ago catalysis. *Nature*, 465(7298):584–589, 2010.

P. S. Chen, J. L. Su, and M. C. Hung. Dysregulation of microRNAs in cancer. *J. Biomed. Sci.*, 19:90, 2012a.

X. Chen, H. Liang, J. Zhang, K. Zen, and C. Y. Zhang. Secreted micrornas: a new form of intercellular communication. *Trends in cell biology*, 22(3):125–32, 2012b.

A. D. Chisholm and J. Hardin. Epidermal morphogenesis. *WormBook*, pages 1–22, 2005.

D. Cifuentes, H. Xue, D. W. Taylor, H. Patnode, Y. Mishima, S. Cheloufi, E. Ma, S. Mane, G. J. Hannon, N. D. Lawson, S. A. Wolfe, and A. J. Giraldez. A novel miRNA processing pathway independent of Dicer requires Argonaute2 catalytic activity. *Science*, 328(5986):1694–1698, 2010.

D. E. Cikaluk, N. Tahbaz, L. C. Hendricks, G. E. DiMattia, D. Hansen, D. Pilgrim, and T. C. Hobman. Gerp95, a membrane-associated protein that belongs to a family of proteins involved in stem cell differentiation. *Mol Biol Cell*, 10(10):3357–72, 1999.

C. P. Concepcion, Y. C. Han, P. Mu, C. Bonetti, E. Yao, A. D'Andrea, J. A. Vidigal, W. P. Maughan, P. Ogrodowski, and A. Ventura. Intact p53-dependent responses in miR-34-deficient mice. *PLoS Genet.*, 8(7):e1002797, 2012.

E. Conibear and T. H. Stevens. Vps52p, Vps53p, and Vps54p form a novel multisubunit complex required for protein sorting at the yeast late Golgi. *Mol. Biol. Cell*, 11(1):305–323, 2000.

C. C. Conine, P. J. Batista, W. Gu, J. M. Claycomb, D. A. Chaves, M. Shirayama, and C. C. Mello. Argonautes ALG-3 and ALG-4 are required for spermatogenesis-specific 26G-RNAs and thermotolerant sperm in *Caenorhabditis elegans*. *Proc Natl Acad Sci U S A*, 107(8):3588–93, 2010.

A. M. Denli, B. B. Tops, R. H. Plasterk, R. F. Ketting, and G. J. Hannon. Processing of primary micrornas by the microprocessor complex. *Nature*, 432(7014):231–5, 2004.

L. Ding and M. Han. GW182 family proteins are crucial for microRNA-mediated gene silencing. *Trends Cell Biol.*, 17(8):411–416, 2007.

L. Ding, A. Spencer, K. Morita, and M. Han. The developmental timing regulator AIN-1 interacts with miRISCs and may target the argonaute protein ALG-1 to cytoplasmic P bodies in *C elegans*. *Mol. Cell*, 19(4):437–447, 2005.

S. W. Ding and O. Voinnet. Antiviral immunity directed by small RNAs. *Cell*, 130(3):413–26, 2007.

S. Djuranovic, A. Nahvi, and R. Green. miRNA-mediated gene silencing by translational repression followed by mRNA deadenylation and decay. *Science*, 336(6078):237–240, 2012.

M. Dlakic. DUF283 domain of Dicer proteins has a double-stranded RNA-binding fold. *Bioinformatics*, 22(22):2711–2714, 2006.

T. F. Duchaine, J. A. Wohlschlegel, S. Kennedy, Y. Bei, D. Conte, K. Pang, D. R. Brownell, S. Harding, S. Mitani, G. Ruvkun, J. R. Yates, and C. C. Mello. Functional proteomics reveals the biochemical niche of *C elegans* DCR-1 in multiple small-RNA-mediated pathways. *Cell*, 124(2):343–354, 2006.

M. S. Ebert and P. A. Sharp. Roles for microRNAs in conferring robustness to biological processes. *Cell*, 149(3):515–524, 2012.

E. Elkayam, C. D. Kuhn, A. Tocilj, A. D. Haase, E. M. Greene, G. J. Hannon, and L. Joshua-Tor. The structure of human argonaute-2 in complex with miR-20a. *Cell*, 150(1):100–110, 2012.

A. Eulalio, I. Behm-Ansmant, D. Schweizer, and E. Izaurralde. P-body formation is a consequence, not the cause, of RNA-mediated gene silencing. *Mol. Cell. Biol.*, 27(11):3970–3981, 2007.

A. Eulalio, F. Tritschler, and E. Izaurralde. The GW182 protein family in animal cells: new insights into domains required for miRNA-mediated gene silencing. *RNA*, 15(8):1433–1442, 2009.

M. R. Fabian and N. Sonenberg. The mechanics of miRNA-mediated gene silencing: a look under the hood of miRISC. *Nat. Struct. Mol. Biol.*, 19(6):586–593, 2012.

M. R. Fabian, N. Sonenberg, and W. Filipowicz. Regulation of mRNA translation and stability by microRNAs. *Annu Rev Biochem*, 79:351–79, 2010.

D. Fasshauer, R. B. Sutton, A. T. Brunger, and R. Jahn. Conserved structural features of the synaptic fusion complex: SNARE proteins reclassified as Q- and R-SNAREs. *Proc. Natl. Acad. Sci. U.S.A.*, 95(26):15781–15786, 1998.

D. S. Fay, S. Keenan, and M. Han. fzr-1 and lin-35/rb function redundantly to control cell proliferation in *C. elegans* as revealed by a nonbiased synthetic screen. *Genes and development*, 16(4):503–17, 2002.

K. Forstemann, M. D. Horwich, L. Wee, Y. Tomari, and P. D. Zamore. Drosophila microRNAs are sorted into functionally distinct argonaute complexes after production by dicer-1. *Cell*, 130(2):287–97, 2007.

C. Frokjaer-Jensen, M. W. Davis, C. E. Hopkins, B. J. Newman, J. M. Thummel, S. P. Olesen, M. Grunnet, and E. M. Jorgensen. Single-copy insertion of transgenes in *Caenorhabditis elegans*. *Nature genetics*, 40(11):1375–83, 2008.

R. Garzon, G. Marcucci, and C. M. Croce. Targeting microRNAs in cancer: rationale, strategies and challenges. *Nat Rev Drug Discov*, 9(10):775–789, 2010.

A. Gerondopoulos, L. Langemeyer, J. R. Liang, A. Linford, and F. A. Barr. BLOC-3 mutated in Hermansky-Pudlak syndrome is a Rab32/38 guanine nucleotide exchange factor. *Curr. Biol.*, 22(22):2135–2139, 2012.

D. Gibbings, P. Leblanc, F. Jay, D. Pontier, F. Michel, Y. Schwab, S. Alais, T. Lagrange, and O. Voinnet. Human prion protein binds argonaute and promotes accumulation of microrna effector complexes. *Nat Struct Mol Biol*, 19(5):517–24, S1, 2012a.

D. Gibbings, S. Mostowy, F. Jay, Y. Schwab, P. Cossart, and O. Voinnet. Selective autophagy degrades DICER and AGO2 and regulates miRNA activity. *Nat. Cell Biol.*, 2012b.

D. Gibbings and O. Voinnet. Control of rna silencing and localization by endolysosomes. *Trends Cell Biol*, 20(8):491–501, 2010.

D. J. Gibbings, C. Ciaudo, M. Erhardt, and O. Voinnet. Multivesicular bodies associate with components of miRNA effector complexes and modulate miRNA activity. *Nat Cell Biol*, 11(9):1143–9, 2009.

A. J. Giraldez, R. M. Cinalli, M. E. Glasner, A. J. Enright, J. M. Thomson, S. Baskerville, S. M. Hammond, D. P. Bartel, and A. F. Schier. MicroRNAs regulate brain morphogenesis in zebrafish. *Science*, 308(5723):833–838, 2005.

A. J. Giraldez, Y. Mishima, J. Rihel, R. J. Grocock, S. Van Dongen, K. Inoue, A. J. Enright, and A. F. Schier. Zebrafish MiR-430 promotes deadenylation and clearance of maternal mRNAs. *Science*, 312(5770):75–9, 2006.

A. Git, I. Spiteri, C. Blenkiron, M. J. Dunning, J. C. Pole, S. F. Chin, Y. Wang, J. Smith, F. J. Livesey, and C. Caldas. PMC42, a breast progenitor cancer cell line, has normal-like mRNA and microRNA transcriptomes. *Breast Cancer Res.*, 10(3):R54, 2008.

R. I. Gregory, K. P. Yan, G. Amuthan, T. Chendrimada, B. Doratotaj, N. Cooch, and R. Shiekhattar. The Microprocessor complex mediates the genesis of microRNAs. *Nature*, 432(7014):235–240, 2004.

A. Grishok, A. E. Pasquinelli, D. Conte, N. Li, S. Parrish, I. Ha, D. L. Baillie, A. Fire, G. Ruvkun, and C. C. Mello. Genes and mechanisms related to RNA interference regulate expression of the small temporal RNAs that control *C. elegans* developmental timing. *Cell*, 106(1):23–34, 2001.

H. Grosshans, T. Johnson, K. L. Reinert, M. Gerstein, and F. J. Slack. The temporal patterning microRNA let-7 regulates several transcription factors at the larval to adult transition in *C elegans*. *Dev. Cell*, 8(3):321–330, 2005.

I. Guller and A. P. Russell. MicroRNAs in skeletal muscle: their role and regulation in development, disease and function. *J. Physiol. (Lond.)*, 588(Pt 21):4075–4087, 2010.

H. Guo, N. T. Ingolia, J. S. Weissman, and D. P. Bartel. Mammalian microRNAs predominantly act to decrease target mRNA levels. *Nature*, 466(7308):835–840, 2010.

A. M. Gurtan, V. Lu, A. Bhutkar, and P. A. Sharp. In vivo structure-function analysis of human Dicer reveals directional processing of precursor miRNAs. *RNA*, 18(6):1116–1122, 2012.

C. M. Hammell, I. Lubin, P. R. Boag, T. K. Blackwell, and V. Ambros. *nhl-2* modulates microrna activity in *Caenorhabditis elegans*. *Cell*, 136(5):926–38, 2009.

J. Hardin. Mechanotransduction: getting morphogenesis down pat. *Curr. Biol.*, 21(9):R309–311, 2011.

B. D. Harfe, M. T. McManus, J. H. Mansfield, E. Hornstein, and C. J. Tabin. The RNaseIII enzyme Dicer is required for morphogenesis but not patterning of the vertebrate limb. *Proc. Natl. Acad. Sci. U.S.A.*, 102(31):10898–10903, 2005.

L. He, X. He, L. P. Lim, E. de Stanchina, Z. Xuan, Y. Liang, W. Xue, L. Zender, J. Magnus, D. Ridzon, A. L. Jackson, P. S. Linsley, C. Chen, S. W. Lowe, M. A. Cleary, and G. J. Hannon. A microRNA component of the p53 tumour suppressor network. *Nature*, 447(7148):1130–1134, 2007.

C. U. Hellen and P. Sarnow. Internal ribosome entry sites in eukaryotic mRNA molecules. *Genes Dev.*, 15(13):1593–1612, 2001.

D. G. Hendrickson, D. J. Hogan, H. L. McCullough, J. W. Myers, D. Herschlag, J. E. Ferrell, and P. O. Brown. Concordant regulation of translation and mRNA abundance for hundreds of targets of a human microRNA. *PLoS Biol.*, 7(11):e1000238, 2009.

I. Heo, C. Joo, J. Cho, M. Ha, J. Han, and V. N. Kim. Lin28 mediates the terminal uridylation of let-7 precursor MicroRNA. *Mol. Cell*, 32(2):276–284, 2008.

D. Hochbaum, Y. Zhang, C. Stuckenholz, P. Labhart, V. Alexiadis, R. Martin, H. J. Knolker, and A. L. Fisher. DAF-12 regulates a connected network of genes to ensure robust developmental decisions. *PLoS Genet.*, 7(7):e1002179, 2011.

M. C. Hresko, B. D. Williams, and R. H. Waterston. Assembly of body wall muscle and muscle cell attachment structures in *Caenorhabditis elegans*. *J. Cell Biol.*, 124(4):491–506, 1994.

G. Hutvagner and M. J. Simard. Argonaute proteins: key players in RNA silencing. *Nat Rev Mol Cell Biol*, 9(1):22–32, 2008.

G. Hutvagner, M. J. Simard, C. C. Mello, and P. D. Zamore. Sequence-specific inhibition of small rna function. *PLoS Biol*, 2(4):E98, 2004.

G. Hutvagner and P. D. Zamore. A microRNA in a multiple-turnover RNAi enzyme complex. *Science*, 297(5589):2056–2060, 2002.

N. T. Ingolia, S. Ghaemmaghami, J. R. Newman, and J. S. Weissman. Genome-wide analysis in vivo of translation with nucleotide resolution using ribosome profiling. *Science*, 324(5924):218–223, 2009.

M. Isik, H. C. Korswagen, and E. Berezikov. Expression patterns of intronic microRNAs in *Caenorhabditis elegans*. *Silence*, 1(1):5, 2010.

S. Iwasaki, T. Kawamata, and Y. Tomari. Drosophila argonaute1 and argonaute2 employ distinct mechanisms for translational repression. *Mol Cell*, 34(1):58–67, 2009.

S. Iwasaki, M. Kobayashi, M. Yoda, Y. Sakaguchi, S. Katsuma, T. Suzuki, and Y. Tomari. Hsc70/Hsp90 chaperone machinery mediates ATP-dependent RISC loading of small RNA duplexes. *Mol. Cell*, 39(2):292–299, 2010.

G. Jannot, S. Bajan, N. J. Giguere, S. Bouasker, I. H. Banville, S. Piquet, G. Hutvagner, and M. J. Simard. The ribosomal protein rack1 is required for microrna function in both *C. elegans* and humans. *EMBO reports*, 12(6):581–6, 2011a.

G. Jannot, M. E. Boisvert, I. H. Banville, and M. J. Simard. Two molecular features contribute to the Argonaute specificity for the microRNA and RNAi pathways in *C elegans*. *RNA*, 14(5):829–835, 2008.

G. Jannot, A. Vasquez-Rifo, and M. J. Simard. Argonaute pull-down and risc analysis using 2'-o-methylated oligonucleotides affinity matrices. *Methods Mol Biol*, 725:233–49, 2011b.

Z. Jiang, N. Yu, P. Kuang, M. Chen, F. Shao, G. Martin, D. H. Chui, W. V. Cardoso, X. Ai, and J. Lu. Trinucleotide repeat containing 6a (Tnrc6a)-mediated microRNA function is required for development of yolk sac endoderm. *J. Biol. Chem.*, 287(8):5979–5987, 2012.

S. M. Johnson, H. Grosshans, J. Shingara, M. Byrom, R. Jarvis, A. Cheng, E. Labourier, K. L. Reinert, D. Brown, and F. J. Slack. RAS is regulated by the let-7 microRNA family. *Cell*, 120(5):635–647, 2005.

M. Johnston, M. C. Geoffroy, A. Sobala, R. Hay, and G. Hutvagner. HSP90 protein stabilizes unloaded argonaute complexes and microscopic P-bodies in human cells. *Mol. Biol. Cell*, 21(9):1462–1469, 2010.

R. J. Johnston and O. Hobert. A microRNA controlling left/right neuronal asymmetry in *Caenorhabditis elegans*. *Nature*, 426(6968):845–9, 2003.

M. Jovanovic, L. Reiter, A. Clark, M. Weiss, P. Picotti, H. Rehrauer, A. Frei, L. J. Neukomm, E. Kaufman, B. Wollscheid, M. J. Simard, E. A. Miska, R. Aebersold, A. P. Gerber, and M. O. Hengartner. RIP-chip-SRM–a new combinatorial large-scale approach identifies a set of translationally regulated bantam/miR-58 targets in *C elegans*. *Genome Res.*, 22(7):1360–1371, 2012.

H. Kaji, J. Kamiie, H. Kawakami, K. Kido, Y. Yamauchi, T. Shinkawa, M. Taoka, N. Takahashi, and T. Isobe. Proteomics reveals N-linked glycoprotein diversity in *Caenorhabditis elegans* and suggests an atypical translocation mechanism for integral membrane proteins. *Mol. Cell Proteomics*, 6(12):2100–2109, 2007.

C. Kanellopoulou, S. A. Muljo, A. L. Kung, S. Ganesan, R. Drapkin, T. Jenuwein, D. M. Livingston, and K. Rajewsky. Dicer-deficient mouse embryonic stem cells are defective in differentiation and centromeric silencing. *Genes Dev.*, 19(4):489–501, 2005.

T. Kawamata and Y. Tomari. Making RISC. *Trends Biochem. Sci.*, 35(7):368–376, 2010.

Y. Kawamura, K. Saito, T. Kin, Y. Ono, K. Asai, T. Sunohara, T. N. Okada, M. C. Siomi, and H. Siomi. Drosophila endogenous small RNAs bind to Argonaute 2 in somatic cells. *Nature*, 453(7196):793–797, 2008.

S. Kennedy, D. Wang, and G. Ruvkun. A conserved siRNA-degrading RNase negatively regulates RNA interference in *C elegans*. *Nature*, 427(6975):645–649, 2004.

C. J. Kenyon. The genetics of ageing. *Nature*, 464(7288):504–512, 2010.

Y. K. Kim, I. Heo, and V. N. Kim. Modifications of small RNAs and their associated proteins. *Cell*, 143(5):703–709, 2010.

M. Kiriakidou, G. S. Tan, S. Lamprinaki, M. De Planell-Saguer, P. T. Nelson, and Z. Mourelatos. An mRNA m7G cap binding-like motif within human Ago2 represses translation. *Cell*, 129(6):1141–1151, 2007.

C. Klattenhoff and W. Theurkauf. Biogenesis and germline functions of piRNAs. *Development*, 135(1):3–9, 2008.

S. W. Knight and B. L. Bass. A role for the RNase III enzyme DCR-1 in RNA interference and germ line development in *Caenorhabditis elegans*. *Science*, 293(5538):2269–71, 2001.

S. B. Koralov, S. A. Muljo, G. R. Galler, A. Krek, T. Chakraborty, C. Kanellopoulou, K. Jensen, B. S. Cobb, M. Merkenschlager, N. Rajewsky, and K. Rajewsky. Dicer ablation affects antibody diversity and cell survival in the B lymphocyte lineage. *Cell*, 132(5):860–874, 2008.

V. L. Koumandou, J. B. Dacks, R. M. Coulson, and M. C. Field. Control systems for membrane fusion in the ancestral eukaryote; evolution of tethering complexes and SM proteins. *BMC Evol. Biol.*, 7:29, 2007.

J. Krol, I. Loedige, and W. Filipowicz. The widespread regulation of microrna biogenesis, function and decay. *Nature reviews. Genetics*, 11(9):597–610, 2010.

R. C. Lee, R. L. Feinbaum, and V. Ambros. The *C. elegans* heterochronic gene lin-4 encodes small rnas with antisense complementarity to lin-14. *Cell*, 75(5):843–54, 1993.

Y. S. Lee, S. Pressman, A. P. Andress, K. Kim, J. L. White, J. J. Cassidy, X. Li, K. Lubell, H. Lim do, I. S. Cho, K. Nakahara, J. B. Preall, P. Bellare, E. J. Sontheimer, and R. W. Carthew. Silencing by small rnas is linked to endosomal trafficking. *Nature cell biology*, 11(9):1150–6, 2009.

N. J. Lehrbach, C. Castro, K. J. Murfitt, C. Abreu-Goodger, J. L. Griffin, and E. A. Miska. Post-developmental microRNA expression is required for normal physiology, and regulates aging in parallel to insulin/IGF-1 signaling in *C elegans*. *RNA*, 2012.

I. Letunic, T. Doerks, and P. Bork. SMART 7: recent updates to the protein domain annotation resource. *Nucleic Acids Res.*, 40(Database issue):D302–305, 2012.

A. K. Leung, J. M. Calabrese, and P. A. Sharp. Quantitative analysis of Argonaute protein reveals microRNA-dependent localization to stress granules. *Proc. Natl. Acad. Sci. U.S.A.*, 103(48):18125–18130, 2006.

H. Liewen, I. Meinhold-Heerlein, V. Oliveira, R. Schwarzenbacher, G. Luo, A. Wadle, M. Jung, M. Pfreundschuh, and F. Stenner-Liewen. Characterization of the human GARP (Golgi associated retrograde protein) complex. *Exp. Cell Res.*, 306(1):24–34, 2005.

J. Liu, M. A. Carmell, F. V. Rivas, C. G. Marsden, J. M. Thomson, J. J. Song, S. M. Hammond, L. Joshua-Tor, and G. J. Hannon. Argonaute2 is the catalytic engine of mammalian RNAi. *Science*, 305(5689):1437–41, 2004.

J. Lu, G. Getz, E. A. Miska, E. Alvarez-Saavedra, J. Lamb, D. Peck, A. Sweet-Cordero, B. L. Ebert, R. H. Mak, A. A. Ferrando, J. R. Downing, T. Jacks, H. R. Horvitz, and T. R. Golub. MicroRNA expression profiles classify human cancers. *Nature*, 435(7043):834–838, 2005.

A. Lujambio and S. W. Lowe. The microcosmos of cancer. *Nature*, 482(7385):347–355, 2012.

E. Lund, S. Guttinger, A. Calado, J. E. Dahlberg, and U. Kutay. Nuclear export of microRNA precursors. *Science*, 303(5654):95–98, 2004.

E. Lund, M. Liu, R. S. Hartley, M. D. Sheets, and J. E. Dahlberg. Deadenylation of maternal mRNAs mediated by miR-427 in *Xenopus laevis* embryos. *RNA*, 15(12):2351–63, 2009.

L. Luo, M. Hannemann, S. Koenig, J. Hegermann, M. Ailion, M. K. Cho, N. Sasidharan, M. Zweckstetter, S. A. Rensing, and S. Eimer. The *Caenorhabditis elegans* garp complex contains the conserved vps51 subunit and is required to maintain lysosomal morphology. *Mol Biol Cell*, 22(14):2564–78, 2011.

J. Ma, M. Flemr, P. Stein, P. Berninger, R. Malik, M. Zavolan, P. Svoboda, and R. M. Schultz. MicroRNA activity is suppressed in mouse oocytes. *Curr. Biol.*, 20(3):265–270, 2010.

M. J. Macias, S. Wiesner, and M. Sudol. WW and SH3 domains, two different scaffolds to recognize proline-rich ligands. *FEBS Lett.*, 513(1):30–37, 2002.

I. J. MacRae, E. Ma, M. Zhou, C. V. Robinson, and J. A. Doudna. In vitro reconstitution of the human RISC-loading complex. *Proc. Natl. Acad. Sci. U.S.A.*, 105(2):512–517, 2008.

K. S. Makarova, Y. I. Wolf, J. van der Oost, and E. V. Koonin. Prokaryotic homologs of Argonaute proteins are predicted to function as key components of a novel system of defense against mobile genetic elements. *Biol. Direct*, 4:29, 2009.

N. J. Martinez, M. C. Ow, J. S. Reece-Hoyes, M. I. Barrasa, V. R. Ambros, and A. J. Walhout. Genome-scale spatiotemporal analysis of *Caenorhabditis elegans* microRNA promoter activity. *Genome Res*, 18(12):2005–15, 2008.

C. Mello and A. Fire. DNA transformation. *Methods Cell Biol.*, 48:451–482, 1995.

C. C. Mello, J. M. Kramer, D. Stinchcomb, and V. Ambros. Efficient gene transfer in C.elegans: extrachromosomal maintenance and integration of transforming sequences. *EMBO J.*, 10(12):3959–3970, 1991.

J. T. Mendell and E. N. Olson. MicroRNAs in stress signaling and human disease. *Cell*, 148(6):1172–1187, 2012.

W. J. Meyer, S. Schreiber, Y. Guo, T. Volkmann, M. A. Welte, and H. A. Muller. Overlapping functions of argonaute proteins in patterning and morphogenesis of Drosophila embryos. *PLoS Genet*, 2(8):e134, 2006.

S. Mi, T. Cai, Y. Hu, Y. Chen, E. Hodges, F. Ni, L. Wu, S. Li, H. Zhou, C. Long, S. Chen, G. J. Hannon, and Y. Qi. Sorting of small RNAs into Arabidopsis argonaute complexes is directed by the 5' terminal nucleotide. *Cell*, 133(1):116–27, 2008.

Y. Mishima, C. Abreu-Goodger, A. A. Staton, C. Stahlhut, C. Shou, C. Cheng, M. Gerstein, A. J. Enright, and A. J. Giraldez. Zebrafish miR-1 and miR-133 shape muscle gene expression and regulate sarcomeric actin organization. *Genes Dev.*, 23(5):619–632, 2009.

E. A. Miska, E. Alvarez-Saavedra, A. L. Abbott, N. C. Lau, A. B. Hellman, S. M. McGonagle, D. P. Bartel, V. R. Ambros, and H. R. Horvitz. Most *Caenorhabditis elegans* microRNAs are individually not essential for development or viability. *PLoS Genet.*, 3(12):e215, 2007.

E. A. Miska, E. Alvarez-Saavedra, M. Townsend, A. Yoshii, N. Sestan, P. Rakic, M. Constantine-Paton, and H. R. Horvitz. Microarray analysis of microRNA expression in the developing mammalian brain. *Genome Biol.*, 5(9):R68, 2004.

T. Miyoshi, A. Takeuchi, H. Siomi, and M. C. Siomi. A direct role for Hsp90 in pre-RISC formation in Drosophila. *Nat. Struct. Mol. Biol.*, 17(8):1024–1026, 2010.

S. Morita, T. Horii, M. Kimura, Y. Goto, T. Ochiya, and I. Hatada. One Argonaute family member, Eif2c2 (Ago2), is essential for development and appears not to be involved in DNA methylation. *Genomics*, 89(6):687–96, 2007.

E. G. Moss, R. C. Lee, and V. Ambros. The cold shock domain protein LIN-28 controls developmental timing in *C. elegans* and is regulated by the *lin-4* rna. *Cell*, 88(5):637–46, 1997.

E. P. Murchison, J. F. Partridge, O. H. Tam, S. Cheloufi, and G. J. Hannon. Characterization of Dicer-deficient murine embryonic stem cells. *Proc. Natl. Acad. Sci. U.S.A.*, 102(34):12135–12140, 2005.

M. A. Newman, J. M. Thomson, and S. M. Hammond. Lin-28 interaction with the Let-7 precursor loop mediates regulated microRNA processing. *RNA*, 14(8):1539–1549, 2008.

A. S. Nicot, H. Fares, B. Payrastre, A. D. Chisholm, M. Labouesse, and J. Laporte. The phosphoinositide kinase PIKfyve/Fab1p regulates terminal lysosome maturation in *Caenorhabditis elegans*. *Mol. Biol. Cell*, 17(7):3062–3074, 2006.

K. Okamura, J. W. Hagen, H. Duan, D. M. Tyler, and E. C. Lai. The mirtron pathway generates microRNA-class regulatory RNAs in Drosophila. *Cell*, 130(1):89–100, 2007.

K. Okamura, M. D. Phillips, D. M. Tyler, H. Duan, Y. T. Chou, and E. C. Lai. The regulatory activity of microRNA* species has substantial influence on microRNA and 3' UTR evolution. *Nat. Struct. Mol. Biol.*, 15(4):354–363, 2008.

C. T. Pager, K. A. Wehner, G. Fuchs, and P. Sarnow. MicroRNA-mediated gene silencing. *Prog Mol Biol Transl Sci*, 90:187–210, 2009.

J. M. Pare, J. Lopez-Orozco, and T. C. Hobman. MicroRNA-binding is required for recruitment of human Argonaute 2 to stress granules and P-bodies. *Biochem. Biophys. Res. Commun.*, 414(1):259–264, 2011.

J. H. Park, S. Ahn, S. Kim, J. Lee, J. W. Nam, and C. Shin. Degradome sequencing reveals an endogenous microRNA target in C. elegans. *FEBS Lett.*, 587(7):964–969, 2013.

D. H. Parry, J. Xu, and G. Ruvkun. A whole-genome rnai screen for *C elegans* miRNA pathway genes. *Curr Biol*, 17(23):2013–22, 2007.

D. M. Pavelec, J. Lachowiec, T. F. Duchaine, H. E. Smith, and S. Kennedy. Requirement for the ERI/DICER complex in endogenous RNA interference and sperm development in *Caenorhabditis elegans*. *Genetics*, 183(4):1283–1295, 2009.

F. J. Perez-Victoria, G. A. Mardones, and J. S. Bonifacino. Requirement of the human garp complex for mannose 6-phosphate-receptor-dependent sorting of cathepsin d to lysosomes. *Mol Biol Cell*, 19(6):2350–62, 2008.

F. J. Perez-Victoria, C. Schindler, J. G. Magadan, G. A. Mardones, C. Delevoye, M. Romao, G. Raposo, and J. S. Bonifacino. Ang2/fat-free is a conserved subunit of the Golgi-associated retrograde protein complex. *Mol. Biol. Cell*, 21(19):3386–3395, 2010.

R. C. Piper and D. J. Katzmann. Biogenesis and function of multivesicular bodies. *Annu. Rev. Cell Dev. Biol.*, 23:519–547, 2007.

E. Piskounova, C. Polytarchou, J. E. Thornton, R. J. LaPierre, C. Pothoulakis, J. P. Hagan, D. Iliopoulos, and R. I. Gregory. Lin28A and Lin28B inhibit let-7 microRNA biogenesis by distinct mechanisms. *Cell*, 147(5):1066–1079, 2011.

C. G. Proud. eIF2 and the control of cell physiology. *Semin. Cell Dev. Biol.*, 16(1):3–12, 2005.

H. Qin, F. Chen, X. Huan, S. Machida, J. Song, and Y. A. Yuan. Structure of the Arabidopsis thaliana DCL4 DUF283 domain reveals a noncanonical double-stranded RNA-binding fold for protein-protein interaction. *RNA*, 16(3):474–481, 2010.

A. Ravi, A. M. Gurtan, M. S. Kumar, A. Bhutkar, C. Chin, V. Lu, J. A. Lees, T. Jacks, and P. A. Sharp. Proliferation and tumorigenesis of a murine sarcoma cell line in the absence of DICER1. *Cancer Cell*, 21(6):848–855, 2012.

B. J. Reinhart, F. J. Slack, M. Basson, A. E. Pasquinelli, J. C. Bettinger, A. E. Rougvie, H. R. Horvitz, and G. Ruvkun. The 21-nucleotide let-7 rna regulates developmental timing in *Caenorhabditis elegans*. *Nature*, 403(6772):901–6, 2000.

J. D. Richter. Cytoplasmic polyadenylation in development and beyond. *Microbiol. Mol. Biol. Rev.*, 63(2):446–456, 1999.

J. D. Richter and P. Lasko. Translational control in oocyte development. *Cold Spring Harb Perspect Biol*, 3(9):a002758, 2011.

D. L. Riddle, T. Blumenthal, B. J. Meyer, and J. Priess. *C. elegans II*. Cold Spring Harbor Laboratory Press, 2nd edition, 1997.

T. A. Rouault. The role of iron regulatory proteins in mammalian iron homeostasis and disease. *Nat. Chem. Biol.*, 2(8):406–414, 2006.

S. Ruegger and H. Grosshans. MicroRNA turnover: when, how, and why. *Trends Biochem. Sci.*, 37(10):436–446, 2012.

R. Russ and F. J. Slack. Cigarette-Smoke-Induced Dysregulation of MicroRNA Expression and Its Role in Lung Carcinogenesis. *Pulm Med*, 2012:791234, 2012.

A. Rybak, H. Fuchs, L. Smirnova, C. Brandt, E. E. Pohl, R. Nitsch, and F. G. Wulczyn. A feedback loop comprising lin-28 and let-7 controls pre-let-7 maturation during neural stem-cell commitment. *Nat. Cell Biol.*, 10(8):987–993, 2008.

S. Sarin, M. M. O'Meara, E. B. Flowers, C. Antonio, R. J. Poole, D. Didiano, R. J. Johnston, S. Chang, S. Narula, and O. Hobert. Genetic screens for *Caenorhabditis elegans* mutants defective in left/right asymmetric neuronal fate specification. *Genetics*, 176(4):2109–2130, 2007.

H. M. Sasaki and Y. Tomari. The true core of RNA silencing revealed. *Nat. Struct. Mol. Biol.*, 19(7):657–660, 2012.

A. N. Sawh and T. F. Duchaine. Turning Dicer on its head. *Nat. Struct. Mol. Biol.*, 19(4):365–366, 2012.

N. T. Schirle and I. J. MacRae. The crystal structure of human Argonaute2. *Science*, 336(6084):1037–1040, 2012.

W. R. Shaw, J. Armisen, N. J. Lehrbach, and E. A. Miska. The conserved miR-51 microRNA family is redundantly required for embryonic development and pharynx attachment in *Caenorhabditis elegans*. *Genetics*, 185(3):897–905, 2010.

Z. Shi and G. Ruvkun. The mevalonate pathway regulates microrna activity in *Caenorhabditis elegans*. *Proc Natl Acad Sci U S A*, 109(12):4568–73, 2012.

F. Simmer, M. Tijsterman, S. Parrish, S. P. Koushika, M. L. Nonet, A. Fire, J. Ahringer, and R. H. Plasterk. Loss of the putative RNA-directed RNA polymerase RRF-3 makes *C elegans* hypersensitive to RNAi. *Curr. Biol.*, 12(15):1317–1319, 2002.

S. Siniossoglou and H. R. Pelham. Vps51p links the VFT complex to the SNARE Tlg1p. *J. Biol. Chem.*, 277(50):48318–48324, 2002.

M. C. Siomi, K. Saito, and H. Siomi. How selfish retrotransposons are silenced in Drosophila germline and somatic cells. *FEBS Lett*, 582(17):2473–8, 2008.

M. C. Siomi, K. Sato, D. Pezic, and A. A. Aravin. PIWI-interacting small RNAs: the vanguard of genome defence. *Nat. Rev. Mol. Cell Biol.*, 12(4):246–258, 2011.

F. J. Slack, M. Basson, Z. Liu, V. Ambros, H. R. Horvitz, and G. Ruvkun. The lin-41 rbcc gene acts in the *C. elegans* heterochronic pathway between the let-7 regulatory rna and the lin-29 transcription factor. *Molecular cell*, 5(4):659–69, 2000.

T. Spruce, B. Pernaute, A. Di-Gregorio, B. S. Cobb, M. Merkenschlager, M. Manzanares, and T. A. Rodriguez. An early developmental role for miRNAs in the maintenance of extraembryonic stem cells in the mouse embryo. *Dev. Cell*, 19(2):207–219, 2010.

M. Stadler, K. Artiles, J. Pak, and A. Fire. Contributions of mrna abundance, ribosome loading, and post- or peri-translational effects to temporal repression of *C. elegans* heterochronic miRNA targets. *Genome Res*, 2012.

F. A. Steiner, S. W. Hoogstrate, K. L. Okihara, K. L. Thijssen, R. F. Ketting, R. H. Plasterk, and T. Sijen. Structural features of small RNA precursors determine Argonaute loading in *Caenorhabditis elegans*. *Nat. Struct. Mol. Biol.*, 14(10):927–933, 2007.

H. Su, M. I. Trombly, J. Chen, and X. Wang. Essential and overlapping functions for mammalian Argonautes in microRNA silencing. *Genes Dev*, 23(3):304–17, 2009.

N. Suh, L. Baehner, F. Moltzahn, C. Melton, A. Shenoy, J. Chen, and R. Blelloch. MicroRNA function is globally suppressed in mouse oocytes and early embryos. *Curr. Biol.*, 20(3):271–277, 2010.

N. Suh and R. Blelloch. Small RNAs in early mammalian development: from gametes to gastrulation. *Development*, 138(9):1653–1661, 2011.

J. E. Sulston and H. R. Horvitz. Post-embryonic cell lineages of the nematode, *Caenorhabditis elegans*. *Dev. Biol.*, 56(1):110–156, 1977.

J. E. Sulston, E. Schierenberg, J. G. White, and J. N. Thomson. The embryonic cell lineage of the nematode *Caenorhabditis elegans*. *Dev. Biol.*, 100(1):64–119, 1983.

Y. Suzuki, M. Minami, M. Suzuki, K. Abe, S. Zenno, M. Tsujimoto, K. Matsumoto, and Y. Minami. The Hsp90 inhibitor geldanamycin abrogates colocalization of eIF4E and eIF4E-transporter into stress granules and association of eIF4E with eIF4G. *J. Biol. Chem.*, 284(51):35597–35604, 2009.

H. Tabara, M. Sarkissian, W. G. Kelly, J. Fleenor, A. Grishok, L. Timmons, A. Fire, and C. C. Mello. The rde-1 gene, RNA interference, and transposon silencing in *C elegans*. *Cell*, 99(2):123–132, 1999.

N. Tahbaz, J. B. Carmichael, and T. C. Hobman. Gerp95 belongs to a family of signal-transducing proteins and requires hsp90 activity for stability and golgi localization. *The Journal of biological chemistry*, 276(46):43294–9, 2001.

N. Tahbaz, F. A. Kolb, H. Zhang, K. Jaronczyk, W. Filipowicz, and T. C. Hobman. Characterization of the interactions between mammalian PAZ PIWI domain proteins and Dicer. *EMBO Rep.*, 5(2):189–194, 2004.

M. G. Thomas, M. Loschi, M. A. Desbats, and G. L. Boccaccio. RNA granules: the good, the bad and the ugly. *Cell. Signal.*, 23(2):324–334, 2011.

K. L. Thompson-Peer, J. Bai, Z. Hu, and J. M. Kaplan. HBL-1 patterns synaptic remodeling in *C elegans*. *Neuron*, 73(3):453–465, 2012.

Y. Tomari, T. Du, and P. D. Zamore. Sorting of Drosophila small silencing RNAs. *Cell*, 130(2):299–308, 2007.

B. B. Tops, R. H. Plasterk, and R. F. Ketting. The *Caenorhabditis elegans* Argonautes ALG-1 and ALG-2: almost identical yet different. *Cold Spring Harb Symp Quant Biol*, 71:189–94, 2006.

M. van Kouwenhove, M. Kedde, and R. Agami. MicroRNA regulation by RNA-binding proteins and its implications for cancer. *Nat. Rev. Cancer*, 11(9):644–656, 2011.

A. Vasquez-Rifo, G. Jannot, J. Armisen, M. Labouesse, S. I. Bukhari, E. L. Rondeau, E. A. Miska, and M. J. Simard. Developmental characterization of the microrna-specific *C. elegans* argonautes alg-1 and alg-2. *PLoS One*, 7(3):e33750, 2012.

H. Vaucheret. Post-transcriptional small RNA pathways in plants: mechanisms and regulations. *Genes Dev.*, 20(7):759–771, 2006.

R. Vazquez-Martinez and M. M. Malagon. Rab proteins and the secretory pathway: the case of rab18 in neuroendocrine cells. *Front Endocrinol (Lausanne)*, 2:1, 2011.

M. C. Vella, E. Y. Choi, S. Y. Lin, K. Reinert, and F. J. Slack. The *C. elegans* microrna let-7 binds to imperfect let-7 complementary sites from the lin-41 3'utr. *Genes Dev*, 18(2):132–7, 2004.

M. C. Vella and F. J. Slack. *C elegans* microRNAs. *WormBook*, pages 1–9, 2005.

A. Ventura and T. Jacks. MicroRNAs and cancer: short RNAs go a long way. *Cell*, 136(4):586–591, 2009.

A. Ventura, A. G. Young, M. M. Winslow, L. Lintault, A. Meissner, S. J. Erkeland, J. Newman, R. T. Bronson, D. Crowley, J. R. Stone, R. Jaenisch, P. A. Sharp, and T. Jacks. Targeted deletion reveals essential and overlapping functions of the miR-17 through 92 family of miRNA clusters. *Cell*, 132(5):875–886, 2008.

S. R. Viswanathan, G. Q. Daley, and R. I. Gregory. Selective blockade of microRNA processing by Lin28. *Science*, 320(5872):97–100, 2008.

H. W. Wang, C. Noland, B. Siridechadilok, D. W. Taylor, E. Ma, K. Felderer, J. A. Doudna, and E. Nogales. Structural insights into RNA processing by the human RISC-loading complex. *Nat. Struct. Mol. Biol.*, 16(11):1148–1153, 2009.

L. Wang and J. Wang. MicroRNA-mediated breast cancer metastasis: from primary site to distant organs. *Oncogene*, 31(20):2499–2511, 2012.

M. B. Warf, W. E. Johnson, and B. L. Bass. Improved annotation of *C elegans* microRNAs by deep sequencing reveals structures associated with processing by Drosha and Dicer. *RNA*, 17(4):563–577, 2011.

M. B. Warf, B. A. Shepherd, W. E. Johnson, and B. L. Bass. Effects of ADARs on small RNA processing pathways in *C elegans*. *Genome Res.*, 22(8):1488–1498, 2012.

L. Weill, E. Belloc, F. A. Bava, and R. Mendez. Translational control by changes in poly(A) tail length: recycling mRNAs. *Nat. Struct. Mol. Biol.*, 19(6):577–585, 2012.

N. C. Welker, D. M. Pavelec, D. A. Nix, T. F. Duchaine, S. Kennedy, and B. L. Bass. Dicer's helicase domain is required for accumulation of some, but not all, *C elegans* endogenous siRNAs. *RNA*, 16(5):893–903, 2010.

J. O. Westholm and E. C. Lai. Mirtrons: microRNA biogenesis via splicing. *Biochimie*, 93(11):1897–1904, 2011.

E. Wienholds, M. J. Koudijs, F. J. van Eeden, E. Cuppen, and R. H. Plasterk. The microRNA-producing enzyme Dicer1 is essential for zebrafish development. *Nat. Genet.*, 35(3):217–218, 2003.

B. Wightman, I. Ha, and G. Ruvkun. Posttranscriptional regulation of the heterochronic gene lin-14 by lin-4 mediates temporal pattern formation in *C. elegans*. *Cell*, 75(5):855–62, 1993.

M. Wildwater, N. Sander, G. de Vreede, and S. van den Heuvel. Cell shape and Wnt signaling redundantly control the division axis of *C elegans* epithelial stem cells. *Development*, 138(20):4375–4385, 2011.

E. Wu, C. Thivierge, M. Flamand, G. Mathonnet, A. A. Vashisht, J. Wohlschlegel, M. R. Fabian, N. Sonenberg, and T. F. Duchaine. Pervasive and cooperative deadenylation of 3'UTRs by embryonic microRNA families. *Mol. Cell*, 40(4):558–570, 2010.

N. Yanaihara, N. Caplen, E. Bowman, M. Seike, K. Kumamoto, M. Yi, R. M. Stephens, A. Okamoto, J. Yokota, T. Tanaka, G. A. Calin, C. G. Liu, C. M. Croce, and C. C. Harris. Unique microRNA molecular profiles in lung cancer diagnosis and prognosis. *Cancer Cell*, 9(3):189–198, 2006.

J. S. Yang, M. D. Phillips, D. Betel, P. Mu, A. Ventura, A. C. Siepel, K. C. Chen, and E. C. Lai. Widespread regulatory activity of vertebrate microRNA* species. *RNA*, 17(2):312–326, 2011.

B. Yao, L. B. La, Y. C. Chen, L. J. Chang, and E. K. Chan. Defining a new role of GW182 in maintaining miRNA stability. *EMBO Rep.*, 13(12):1102–1108, 2012.

R. Yi, D. O'Carroll, H. A. Pasolli, Z. Zhang, F. S. Dietrich, A. Tarakhovsky, and E. Fuchs. Morphogenesis in skin is governed by discrete sets of differentially expressed microRNAs. *Nat. Genet.*, 38(3):356–362, 2006.

R. Yi, Y. Qin, I. G. Macara, and B. R. Cullen. Exportin-5 mediates the nuclear export of pre-microRNAs and short hairpin RNAs. *Genes Dev.*, 17(24):3011–3016, 2003.

I. M. Yu and F. M. Hughson. Tethering factors as organizers of intracellular vesicular traffic. *Annu. Rev. Cell Dev. Biol.*, 26:137–156, 2010.

H. Zahreddine, H. Zhang, M. Diogon, Y. Nagamatsu, and M. Labouesse. CRT-1/calreticulin and the E3 ligase EEL-1/HUWE1 control hemidesmosome maturation in *C elegans* development. *Curr. Biol.*, 20(4):322–327, 2010.

H. Zhang and A. Z. Fire. Cell autonomous specification of temporal identity by *Caenorhabditis elegans* microrna lin-4. *Developmental biology*, 344(2):603–10, 2010.

H. Zhang and M. Labouesse. The making of hemidesmosome structures in vivo. *Dev Dyn*, 239(5):1465–76, 2010.

H. Zhang, F. Landmann, H. Zahreddine, D. Rodriguez, M. Koch, and M. Labouesse. A tension-induced mechanotransduction pathway promotes epithelial morphogenesis. *Nature*, 471(7336):99–103, 2011.

L. Zhang, L. Ding, T. H. Cheung, M. Q. Dong, J. Chen, A. K. Sewell, X. Liu, J. R. Yates, and M. Han. Systematic identification of *C elegans* miRISC proteins, miRNAs, and mRNA targets by their interactions with GW182 proteins AIN-1 and AIN-2. *Mol. Cell*, 28(4):598–613, 2007.

G. X. Zheng, A. Ravi, J. M. Calabrese, L. A. Medeiros, O. Kirak, L. M. Dennis, R. Jaenisch, C. B. Burge, and P. A. Sharp. A latent pro-survival function for the mir-290-295 cluster in mouse embryonic stem cells. *PLoS Genet.*, 7(5):e1002054, 2011.

M. Zhong, W. Niu, Z. J. Lu, M. Sarov, J. I. Murray, J. Janette, D. Raha, K. L. Sheaffer, H. Y. Lam, E. Preston, C. Slightham, L. W. Hillier, T. Brock, A. Agarwal, R. Auerbach, A. A. Hyman, M. Gerstein, S. E. Mango, S. K. Kim, R. H. Waterston, V. Reinke, and M. Snyder. Genome-wide identification of binding sites defines distinct functions for *Caenorhabditis elegans* PHA-4/FOXA in development and environmental response. *PLoS Genet*, 6(2):e1000848, 2010.

D. F. Zielinska, F. Gnad, K. Schropp, J. R. Winiewski, and M. Mann. Mapping N-glycosylation sites across seven evolutionarily distant species reveals a divergent substrate proteome despite a common core machinery. *Mol. Cell*, 46(4):542–548, 2012.

Y. Zou, H. Chiu, D. Domenger, C. F. Chuang, and C. Chang. The lin-4 microRNA targets the LIN-14 transcription factor to inhibit netrin-mediated axon attraction. *Sci Signal*, 5(228):ra43, 2012.

Appendix A

A primer on *C. elegans* embryonic development

A.1 *Caenorhabditis elegans*

The *Caenorhabditis elegans* is a free living nematode species, constituted by males and protandrious [1] hermaphrodites. Anatomically, their vermiform body is protected by a cuticle, produced by a subjacent syncitial hypodermis. Inside of it, gonads and the muscular, nervous, excretory and digestive systems are found. As result of the *C. elegans* development a fixed number of somatic nuclei is produced [2], 959 in hermaphrodites and 1031 in males. The *C. elegans* species has a short life cycle (3 days at 25°C), and passes through four larval stages (L1 to L4) to reach adulthood. Under unfavorable conditions L2 stage worms can enter an alternative stage to form 'dauer larvae'. The fast life cycle, reproductive mode with copious progeny and the array of available experimental techniques among other features make *C. elegans* a very good model organism for genetic studies (Riddle *et al.*, 1997).

A.2 Embryonic development

The *C. elegans* embryonic development, start with fertilization of the ovocyte by sperm leading to the completion of meiosis and production of the eggshell. The egg contains all the material supply necessary to develop and hatch into a L1 stage worm. Overall, during embryonic development this animal acquire most of its somatic cells and organs. In contrast, the germ cells start to proliferate only post-embryonically and concomitantly all the reproductive organs form (somatic gonad, spermatecha, uterus and vulva, male copulatory organ). Additional

1. Self-fertilizing, produce sperm first and then ovocytes
2. this feature is known as eutely.

post-embryonic divisions also occur at other tissues, including the hypodermis[3], muscle and gut.

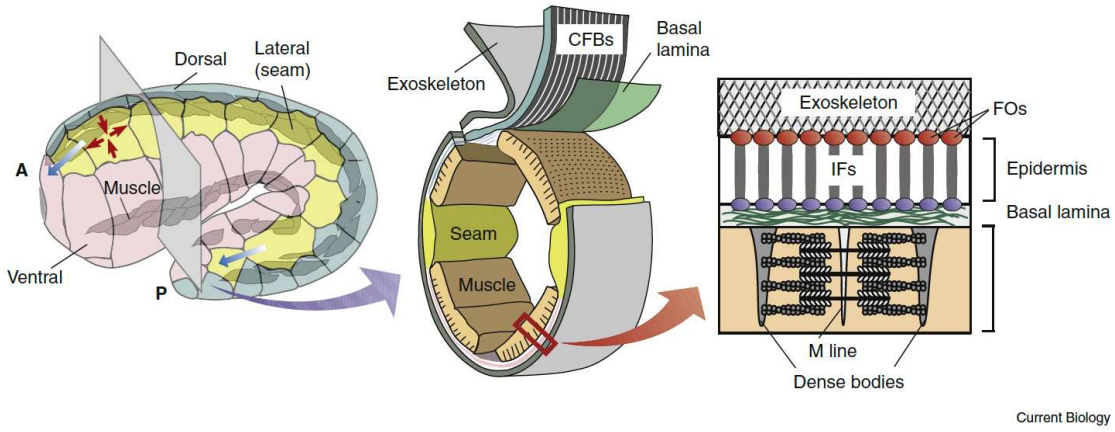

Figure A.1: **Anatomy of epidermal and muscle attachment structures.** At the left, a 1.5 fold stage worm is depicted. Fully enclosed by the dorsal (blue), lateral (seam cells in yellow) and ventral (pink) hypodermal cells. The underneath muscle rows are depicted in grey color. The forces produced by the hypodermal cells (red arrows) contribute to anteroposterior (A and P) elongation. At the center a transversal worm section illustrates the connection of muscle and hypodermal cells to a common basal lamina. In addition, hypodermal cells contact the exoskeleton and display circumferential actin bundles (CFB). At the left, the structural components that mediate the physical muscle-hypodermis tissue attachements are indicated. The fibrous organelles (FOs) connected by intermediate filaments (IFs) mediate the attachement of the hypodermal cells to the exoskeleton and the basal lamina. Muscle cells attach to the same lamina by means of dense bodies. Figure reproduced with permission from (Hardin, 2011).

The embryonic development can be divided into an initial phase of cell proliferation, the 'pre-morphogenetic' phase, followed by a phase where most division cease but dramatic tissue rearrangements and organ formation happen (so called the 'morphogenetic phase'). During the initial premorphogenetic phase rapid cell divisions take place, and the embryo becomes an ovoid mass of approximately 550 cells. Some cell rearrengements take place during this phase, for example, the endoderm precursors invaginate into the embryo interior (gastrulation). During the morphogenetic phase the embryo will transform from a ovoid mass of cells into a worm with most of its organs. This involves the following processes:

– **Epidermal cell intercalation**. The previously specified epidermal cells are initially located at the dorsal part of the embryo arranged in several anteroposterior rows. As result of the epidermal 'intercalation' process the two more dorsally located rows merge into a single row of cells.

3. the 'hypodermis' and 'epidermis' denominations are considered equivalent in the worm.

- **Epidermal cell migration and ventral enclosure.** A set of the dorsal epidermal cells actively extend cytoplasmic protusions towards the ventral side of the embryo from both lateral sides. Once the two extending sets of epidermal cells have reached the ventral side, they establish close contact with each other and seal into a single epithelial sheet (the 'ventral enclosure' process). In this manner the embryo becomes completely covered by an epithelial sheet.
- **Embryonic elongation.** Once the embryo is completely surrounded by its epidermis the 'elongation' process starts. In this dynamic process the embryo passes from an ovoid to a stretched vermiform shape by a stark enlargement of its anteroposterior axis. Two distinct phases of the elongation process are recognized. During 'early elongation' the contractile force generated by the cytoskeleton of the hypodermal cells is transmited throughout the epithelial sheets and embryo, as consequence the embryo shape changes from the 'comma' stage to the '1.5 fold' stage. During 'late elongation' the participation of both the epithelial cells and muscular tissue is required. Embryos of mutants defective in muscle contractility or with defective extracellular matrix components, paralyze at the '2-fold' stage, a diagnostic phenotype named 'Pat' (paralyzed at 2-fold). The muscle and hypodermal cells coordinate their action given that they are physically attached. Both cell types are adhered to a common basal lamina, the hypodermal cells attach to the lamina by a cytoskeletal structure named the fibrous organelle (FO). The FO consist of hemidesmosomes connected through intermediate filaments, FO components include plectin (VAB-10) protein and the adaptor protein VAB-19. On the basal side of the hypodermal cells, the FOs contact the basal lamina while at the apical side, FOs establish a mechanical link to the worm exoskeleton (Figure A.1). Importantly, the FOs are properly patterned by the muscular contractions, through processes involving mechanotransduction (Zhang *et al.* (2011)). The action and mechanical coupling of these two tissues will allow embryo elongation from the '2-fold' stage until completion.

Appendix B

A primer on vesicular trafficking

B.1 Introduction

Membranes define the boundaries of many compartments inside the cells. Given that most macromolecules can not freely diffuse through membranes, the maintenance of the different membrane-bound compartments and the material exchange between compartments requires specialized systems. Among those different systems, several are mediated by vesicles which form from a donor compartment and fuse to a target membrane. A set of factors have been proposed to define the specificity of this vesicular system, including SNARE proteins, the small GTPases of the Rab family, vesicle tethering complexes and other components. The roles of vesicle trafficking include: 1) The exchange of biomolecules between the cell and its environment by the process of endocytosis and exocytosis; 2)The sorting and recycling of many proteins to their appropriate organelles and; 3) The degradation of membrane proteins, the biomolecules enclosed in vesicles, and even cytosolic components (through the process of autophagy).

B.1.1 Trafficking components

Among the phethora of trafficking components, two are briefly described here: Rabs and SNARES.

The rab family of small GTPases can directly associate to the membranes upon prenylation, a lipidic modification that allows membrane anchoring. These proteins switch from Guanosine diphosphate (GDP) to Guanosine triphosphate (GTP) bound states and when activated function by recruiting 'Rab effector' proteins.

SNARE (soluble NSF attachment protein receptor) proteins are a set of protein families that

share a common 60-70 aminoacids long motif (the SNARE motif), that mediates the formation of SNARE complexes. SNARE proteins in the vesicle and target membranes form complexes *in trans*. Three SNARE proteins interact to form a four helix bundle, and this complex is key to bring the vesicle and target membranes into very close proximity for the subsequent membrane fusion process (Fasshauer *et al.*, 1998).

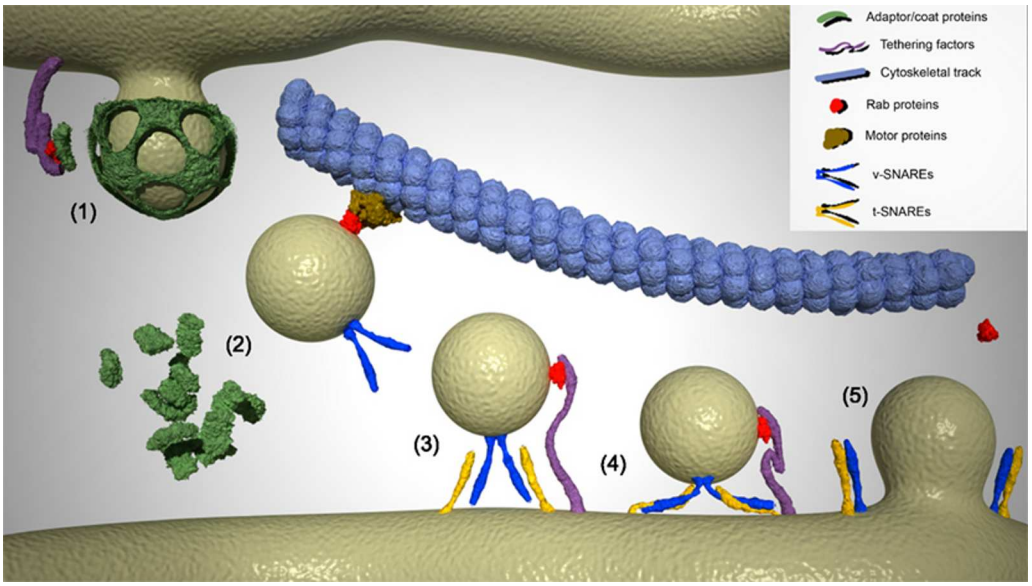

Figure B.1: **Schematic of the processes of vesicular traffic.** Figure reproduced with permission from Vazquez-Martinez and Malagon (2011).

B.1.2 Tethering complexes

Vesicles bud from a donor compartment, enclosing the molecules to be transported (termed 'cargo') with the help of 'coat proteins' (*e.g* clathrin) and are transported towards their target membrane. The process that culminates with the fusion of a vesicle to its target membrane is divided in three phases. The initial 'tethering' phase, correspond to the first contact between the incoming vesicle and the target membrane, it is mediated by 'tethering complexes' that establish a physical bridge between the vesicle and the target membranes through interactions with proteins of both compartments, like small GTPases of distinct families and the SNARE proteins. Tethering is followed by the 'docking' phase, were membrane-spanning SNARE proteins sitting at the target and vesicle interact *in trans* to bring the vesicle and the target membrane into close proximity. Finally, the 'fusion' phase take place, whereby the contents of the vesicle are released (Figure B.1).

The tethering complexes are a structurally diverse set of proteins. They are usually partition into two classes: coiled coils homodimers (*e.g.* p115/Uso1) and multisubunit complexes (re-

viewed in Yu and Hughson 2010). Tethering complexes are specifically localized to the target membranes where the incoming vesicles will fuse (Figure B.2). The multisubunit complexes include (Koumandou *et al.*, 2007):

- **TRAPPI complex**. It is involved in intra-Golgi anterograde transport.
- **DSL1 complex**. Involved in Golgi to ER retrograde transport.
- **COG complex**. Involved in transport through the Golgi.
- **HOPS complex**. Role in transport from endosomes to lysosomes.
- **GARP complex**. It is involved in endosome to Golgi transport.
- **Exocyst complex**. Role in transport of vesicles to the plasma membrane.

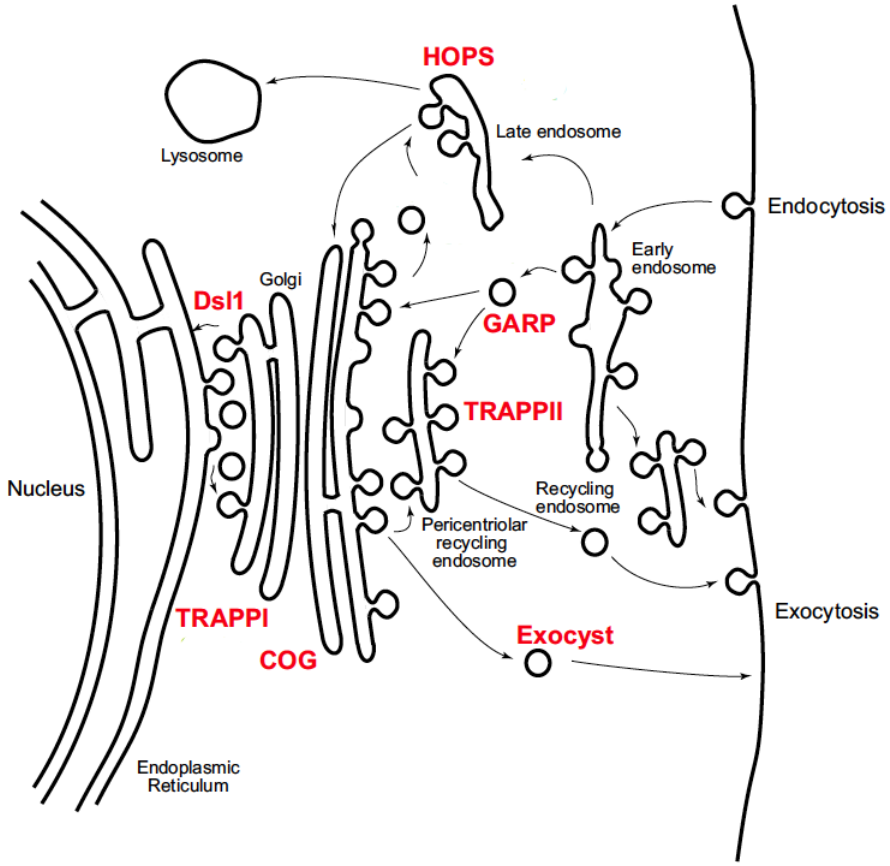

Figure B.2: **Intracellular tethering complexes.** The indicated tethering complexes (named in red) are shown at their intracellular locations. Figure reproduced with permission from (Koumandou *et al.*, 2007).

Of particular interest among the tethering factors in this thesis, is the GARP (Golgi Associated Retrograde Protein) complex, a highly conserved complex composed of four subunits in yeast, mammals and *C. elegans* (VPS-51/-52-/-53/-54). This complex has been proposed to have a distant similarity to the COG, DSL1 and exocyst complexes (Koumandou *et al.*, 2007).

Biochemical and structural analysis propose that the GARP complex has a core formed by the interacting amino-terminal coiled coil regions of its subunits, while the carboxy-terminus engage in interactions necessary for tethering (reviewed in Bonifacino and Hierro 2011).

B.1.3 Endosomal sorting

The endosomal compartment intersects several trafficking routes, and its principal role is to mediate the sorting of proteins either to recycle them back to another compartment (plasma membrane or Golgi complex) or direct them towards lysosomal degradation. In general, this compartment transition from early to late endosomes, develops intraluminal vesicles (becoming Multivesicular endosomes or Multivesicular Bodies (MVBs)) and ultimately fuses to lysosomes to release and degrade their content. During this transition processes, proteins located at the endosomal membrane are sorted. The ones targeted for lysosomal degradation are incorporated into the MVBs intraluminal vesicles and destroyed upon fusion with the lysosomes, the ones recycled leave the endosome through vesicles.

A series of proteins, known as ESCRT complexes (Endosomal Sorting Complex Required for Transport Complex), function in the trafficking and sorting of proteins at the endosomes. Four complexes are commonly recognized (ESCRT-0, -I, -II, -III). A current model of their action is the following (reviewed in Piper and Katzmann 2007). Proteins destinated to sorting or degradation are ubiquitinated, this ubiquitinated cargo is then brought to endosomes by peripheral ubiquitin (Ub) receptors. Once there, the ESCRT-I and ESCRT-II complexes may function to promote release of the cargo from the peripheral receptor and position it in an environment suitable for further processing. Next, polymerizing ESCRT-III subunits incarcerate the cargo and recruit deubiquitinating enzymes to recycle the cargo-attached Ub molecule. At this point, the cargo is ready for incorporation into MVB intraluminal vesicles, the formation and fission of these vesicles occurs through largely unknown mechanisms. Finally, the cargo contained in the vesicles inside the MVB is degraded upon release of MVB contents into lysosomes.

Appendix C

The microRNA pathway controls germ cells proliferation and differentiation in *C. elegans*

Foreword

The present appendix is constituted by an article published in the journal 'Cell research' (Bukhari *et al.*, 2012). I participated in this study of my colleague Irfan Bukhari by generating plasmids and the corresponding transgenic reporter lines (MJS13 and *alg-1(gk214)*Ex [*plag-2::rfp::alg-1*]). This study defined a role for the microRNA-specfic Argonautes and the microRNA pathway in controlling multiple aspects of germ cells biology.

Cell Research (2012) 22:1034-1045.

www.nature.com/cr

ORIGINAL ARTICLE

The microRNA pathway controls germ cell proliferation and differentiation in *C. elegans*

Syed Irfan Ahmad Bukhari[1], Alejandro Vasquez-Rifo[1], Dominic Gagné[2], Eric R Paquet[1], Monique Zetka[3], Claude Robert[2], Jean-Yves Masson[1], Martin J Simard[1]

[1]Laval University Cancer Research Centre, Hôtel-Dieu de Québec (CHUQ), Quebec City, Québec, Canada G1R 2J6; [2]Laboratoire de génomique fonctionnelle du développement embryonnaire, Centre de recherche en biologie de la reproduction, Pavillon Comtois, Faculté des sciences de l'agriculture et de l'alimentation, Université Laval, Québec, Canada G1V 0A6; [3]Department of Biology, McGill University, 1205 avenue Doctor Penfield, Montréal, QC, Canada H3A 1B1

The discovery of the miRNA pathway revealed a new layer of molecular control of biological processes. To uncover new functions of this gene regulatory pathway, we undertook the characterization of the two miRNA-specific Argonaute proteins in *Caenorhabditis elegans*, ALG-1 and ALG-2. We first observed that the loss-of-function of *alg-1* and *alg-2* genes resulted in reduced progeny number. An extensive analysis of the germline of these mutants revealed a reduced mitotic region, indicating fewer proliferating germ cells. We also observed an early entry into meiosis in *alg-1* and *alg-2* mutant animals. We detected ALG-1 and ALG-2 protein expressions in the distal tip cell (DTC), a specialized cell located at the tip of both *C. elegans* gonadal arms that regulates mitosis-meiosis transition. Re-establishing the expression of *alg-1* specifically in the DTC of mutant animals partially rescued the observed germline defects. Further analyses also support the implication of the miRNA pathway in gametogenesis. Interestingly, we observed that disruption of five miRNAs expressed in the DTC led to similar phenotypes. Finally, gene expression analysis of *alg-1* mutant gonads suggests that the miRNA pathway is involved in the regulation of different pathways important for germline proliferation and differentiation. Collectively, our data indicate that the miRNA pathway plays a crucial role in the control of germ cell biogenesis in *C. elegans*.

***Keywords*:** argonaute; miRNA; germline

Cell Research (2012) **22**:1034-1045. doi:10.1038/cr.2012.31; published online 28 February 2012

Introduction

MiRNAs are 21-23 nucleotides long non-coding RNA molecules processed from hairpin-structured RNAs by Drosha and Dicer RNaseIII enzymes. These short RNA molecules induce translational repression and gene silencing of their target mRNAs via interaction with an Argonaute protein. Members of this protein family are classified into three groups: Argonaute-like proteins (AGO); Piwi-like proteins and *C. elegans*-specific AGOs (WAGOs) (reviewed in [1]). In *C. elegans,* AGO-clade proteins ALG-1 and ALG-2 have been identified to be involved exclusively in the miRNA pathway [2]. MiRNAs regulate a plethora of biological processes including cell proliferation, cell differentiation and apoptosis, processes important to coordinate developmental timing (reviewed in [3, 4]). Since the discovery of the prominent miRNA families of *lin-4* and *let-7* in determining *C. elegans* developmental timing (reviewed in [4]), their mammalian homologs have also been identified to control cell proliferation in human cell lines [5, 6]. Recent studies suggest that mammalian *let-7* miRNA could regulate developmental processes via regulation of several cell cycle-related genes [7, 8]. Since the deletion of a single family of miRNA often fails to induce severe defects *in vivo* [9, 10], it has been suggested that most biological processes are subjected to regulation of a cumulative effect by various miRNAs.

Among these processes, the studies of animals carrying mutations of important components of the miRNA

Correspondence: Jean-Yves Masson[a], Martin J Simard[b]
[a]E-mail: Jean-Yves.Masson@crhdq.ulaval.ca
[b]E-mail: Martin.Simard@crhdq.ulaval.ca
Received 16 August 2011; revised 16 November 2011; accepted 20 December 2011; published online 28 February 2012

pathway indicate the contribution of miRNAs in the animal germline. In *Drosophila*, mutations of *dcr-1*, *ago-1* and *loquacious* genes resulted in defects in germline maintenance [11-14]. In *C. elegans*, alteration of the *dcr-1* gene rendered animals sterile despite retaining a normal gonad due to the strong maternal rescue [15]. Additionally, deletion of the Drosha-encoding gene *drsh-1* also led to sterility in nematode [16].

Here, we report that Argonaute proteins ALG-1 and ALG-2 are expressed in the distal tip cells (DTCs) of the *C. elegans* germline. Mutations in *alg-1* and *alg-2* result in drastically reduced number of progeny. We observed that this reduction in fertility is caused by defects in multiple processes in germline development, including reduced germ cell proliferation and increase in apoptosis. Our findings suggest that ALG-1/2 function, together with a set of miRNAs expressed in the DTCs to regulate diverse biological pathways important to maintain animal germline proliferation and differentiation.

Results

MicroRNA-specific Argonautes are required for germ cell proliferation

Since defects in the development of the germline will be reflected in the progeny number, we first investigated the brood size of ALG-1 and ALG-2 loss-of-function mutants, named as *alg-1(gk214)* and *alg-2(ok304),* respectively. Compared to wild-type animals, we noticed a significantly reduced brood size in *alg-1(gk214)* and *alg-2(ok304)*, though such reduction was more drastic in *alg-1(gk214)* (Table 1). As any defects during germline proliferation, meiosis or gamete formation could affect progeny number, we first asked if these mutants have defects in cell proliferation in the germline. We extruded germline of young adults from wild-type, *alg-1(gk214)* and *alg-2(ok304)* animals, followed by staining of DNA with DAPI to monitor the spatio-temporal progression of different meiotic phases. Cells with crescent-shaped nuclear morphology mark the transition zone, which represents the leptotene/zygotene stage of meiosis [17, 18]. Compared to the wild-type animals, the mitotic regions of *alg-1(gk214)* and *alg-2(ok304)* are shorter as determined by the morphology of the germ cell nuclei (Figure 1A-1C) and by the number of cells in the mitotic region (Table 1). To corroborate our findings from the DAPI staining, we used an antibody specific to HIM-3, a meiosis-specific axis component between sister chromatids [19], as a *bona fide* marker of entry into meiosis. In agreement with our earlier findings, anti-HIM-3 antibody revealed an early entry into meiosis in *alg-1(gk214)* and *alg-2(ok304)*, compared to the wild type (Figure 1D-1F). Similar defects were observed with another loss-of-function allele of the *alg-1* gene (*alg-1(tm492)*) as well as in *alg-1(RNAi)* animals (Supplementary information, Figure S1). These results suggest that ALG-1 and ALG-2 are involved in the regulation of germline proliferation.

Expression of ALG-1 in the DTC controls germ cell proliferation

To better decipher how *alg-1* and *alg-2* control germ cell proliferation and meiosis entry, we next decided to observe the expression pattern of ALG-1 and ALG-2 proteins in animal gonads. By immunostaining of extruded gonads using a newly generated ALG-1-specific antibody (Supplementary information, Figure S2), we observed that ALG-1 is localized to the DTC of the wild-type gonads but not in *alg-1(gk214)* (Figure 2A). To overcome the non-availability of ALG-2-specific antibody, we generated a transgenic line somatically expressing GFP-

Table 1 Phenotypes observed in the germline of *alg-1(gk214)* and *alg-2(ok304)* animals

Strain	Brood size (*N*=25)	Nb of cells in MR (*N*=5)	Oocyte / arm day 1 (*N*=5)	Oocyte / arm day 2 (*N*=5)	Average corpses/ arm (*N*=5)
Wild-type	266.4 ± 3.22	240.3 ± 0.63	9.06 ± 0.06	9.84 ± 0.12	2.98 ± 0.19
alg-1(gk214)	77.0 ± 5.64	203.9 ± 1.26	5.48 ± 0.16	6.08 ± 0.07	4.38 ± 0.18
	*(5.68E−20)	*(1.93E−05)	*(6.51E−06)	*(3.33E−05)	*(0.01)
alg-2(ok304)	178.8 ± 4.27	213.7 ± 0.43	7.0 ± 0.07	7.18 ± 0.24	4.12 ± 0.05
	*(4.24E−14)	*(1.99E−06)	*(1.03E−05)	*(0.0015)	*(0.001)
lag-2p::rfp::alg-1	142.12 ± 5.6	237.2 ± 1.4	6.7 ± 0.17	6.4 ± 0.2	3.28 ± 0.08
	*(3.70E−17)	*(0.134)	*(9.61E−05)	*(8.68E−05)	*(0.184)
	**(5.34E−08)	**(0.0001)	**(0.005)	**(0.186)	**(0.004)

N: number of animals (brood size) or number of replicates (10 animals/replicate); MR: Mitotic region. The brood sizes were defined as the numbers of viable larvae that developed to the L1 stage descended from a single hermaphrodite of its strain. In parenthesis, *P*-values were calculated with a Student's *t*-test to compare numbers with wild-type (*) or *alg-1(gk214)* (**) animals, and represented as ± SEM.

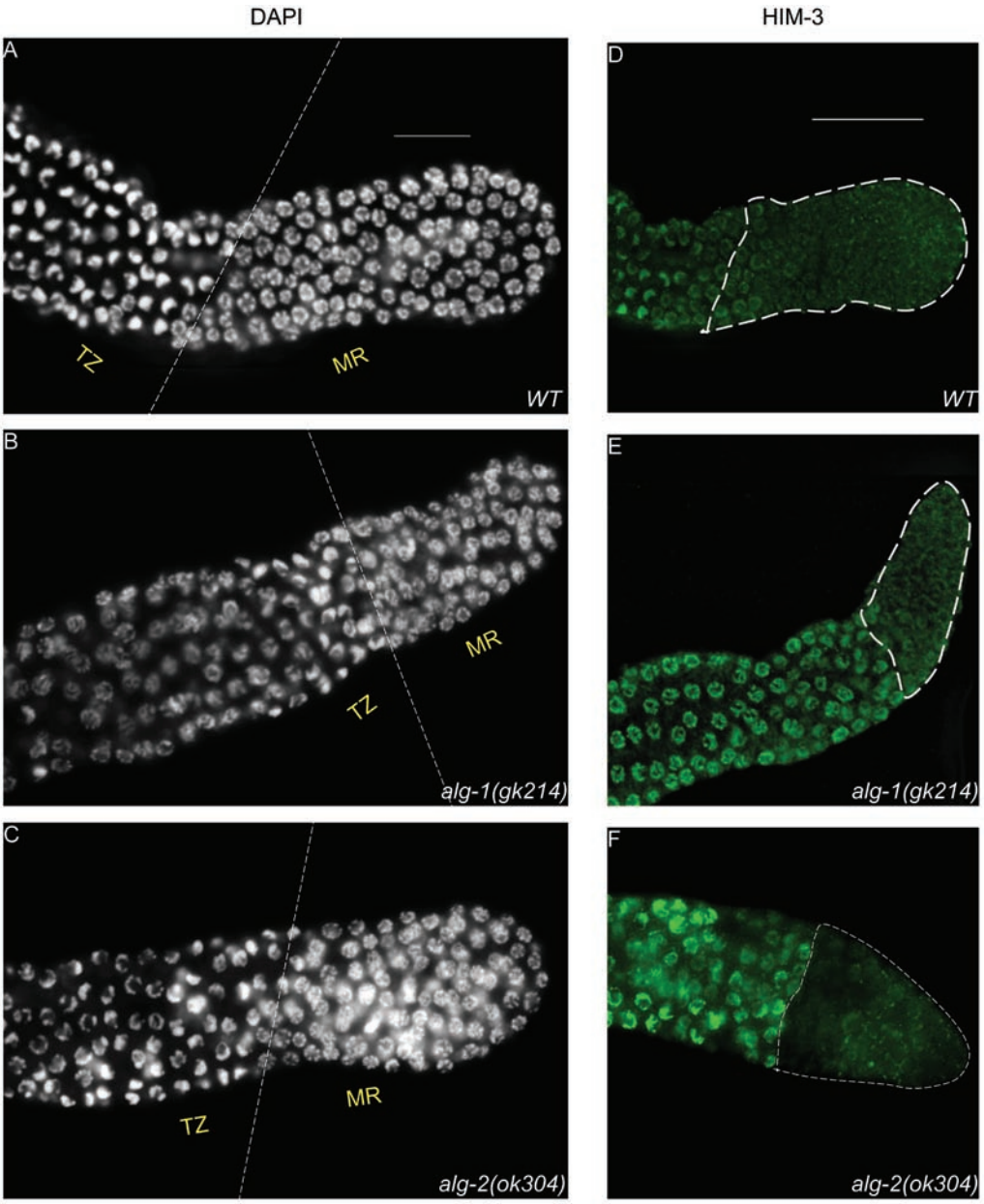

Figure 1 *alg-1* and *alg-2* mutant gonads have shorter mitotic region and display early entry into meiosis. **(A-C)** DAPI-stained germline depicting mitotic region (MR) and transition zone (TZ) in wild-type (WT), *alg-1(gk214)* and *alg-2(ok304)* mutant animals. **(D-F)** Staining with HIM-3 antibody (green) depicting entry into meiosis in wild-type (WT) gonads and *alg-1*(*gk214*) and *alg-2(ok304)*. Scale bar measures 20 μm.

tagged ALG-2 (MJS13) and found that ALG-2 is also localized in the DTC of the gonads (Figure 2B). DTC caps the distal end of the germline, and provides the stem cell niche. These specialized cells are also responsible for maintaining proliferation in the distal part of the gonad arm, which is the mitotic region [20-23]. When the contact between the DTC and germ cells is breached, cells enter into meiosis. To determine whether the presence of ALG-1 in the DTC is crucial to control germ cell proliferation and differentiation, we generated a transgenic line where ALG-1 expression is under control of the promoter of *lag-2*, a membrane-bound Delta/Serrate/LAG-2 ligand expressed exclusively in the DTC [24]. When re-establishing ALG-1 expression in the DTC (Figure 2C), we were able to partially rescue the brood size compared to the *alg-1* mutant (Table 1), as well as fully restore the

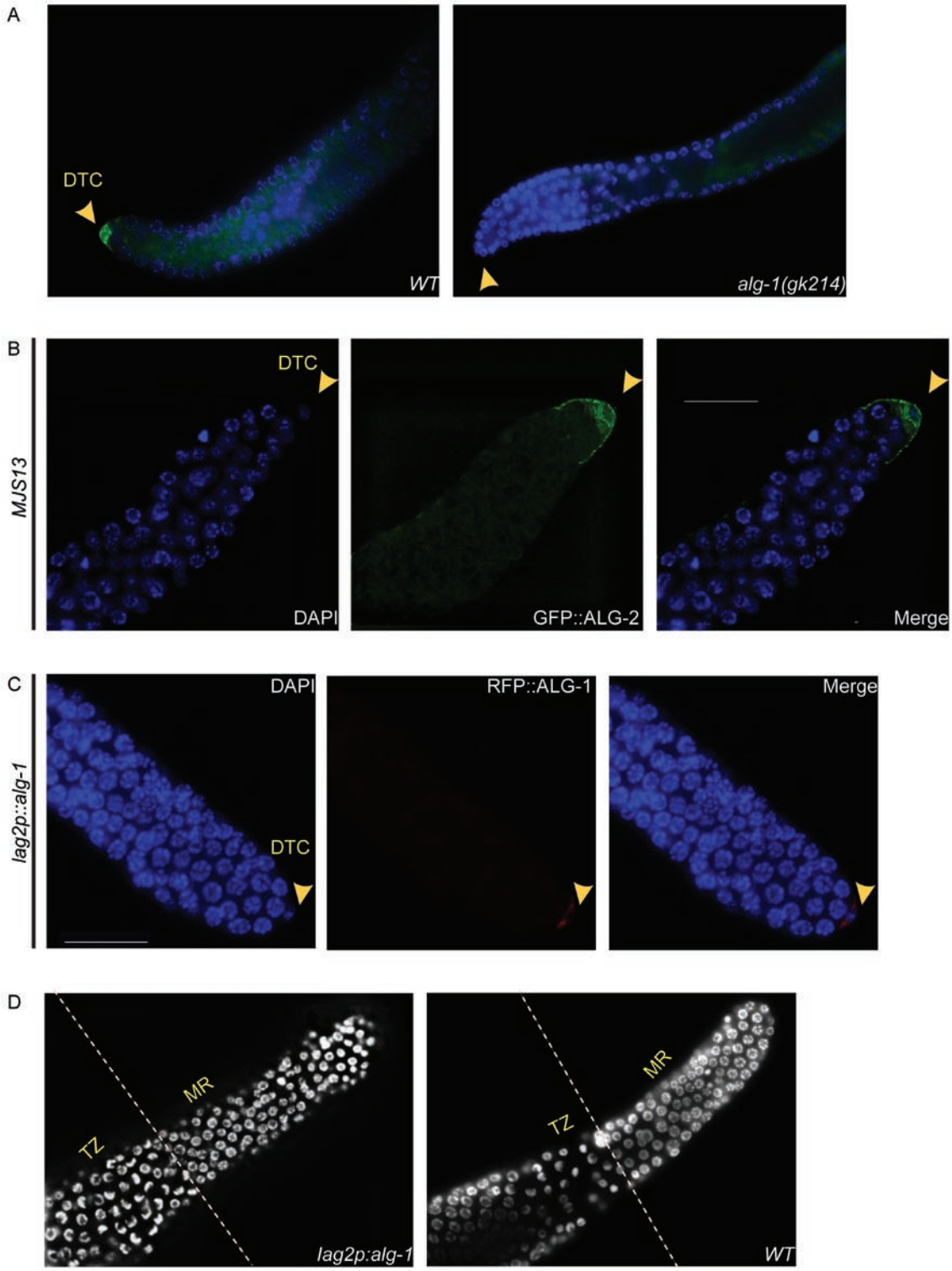

Figure 2 ALG-1 and ALG-2 localize to the DTC. **(A)** Anti-ALG-1 antibody depicts ALG-1 localization to the DTC of wild-type (WT) germline, but not in *alg-1(gk214)*. **(B)** ALG-2 (green) expression in DTC of *gfp::alg-2* (MJS13) transgenic line. Gonads were counter stained with DAPI (blue) to visualize nuclei. **(C)** ALG-1 localized exclusively in DTC of transgenic animals expressing RFP-tagged ALG-1 protein under control of the DTC-specific *lag-2* promoter (lag-2p). Arrows indicate DTC. **(D)** Restoration of mitotic region in *lag-2p::rfp::alg-1*-expressing animals shown by DAPI staining compared to wild-type gonad. Scale bar measures 20 μm.

normal length of the mitotic region (Figure 2D and Table 1, compared to wild type). To further decipher the role of *alg-1* beyond the DTC, we scored the brood size in transgenic animals expressing RFP-tagged ALG-1 under the control of endogenous *alg-1* promoter and 3′UTR. Apart from the DTC, RFP::ALG-1 is also expressed in sheath

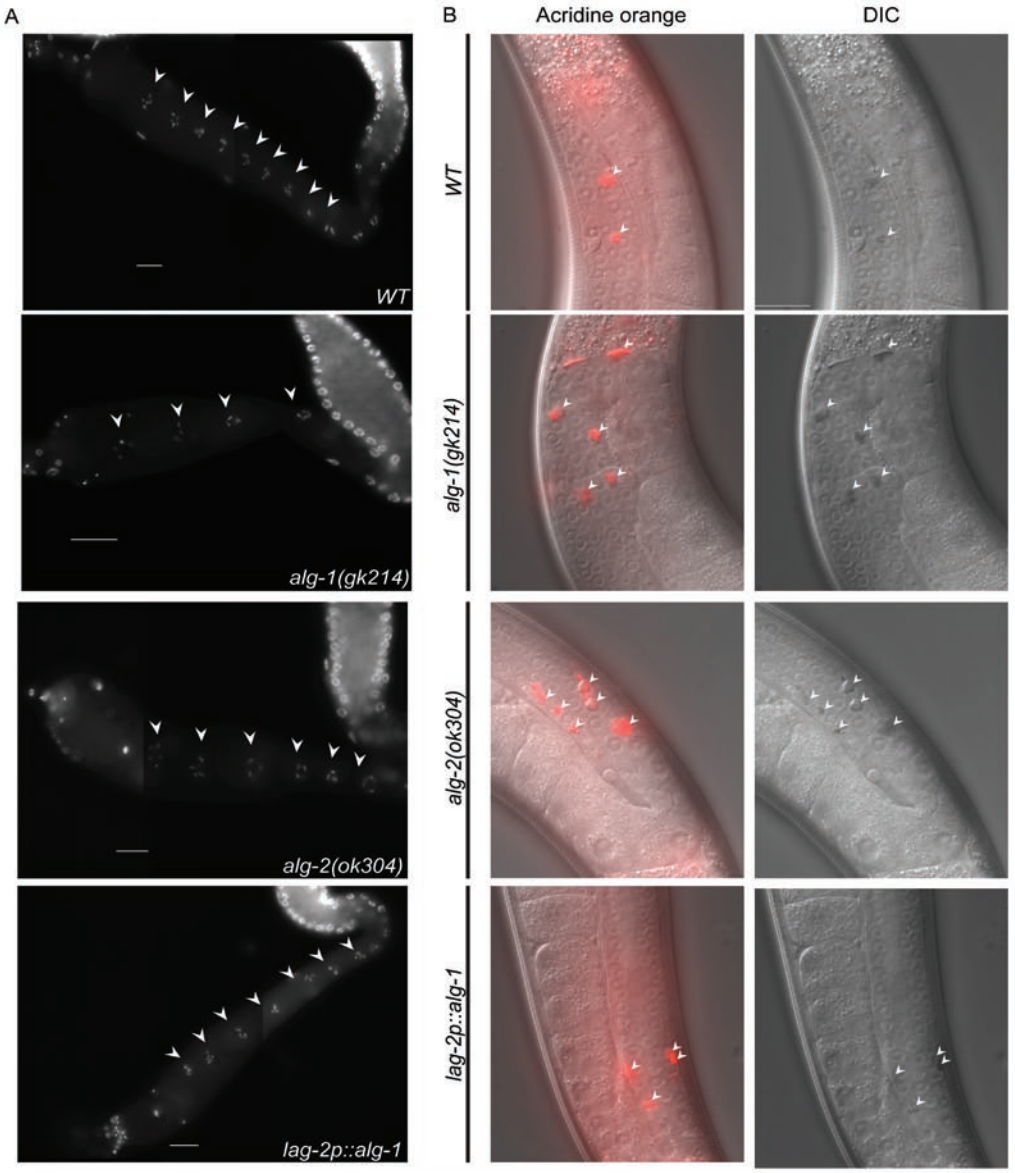

C

Strain	Brood size (N=12)	Brood size after mating with wild-type (N=12)	*p* - value
alg-1(gk214)	77 ± 9.6	120.9 ± 8.2	0.002
alg-2(ok304)	175.58 ± 5.4	210.16 ± 8.6	0.008
plag-2::alg-1	142.33 ± 9.5	146.91 ± 7.2	0.75
WT	274.5 ± 4.04	491.33 ± 20.3	8.19E-07

Figure 3 Effects of ALG-1 and ALG-2 on oocytes. **(A)** DAPI-stained germline. Arrowheads depict oocyte nuclei in diakinesis stage in the proximal gonad arm of wild-type (WT), *alg-1(gk214)*, *alg-2(ok304)* and *plag-2::rfp::alg-1* animals. **(B)** Merged and nomarski DIC micrographs of AO-stained germline in respective genetic backgrounds. Arrowheads mark apoptotic corpses. **(C)** Brood size in *alg-1* and *alg-2* mutant animals as well as in *plag-2::alg-1* and wild-type animals after mating with wild-type males represented as average brood size ± SEM, $P < 0.01$.

cells besides other somatic tissues (AVR, unpublished data). We observed that these transgenic animals showed a significant increase in brood size compared to animals with DTC-expressed *alg-1* (158 ± 2.7 vs 142.12 ± 5.6 for *plag-2::alg-1*; $P < 0.017$). Taken together, our results indicate that ALG-1 plays a role within the DTC as well as in other tissues of the gonads.

ALG-1 and ALG-2 are important for gamete formation and maintenance

Since germ cells undergo proliferation (mitosis), gametogenesis (meiosis and differentiation) or apoptosis, we examined if the loss of the miRNA-specific Argonautes *alg-1* and *alg-2* genes can affect the fates of germ cells in animals. Although we did not observe high incidence of males and the dead eggs phenotype in *alg-1(gk214)* and *alg-2(ok304)* animals (two notable consequences of meiotic defects in *C. elegans*, data not shown), we found that both mutants have significantly reduced number of oocytes than the wild-type animals (Figure 3A and Table 1). Using the vital dye acridine orange (AO), which has been used to stain apoptotic cells in live animals [25], as well as differential interference contrast (DIC) microscopy, we observed increased germ cell corpses in the proximal region of the gonad arm in *alg-1(gk214)* and *alg-2(ok304)* (Figure 3B and Table 1). The fact that both DIC microscopy and AO staining detect the same number of germ cell corpses, suggests that mutants have an increase in apoptosis rather than defective engulfment in the germline. Re-establishing the expression of ALG-1 in the DTC partially restores the number of oocytes and reduces germ cell corpses (Figure 3B and Table 1). We next determined if the decrease in brood size also results from defects in male gametes formation. We observed that sperm nuclei number in *alg-1* and *alg-2* mutant hermaphrodites is not significantly different from the wild-type animals (data not shown). However, when the two Argonaute mutants were mated with wild-type males, we observed a significant increase in the brood size compared to the unmated mutant hermaphrodites, but brood size is significantly smaller than that of the wild-type hermaphrodites mated with wild-type males (Figure 3C). In addition, the brood size of animals with DTC-expressed *alg-1* is not enhanced upon mating with wild-type males (Figure 3C). This observation supports that re-establishing ALG-1 expression in the DTC mainly rescues spermiogenesis, and thus sustains the fact that ALG-1 is required in other gonadal tissues. Together, our data show that ALG-1 and ALG-2 are involved in maintaining *C. elegans* fertility.

miRNAs expressed in the DTC are implicated in germ cell proliferation and differentiation

Since ALG-1 and ALG-2 are imperative to miRNA-induced gene silencing, we next decided to identify candidate miRNAs involved in germline maintenance. Recently, the expression pattern of several *C. elegans* miRNAs has been studied *in vivo* using miRNA promoter::GFP fusion constructs [26]. Of the total of 70 transgenic *C. elegans* strains reported, 8 *pmiRNA::gfp* strains (*plet-7, plin-4, pmir-80, pmir-237, pmir-247-797, pmir-359, pmir-53* and *pmir-71*) exhibited expression in the DTC. We thus examined animals carrying mutant alleles of the eight miRNA genes, to determine if they

Table 2 Different phenotypes observed in miRNA mutants

Strain	Brood size (*N*=20)	Nb of cells in MR (*N*=5)	Oocytes / arm day 1 (*N*=5)	Oocytes / arm day 2 (*N*=5)
Wild-type	266.4 ± 3.7	240.3 ± 0.63	9.06 ± 0.06	9.84 ± 0.12
let-7(n2853)	43.9 ± 3.1 (6.45E−22)	192.02 ± 1.4 (3.40E−06)	5.8 ± 0.07 (1.66E−06)	*ND
lin-4(e912)	30.0 ± 0.9 (1.07E−23)	197.6 ± 1.2 (4.11E−06)	5.6 ± 0.12 (1.81E−06)	*ND
mir-359(n4540)	235.6 ± 6.8 (0.002)	221.3 ± 0.9 (5.39E−05)	7.7 ± 0.12 (0.001)	8.98 ± 0.09 (0.01)
mir-247(n4505)	207.7 ± 5.9 (3.10E−07)	200.94 ± 2.6 (0.0002)	7.6 ± 0.12 (0.0003)	8.84 ± 0.08 (0.003)
mir-237(n4296)	222.1 ± 7.4 (4.37E−05)	213.7 ± 1.9 (5.45E−05)	8.82 ± 0.05 **(0.70)	10.12 ± 0.32 **(0.40)

N: number of animals (brood size) or number of replicates (10 animals/replicate); MR: Mitotic region; ND: Not determined. In parenthesis, *P*-values were calculated with a Student's *t*-test to compare the significance of the numbers with wild-type animals and represented as ± SEM.

*Most of the population died after the first day of fertile adults.

***mir-237(n4296)* animals have similar number of oocytes as the wild-type.

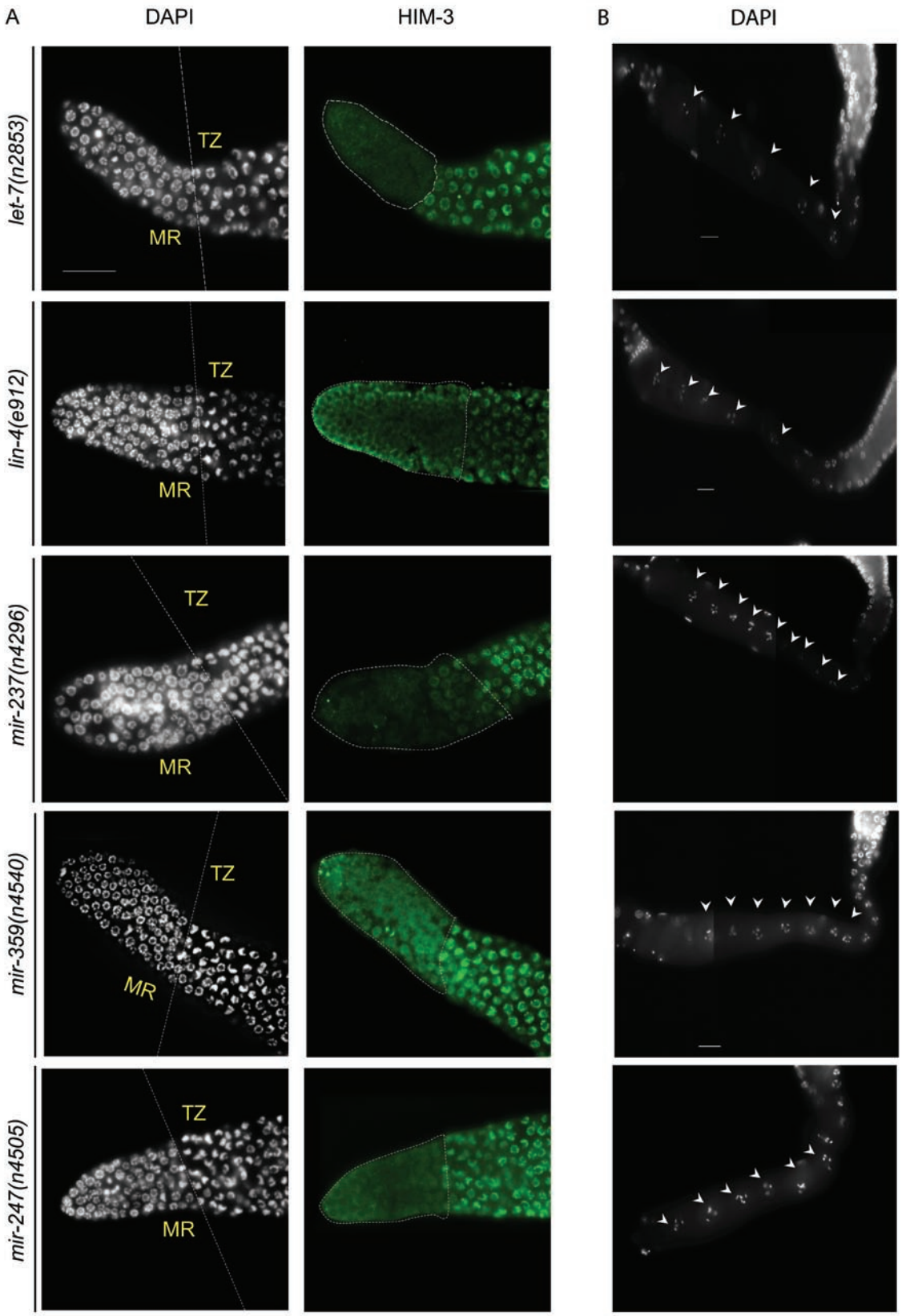

Figure 4 A subset of miRNAs expressed in the DTC affects germline proliferation and oocytes. **(A)** DAPI and HIM-3 staining depicting shorter mitotic region observed in *let-7*, *lin-4*, *miR-237* and *mir-247* in mutant animals. **(B)** DAPI-stained germline. Arrowheads depict oocyte nuclei in diakinesis stage in the proximal gonad arm of miRNA mutant animals.

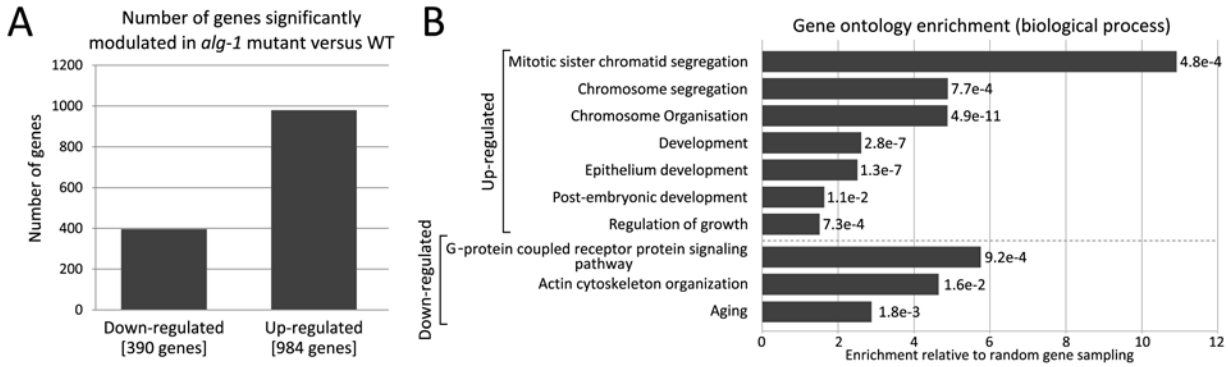

Figure 5 Comparative microarray analyses of genes expressed in the germline. **(A)** Number of genes significantly modulated in extruded *alg-1* mutant versus wild-type gonads. Selected significant genes have a fold change > 2 and a *P*-value < 0.001 (*N* = 4; the list of can be found in Supplementary information, Table S1). **(B)** Gene ontology biological process enrichment performed using DAVID. The upper part corresponds to enrichment obtained when using the list of downregulated genes and the bottom part of the upregulated genes. Numbers to the right represent Benjamini-Hochberg *P*-values.

display phenotypes similar to *alg-1(gk214)* and *alg-2(ok304)*. Among them, we found that *let-7(n2853)*, *lin-4(e912)*, *miR-237(n4296)*, *miR-359(n4540)* and *miR-247(n4505)* mutants displayed similar phenotypes to *alg-1(gk214*) and *alg-2(ok304)*. All five mutant strains had significantly smaller brood size and shorter mitotic region with reduced number of cells within the mitotic region compared to wild type (Figure 4 and Table 2). While the *let-7(n2853)*, *lin-4(e912)*, *miR-359(n4540)* and *mir-247(n4505)* mutant animals have shorter mitotic region as well as fewer number of oocytes, *mir-237(n4296)* mutant animals have only shorter mitotic region but normal oocyte number (Figure 4 and Table 2), and *miR-80(nDf53)*, *mir-71(n4115)* and *mir-53(n4113)* mutant strains have no apparent germline defect (Supplementary information, Figure S3). These observations suggest that a variety of miRNAs regulate different processes at multiple steps in germline biogenesis.

Since the regulation by miRNAs often leads to a decrease in target mRNAs [27-30], we next decided to compare the level of mRNAs found in gonads of wild-type and *alg-1* animals to uncover putative targets of *let-7*, *lin-4*, *miR-237*, *miR-359* and *miR-247* miRNAs in the germline. When we compared microarray data from four independent biological samples, we observed that the level of 1 374 different mRNAs is significantly altered in the absence of *alg-1* (with a threshold of > 2-fold change, $P \leq 0.001$; Figure 5 and Supplementary information, Table S1). A clustering analysis of the gene expression data revealed a significant alteration in the expression of genes associated with biological pathways important for chromosome organization and segregation (Figure 5). Although they are not significantly enriched, we notably found putative targets predicted by either TargetScan [31] or miRWIP [32] algorithm for *let-7*, *lin-4*/*miR-237* (since they are similar in sequence, they are predicted to target the same mRNAs [33]), *miR-359* and *miR-247* miRNAs among mRNAs misregulated in the germline of *alg-1* mutant (Supplementary information, Table S2). Thus, our results implicate that these miRNAs contribute to the regulation of the process of gamete formation and differentiation in *C. elegans* by affecting the expression of multiple mRNA targets.

Discussion

Earlier studies performed in *Drosophila* have highlighted that components of the miRNA pathway are required for germline stem cell self-renewal, [11, 13, 14, 34] and that the maternally expressed *bantam* and *miR-184* miRNAs contribute to oogenesis [35, 36]. While our data revealed that the role of the miRNA pathway in germline maintenance is conserved in *C. elegans*, our results also support for the first time that both miRNA-specific Argonaute proteins ALG-1 and ALG-2 in the stem cell niche are crucial for the proper control of germ cell proliferation and gametes formation.

Previous studies of *C. elegans* strains carrying mutations in Drosha (*drsh-1*) and Dicer (*dcr-1*) genes, two important processors of miRNAs, showed that these mutants were sterile [15, 16]. In our laboratory, we observed that post-embryonic RNAi of ALG-1 on *alg-2* background or vice versa could also render animals sterile (unpublished data). These observations indicate that the miRNA pathway is indispensible in animal reproduction. Our current study showed that germline proliferation is

reduced in both miRNA-specific Argonaute mutants. The restoration of ALG-1 exclusively in the DTC, rescues the mitotic cell number in the germline, which leads to a partial but significant increase in brood size, suggesting that miRNAs play a role in germline cell division. Additionally, our observation of fewer oocytes and increased apoptotic corpses in both *alg-1* and *alg-2* suggests that miRNAs are also important regulators in gamete formation. Consistent with our findings, mice with either global deletion of dicer or with oocyte-specific deletion of AGO2 display failures in oogenesis due to arrest at meiosis I [37-40]. These animals also have severely reduced number of spermatogonia, which could be due to proliferation defects and an increase in apoptosis [39, 41, 42]. However, it has yet to be determined in vertebrates the contribution of miRNAs in gametogenesis, since the loss of Dicer also affects the production of endogenous siRNAs, a type of small RNAs that are also important in this process [43-45].

In *C. elegans*, a single DTC in each gonad arm establishes germline stem cell niche. It controls germ cells fate by employing in part the GLP-1/Notch signaling through a network of RNA-binding regulatory proteins, most notably, Pumilio and FBF, to maintain a balance between proliferation and differentiation [46]. While the RNA-binding proteins GLD-1, GLD-2/GLD-3 promote the meiosis entry of germline stem cells, the activation of the GLP-1/Notch signaling pathway inhibits these signals and retains the cells in mitotic stage [47]. Interestingly, *gld-1* mRNA has been found in ALG-1-immunoprecipitated complex [48], and other evidence also indicates that *gld-1* is subject to regulation by miRNAs [49]. These studies suggest the possibility that miRNAs can regulate the mitosis to meiosis decision by controlling key genes involved in the process.

We demonstrate that mutants of five different miRNAs which are known to localize to the DTC display similar phenotypes as the ones observed in *alg-1* and *alg-2* mutants, suggesting that more than one miRNA participate in stem cell fate regulation. Our extensive microarray analysis of mRNAs expressed in *alg-1* mutant gonads, detected the mis-regulation of more than 1 300 genes. Among them, we observed that the expression of the major sperm proteins (MSPs), was upregulated in *alg-1* mutant gonads. MSP signaling is known to regulate the oocyte production and development. The proximal MSP signaling works coordinately with the distal GLP-1 signaling to regulate the proper oocyte growth and function [50, 51]. We thus envision that GLP-1 and MSP signaling are both subject to the miRNA regulation, and the loss of the miRNA-specific Argonaute genes leads to alterations in both signaling pathways, likely due to imbalance of these proteins, and thus affecting the fertility of the animals. Therefore, the phenotypes observed in the germline of *alg-1* and *alg-2* mutants reflect that different miRNAs are involved in germline biogenesis by regulating different pathways. Hence, it may be difficult to recapitulate the *alg-1* and *alg-2* mutant phenotypes by inactivating specific miRNAs. We therefore propose that the phenotypes of *alg-1* and *alg-2* mutants result from the combinatorial effect of miRNAs and their targets.

Materials and Methods

Strains

All the strains were maintained according to standard protocols [52]. The *let-7(n2853)* and *lin-4(e912)* mutant strains were maintained at 15 °C and *let-7(n2853)* (shifted to 20 °C beyond L4 stage). All other strains were maintained at 20 °C. The *alg-1(gk214)* mutant carries an out-of-frame deletion of 200 bp after the 28th amino acid and terminates by 2 additional amino acids. The *alg-2(ok304)* allele is an out-of-frame deletion that removes the nucleotides encoding amino acids 34-374 and terminates after encoding 8 additional amino acids from another reading frame. They are therefore likely to be null alleles of *alg-1* and *alg-2*. Further details can be found on the *C. elegans* Gene Knockout Consortium website. All mutant strains have been outcrossed at least three times before analyses.

Rescue experiments

Transgenic MJS13 line was generated by microinjecting a mix of reporter plasmids (pRF4), MSp59 (*alg-1p::RFP::alg-1*) and MSp72 (*alg-2p::GFP::alg-2*) and crossed into *alg-1(gk214)* strain. Extrachromosomal arrays were UV integrated. The *plag-2::alg-1* line (MJS26) was generated by microinjecting a mix of pRF4 and MSp151 plasmids and crossed into *alg-1(gk214)* strain. A 3 kb promoter of *lag-2* was excised by *Bam*HI from pJK590 [53] and cloned into *Bam*HI-digested pBluescriptII SK+ to generate MSp147. Using a primer set incorporating *Afl*II and *Not*I sites, the promoter was amplified by PCR, digested and employed to exchange the endogenous *alg-1* promoter from *Afl*II/*Not*I-digested MSp59 plasmid (*alg-1p::RFP::alg-1*) producing MSp150. Latter, the *Not*I RFP cassette was reintroduced to generate MSp151 (*lag-2p::RFP::alg-1*). Both *alg-1* and *alg-2* constructs contain their respective 3′UTR regions.

Cytological methods

For antibody staining, gonads were dissected from young adults (20-22 h post L4) in PBS. Extruded gonads were immersed in fixing solution (1% PFA+0.1% Tween-20) for 5 min at room temperature, followed by freeze crack in liquid nitrogen and transferred to −20 °C methanol for 1 min. The fixed gonads were washed three times in PBS with 0.1% Tween-20 for 15 min, followed by blocking in PBS-T + 1% BSA for 1 h at room temperature. Gonads were then incubated with primary antibodies (α-ALG-1 (1:500) or α-HIM-3 (1:200)) overnight at 4 °C, and probed with Alexa Fluor 488 anti-rabbit as secondary antibody (1:500). Gonads were counter-stained by 1 μg/ml DAPI in antifading agent (Vectashield, Vector Laboratories). Images were captured using Zeiss motorized Axioplan 2 microscope at 630×

consisting of 15-20 serial Z sections of 0.5 μm thickness subsuming entire nuclei. Fluorescence images were acquired with an AxioCam HRm camera and AxioVision acquisition software.

Brood size

Single L4 hermaphrodite from wild-type and mutant strains were transferred to seeded NGM plates and maintained at 20 °C. Animals were transferred to fresh plates each day until they stopped laying eggs. The hatched larvae on each plate were counted and total number of viable larvae that developed to the L1 stage descended from a single hermaphrodite was calculated. The average number of viable larvae from 25 hermaphrodites of a strain was plotted as brood size. Significant differences were determined by Student's *t*-test ($P < 0.05$) and represented as ± SEM.

Scoring mitotic cell number counts and entry into meiosis

Mitotic region was established previously [23]. Cell numbers within mitotic region were determined by counting from the row immediately adjacent to the DTC to the row containing multiple crescent-shaped nuclei, which is the early meiotic prophase I (leptotene/zygotene) or to the row where the nuclei stained positive with α-HIM-3 antibody (marker for entry into meiosis). Entry into meiosis was confirmed by looking at the gonad arm within each category for nuclei that stained positive with α-HIM-3 antibody in mitotic region/ transition zone.

Oocyte count and sperm defect

Gonads from L4 animals past 20 h and 40 h (day-1 and day-2, respectively) were dissected and fixed with fixing solution (1% PFA+0.1% Tween-20) for 30 min at room temperature. Gonads were washed stained by 1 μg/ml DAPI in anti-fading agent (Vectashield, Vector Laboratories) and monitored under the microscope at 630× magnification. Oocytes were counted from the loop of the gonad arm in a linear fashion till the most proximal oocyte also called as (−1). To check the sperm defect, L4 animals of mutant background were mated with wild-type males. Progeny was counted from animals, where cross progeny was monitored and compared to progeny from unmated animals.

AO assay

To obtain the number of corpses in worms, 20-22 h past L4 adult animals were stained with AO. Adult animals were incubated in dark for 1.5 h at room temperature on plates containing 1 ml of M9 with 0.08 mg of AO. Stained adults were transferred to fresh NGM plates to incubate for 45 min to clear the stained bacteria. Worms were mounted on agarose pads and monitored under fluorescence microscope. Stained corpses as well as the ones which were clearly visible under DIC as dark spots were counted.

Microarray analysis

Gonads from wild-type N2 and *alg-1(gk214)* animals from four independent pools (around five hundred gonads for each set) were extruded and immediately placed in cold Tri-Reagent (Sigma) for total RNA extraction. RNA purification was performed using the PicoPure RNA isolation kit (Applied Biosystems), with DNase (Qiagen) treatment on the purification column according to the manufacturer's instructions. Quantity and quality of RNA was verified on a 2100 Bioanalyzer (Agilent Technologies). Samples were stored at −80 °C.

Antisense RNA was produced using the Agilent LowInput QuickAmp Labeling Kit Two Color (Agilent Technologies). A 100 ng of total RNA spiked in with Two-Color RNA Spike-In Kit from Agilent was amplified and labeled as recommended by manufacturer; except for labelled aRNA purification, picopure RNA extraction kit was used. Quantity and labeling of aRNA was determined using a Nanodrop ND-1000 (NanoDrop Technologies).

Samples from four biological replicates of each gonad strain were hybridized on *C. elegans* Oligo Microarray (Agilent Technologies) using a dye-swap design (technical replicates) for a total of four arrays. The manufacturer's protocol provided with Agilent Gene Expression oligo microarrays Version 6.5 (May 2010) was followed adding the acetonitrile and Stabilization and Drying Solution (Agilent Technologies) to wash steps. Slide was scanned on a G2505 B Agilent Microarray scanner and fluorescence values extract using Feature extraction software (Agilent Technologies).

The raw expression data were imported in FlexArray (http://www.genomequebec.mcgill.ca/FlexArray) and analyzed using LIMMA [54]. First background was subtracted and the data were normalized using loess normalization. The experimental design was modeled using the function lmFit and the dye-swap arrays were taken into account. Differential expression was assessed using an empirical Bayes' statistics using the eBayes function. Gene enrichment analysis was performed using DAVID on the gene ontology biological processes [55].

Acknowledgments

We thank members of the Zetka lab for their technical help as well as members of the Simard's group for their critical reading of the manuscript. We also thank Judith Kimble (University of Wisconsin-Madison) and Eric Miska (University of Cambridge) for providing reagents and strains. Some nematode strains were provided by the *Caenorhabditis* Genetics Center, which is funded by the NIH National Center for Research Resources (NCRR) and by the International *C. elegans* Gene Knockout Consortium. This research was supported by NSERC grants (C R, J-Y M and M J S). J-Y M is a Chercheur-Boursier Senior from Fonds de la Recherche en Santé du Québec and M J S is a Canadian Institutes of Health Research New Investigator.

References

1 Hutvagner G, Simard MJ. Argonaute proteins: key players in RNA silencing. *Nat Rev Mol Cell Biol* 2008; **9**:22-32.
2 Grishok A, Pasquinelli AE, Conte D, *et al.* Genes and mechanisms related to RNA interference regulate expression of the small temporal RNAs that control *C. elegans* developmental timing. *Cell* 2001; **106**:23-34.
3 Bartel DP. MicroRNAs: genomics, biogenesis, mechanism, and function. *Cell* 2004; **116**:281-297.
4 Ambros V. MicroRNAs and developmental timing. *Curr Opin Genet Dev* 2011; **21**:511-517.
5 Takamizawa J, Konishi H, Yanagisawa K, *et al.* Reduced expression of the let-7 microRNAs in human lung cancers in association with shortened postoperative survival. *Cancer Res* 2004; **64**:3753-3756.
6 Lee YS, Kim HK, Chung S, Kim KS, Dutta A. Depletion of

human micro-RNA miR-125b reveals that it is critical for the proliferation of differentiated cells but not for the down-regulation of putative targets during differentiation. *J Biol Chem* 2005; **280**:16635-16641.
7 Ramachandran R, Fausett BV, Goldman D. Ascl1a regulates Muller glia dedifferentiation and retinal regeneration through a Lin-28-dependent, let-7 microRNA signalling pathway. *Nat Cell Biol* 2010; **12**:1101-1107.
8 Johnson CD, Esquela-Kerscher A, Stefani G, *et al.* The let-7 microRNA represses cell proliferation pathways in human cells. *Cancer Res* 2007; **67**:7713-7722.
9 Alvarez-Saavedra E, Horvitz HR. Many families of *C. elegans* microRNAs are not essential for development or viability. *Curr Biol* 2010; **20**:367-373.
10 Miska EA, Alvarez-Saavedra E, Abbott AL, *et al*. Most *Caenorhabditis elegans* microRNAs are individually not essential for development or viability. *PLoS Genet* 2007; **3**:e215.
11 Yang L, Chen D, Duan R *et al.* Argonaute 1 regulates the fate of germline stem cells in *Drosophila*. *Development* 2007; **134**:4265-4272.
12 Forstemann K, Tomari Y, Du T, *et al.* Normal microRNA maturation and germ-line stem cell maintenance requires Loquacious, a double-stranded RNA-binding domain protein. *PLoS Biol* 2005; **3**:e236.
13 Jin Z, Xie T. Dcr-1 maintains *Drosophila* ovarian stem cells. *Curr Biol* 2007; **17**:539-544.
14 Hatfield SD, Shcherbata HR, Fischer KA, *et al.* Stem cell division is regulated by the microRNA pathway. *Nature* 2005; **435**:974-978.
15 Knight SW, Bass BL. A role for the RNase III enzyme DCR-1 in RNA interference and germ line development in *Caenorhabditis elegans*. *Science* 2001; **293**:2269-2271.
16 Denli AM, Tops BB, Plasterk RH, Ketting RF, Hannon GJ. Processing of primary microRNAs by the Microprocessor complex. *Nature* 2004; **432**:231-235.
17 Dernburg AF, McDonald K, Moulder G, *et al.* Meiotic recombination in *C. elegans* initiates by a conserved mechanism and is dispensable for homologous chromosome synapsis. *Cell* 1998; **94**:387-398.
18 MacQueen AJ, Villeneuve AM. Nuclear reorganization and homologous chromosome pairing during meiotic prophase require *C. elegans* chk-2. *Genes Dev* 2001; **15**:1674-1687.
19 Zetka MC, Kawasaki I, Strome S, Muller F. Synapsis and chiasma formation in *Caenorhabditis elegans* require HIM-3, a meiotic chromosome core component that functions in chromosome segregation. *Genes Dev* 1999; **13**:2258-2270.
20 Hansen D, Schedl T. The regulatory network controlling the proliferation-meiotic entry decision in the *Caenorhabditis elegans* germ line. *Curr Top Dev Biol* 2006; **76**:185-215.
21 Kimble J, Crittenden SL. Controls of germline stem cells, entry into meiosis, and the sperm/oocyte decision in *Caenorhabditis elegans*. *Annu Rev Cell Dev Biol* 2007; **23**:405-433.
22 Hubbard EJ. *Caenorhabditis elegans* germ line: a model for stem cell biology. *Dev Dyn* 2007; **236**:3343-3357.
23 Crittenden SL, Leonhard KA, Byrd DT, Kimble J. Cellular analyses of the mitotic region in the *Caenorhabditis elegans* adult germ line. *Mol Biol Cell* 2006; **17**:3051-3061.
24 Henderson ST, Gao D, Lambie EJ, Kimble J. lag-2 may encode a signaling ligand for the GLP-1 and LIN-12 receptors of *C. elegans*. *Development* 1994; **120**:2913-2924.
25 Gumienny TL, Lambie E, Hartwieg E, Horvitz HR, Hengartner MO. Genetic control of programmed cell death in the *Caenorhabditis elegans* hermaphrodite germline. *Development* 1999; **126**:1011-1022.
26 Martinez NJ, Ow MC, Reece-Hoyes JS, *et al.* Genome-scale spatiotemporal analysis of *Caenorhabditis elegans* microRNA promoter activity. *Genome Res* 2008; **18**:2005-2015.
27 Lim LP, Lau NC, Garrett-Engele P, *et al.* Microarray analysis shows that some microRNAs downregulate large numbers of target mRNAs. *Nature* 2005; **433**:769-773.
28 Bagga S, Bracht J, Hunter S, *et al.* Regulation by let-7 and lin-4 miRNAs results in target mRNA degradation. *Cell* 2005; **122**:553-563.
29 Guo H, Ingolia NT, Weissman JS, Bartel DP. Mammalian microRNAs predominantly act to decrease target mRNA levels. *Nature* 2010; **466**:835-840.
30 Rehwinkel J, Natalin P, Stark A, *et al.* Genome-wide analysis of mRNAs regulated by Drosha and Argonaute proteins in *Drosophila melanogaster*. *Mol Cell Biol* 2006; **26**:2965-2975.
31 Friedman RC, Farh KK, Burge CB, Bartel DP. Most mammalian mRNAs are conserved targets of microRNAs. *Genome Res* 2009; **19**:92-105.
32 Hammell M, Long D, Zhang L, *et al.* mirWIP: microRNA target prediction based on microRNA-containing ribonucleoprotein-enriched transcripts. *Nat Methods* 2008; **5**:813-819.
33 Ambros V, Lee RC, Lavanway A, Williams PT, Jewell D. MicroRNAs and other tiny endogenous RNAs in *C. elegans*. *Curr Biol* 2003; **13**:807-818.
34 Park JK, Liu X, Strauss TJ, McKearin DM, Liu Q. The miRNA pathway intrinsically controls self-renewal of *Drosophila* germline stem cells. *Curr Biol* 2007; **17**:533-538.
35 Yang Y, Xu S, Xia L, *et al.* The bantam microRNA is associated with *drosophila* fragile X mental retardation protein and regulates the fate of germline stem cells. *PLoS Genet* 2009; **5**:e1000444.
36 Iovino N, Pane A, Gaul U. miR-184 has multiple roles in *Drosophila* female germline development. *Dev Cell* 2009; **17**:123-133.
37 Kaneda M, Tang F, O'Carroll D, Lao K, Surani MA. Essential role for Argonaute2 protein in mouse oogenesis. *Epigenetics Chromatin* 2009; **2**:9.
38 Suh N, Baehner L, Moltzahn F, *et al.* MicroRNA function is globally suppressed in mouse oocytes and early embryos. *Curr Biol* 2010; **20**:271-277.
39 Tang F, Kaneda M, O'Carroll D, *et al.* Maternal microRNAs are essential for mouse zygotic development. *Genes Dev* 2007; **21**:644-648.
40 Murchison EP, Stein P, Xuan Z, *et al*. Critical roles for Dicer in the female germline. *Genes Dev* 2007; **21**:682-693.
41 Hayashi K, Chuva de Sousa Lopes SM, Kaneda M, *et al.* MicroRNA biogenesis is required for mouse primordial germ cell development and spermatogenesis. *PLoS One* 2008; **3**:e1738.
42 Maatouk DM, Loveland KL, McManus MT, Moore K, Harfe BD. Dicer1 is required for differentiation of the mouse male germline. *Biol Reprod* 2008; **79**:696-703.
43 Tam OH, Aravin AA, Stein P, *et al.* Pseudogene-derived small interfering RNAs regulate gene expression in mouse oocytes.

Nature 2008; **453**:534-538.
44 Watanabe T, Takeda A, Tsukiyama T, *et al*. Identification and characterization of two novel classes of small RNAs in the mouse germline: retrotransposon-derived siRNAs in oocytes and germline small RNAs in testes. *Genes Dev* 2006; **20**:1732-1743.
45 Watanabe T, Totoki Y, Toyoda A, *et al*. Endogenous siRNAs from naturally formed dsRNAs regulate transcripts in mouse oocytes. *Nature* 2008; **453**:539-543.
46 Cinquin O, Crittenden SL, Morgan DE, Kimble J. Progression from a stem cell-like state to early differentiation in the *C. elegans* germ line. *Proc Natl Acad Sci USA* 2010; **107**:2048-2053.
47 Kadyk LC, Kimble J. Genetic regulation of entry into meiosis in *Caenorhabditis elegans*. *Development* 1998; **125**:1803-1813.
48 Zisoulis DG, Lovci MT, Wilbert ML, *et al*. Comprehensive discovery of endogenous Argonaute binding sites in *Caenorhabditis elegans*. *Nat Struct Mol Biol* 2010; **17**:173-179.
49 Liu M, Liu P, Zhang L, *et al*. mir-35 is involved in intestine cell G1/S transition and germ cell proliferation in *C. elegans*. *Cell Res* 2011; **21**:1605-1618.
50 Govindan JA, Nadarajan S, Kim S, Starich TA, Greenstein D. Somatic cAMP signaling regulates MSP-dependent oocyte growth and meiotic maturation in *C. elegans*. *Development* 2009; **136**:2211-2221.
51 Nadarajan S, Govindan JA, McGovern M, Hubbard EJ, Greenstein D. MSP and GLP-1/Notch signaling coordinately regulate actomyosin-dependent cytoplasmic streaming and oocyte growth in *C. elegans*. *Development* 2009; **136**:2223-2234.
52 Brenner S. The genetics of *Caenorhabditis elegans*. *Genetics* 1974; **77**:71-94.
53 Blelloch R, Anna-Arriola SS, Gao D, *et al*. The *gon-1* gene is required for gonadal morphogenesis in *Caenorhabditis elegans*. *Dev Biol* 1999; **216**:382-393.
54 Smyth GK. Linear models and empirical bayes methods for assessing differential expression in microarray experiments. *Stat Appl Genet Mol Biol* 2004; **3**:Article3.
55 Huang da W, Sherman BT, Lempicki RA. Systematic and integrative analysis of large gene lists using DAVID bioinformatics resources. *Nat Protoc* 2009; **4**:44-57.

(**Supplementary information** is linked to the online version of the paper on the *Cell Research* website.)

Appendix D

Argonaute pull-down and RISC analysis using 2'-O-methylated oligonucleotides affinity matrices

Foreword

The present appendix is constituted by a book chapter published in 'Methods Mol Biol.' (Jannot *et al.*, 2011b). I participated in the redaction of this study of my colleague Guillaume Jannot. This study details a methodological procedure used to pull-down small RNAs and their associated proteins. This is exemplified by the isolation by affinity chromatography of let-7 miRISC from *C. elegans* extracts.

Chapter 16

Argonaute Pull-Down and RISC Analysis Using 2′-*O*-Methylated Oligonucleotides Affinity Matrices

Guillaume Jannot, Alejandro Vasquez-Rifo, and Martin J. Simard

Abstract

During the last decade, several novel small non-coding RNA pathways have been unveiled, which reach out to many biological processes. Common to all these pathways is the binding of a small RNA molecule to a protein member of the Argonaute family, which forms a minimal core complex called the RNA-induced silencing complex or RISC. The RISC targets mRNAs in a sequence-specific manner, either to induce mRNA cleavage through the intrinsic activity of the Argonaute protein or to abrogate protein synthesis by a mechanism that is still under investigation. We describe here, in details, a method for the affinity chromatography of the *let-7* RISC starting from extracts of the nematode *Caenorhabditis elegans*. Our method exploits the sequence specificity of the RISC and makes use of biotinylated and 2′-*O*-methylated oligonucleotides to trap and pull-down small RNAs and their associated proteins. Importantly, this technique may easily be adapted to target other small RNAs expressed in different cell types or model organisms. This method provides a useful strategy to identify the proteins associated with the RISC, and hence gain insight in the functions of small RNAs.

Key words: 2′-*O*- methyl oligonucleotides, Argonaute, *Let-7* microRNA, Affinity chromatography, TaqMan chemistry

1. Introduction

RNA-mediated gene silencing pathways can be triggered either by the introduction of exogenous double-stranded RNA molecules (RNA *interference* or RNAi) or by the endogenous expression of microRNAs. They constitute two distinct pathways that lead to posttranscriptional down regulation of targeted messenger RNA (mRNA) through either degradation of the mRNAs or inhibition of protein synthesis. RNAi is commonly used in research laboratory as a simple, but powerful technique to knockdown the expression of specific genes. The microRNA pathway can be described as an endogenous process, which is conserved across many species and is

Tom C. Hobman and Thomas F. Duchaine (eds.), *Argonaute Proteins: Methods and Protocols*,
Methods in Molecular Biology, vol. 725, DOI 10.1007/978-1-61779-046-1_16,

used to control cell homeostasis. It is estimated that 60% of human genes could be regulated by microRNA molecules and it is now becoming clear that the mis-expression of these small RNA molecules contributes to the development of a large spectrum of human diseases. Moreover, the recent findings involving small RNA in the control of spermatogenesis and in the silencing of transposable elements in the germline highlight their role in an important diversity of developmental processes in animals (reviewed in ref. (1)). Essential to all small RNA-mediated gene regulation pathways is a ribonucleoprotein complex called RNA-induced silencing complex (RISC) composed of, at least, one 21–23 nucleotides long, single-stranded RNA and a member of the Argonaute protein family (2). The activity of the RISC on its target depends on the base-pairing between the small RNA and the mRNA. When pairing is perfect, the RISC mediates mRNA cleavage through the endonuclease activity of the Argonaute protein. When the pairing is imperfect, the RISC prevents protein synthesis by a mechanism that is still unclear.

In 2004, Hutvágner *et al.* reported that modified antisense oligonucleotides can block RISC-mediated gene regulation in vivo (3) through base pairing with the small guide RNAs in this complex. The replacement of the hydroxyl group by a methyl group, as shown in Fig. 1, makes the oligonucleotide resistant to cellular ribonucleases (4) and allows the sequence-specific purification of the RISC. A biotinylated 2′-*O*-methylated oligonucleotide is bound to the RISC, and pull-down is performed using streptavidin-coupled magnetic beads. This approach is useful to identify the proteins associated with small RNAs in vivo, as well as to characterize their molecular functions (for examples of utilization, see (5–8)).

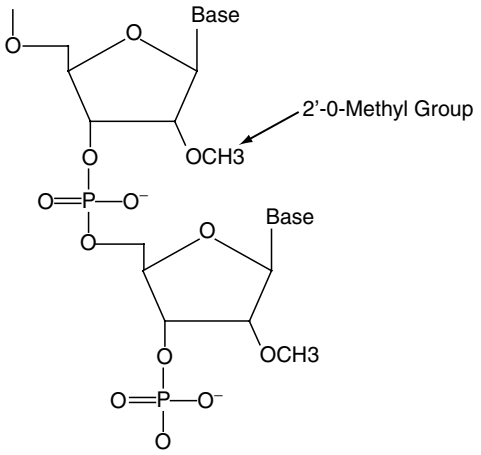

Fig. 1. Representative backbone of a single-stranded 2′-*O*-methylated oligonucleotide is shown. Each hydrogen from 2′ hydroxyl groups was replaced by a CH_3 (methyl) group. This modification confers resistance to most RNase activities.

2. Materials

2.1. Caenorhabditis elegans Culture and Extract Preparation

1. The wild-type *C. elegans* Bristol, N2 strain, was obtained from the *Caenorhabditis* Genetics Center (CGC, University of Minnesota, USA). The transgenic *C. elegans* strain expressing ALG-1 protein tagged at the N-terminus with the Green Fluorescent Protein (GFP) was generated in the laboratory as previously described in (3).
2. *Escherichia coli* (OP50) in TB liquid culture, as a food source for *C. elegans*.
3. TB medium (1 L): 12 g bacto-peptone, 24 g bacto-yeast extract, 4 mL glycerol, in 900 mL of water. Sterilize by autoclaving and cool down to <60°C. Add 100 mL of sterile 10× TB phosphates and store at room temperature (RT).
4. 10× TB phosphate (1 L): 23.1 g KH_2PO_4, 125.4 g K_2HPO_4. Sterilize by autoclaving. Store at RT.
5. Nematode growth medium (NGM) (1 L): 20 g agarose, 3 g NaCl, 2.5 g bacto-peptone. Sterilize by autoclaving and cool down to <60°C. Add, 1 mL 1 M $MgSO_4$, 1 mL 1 M $CaCl_2$, 1 mL cholesterol stock solution (5 mg/mL in ethanol), and 25 mL PPB stock solution.
6. PPB stock solution (1 L): 98 g KH_2PO_4 and 48 g K_2HPO_4. Dissolve the salts in deionized water (final volume 1 L). Sterilize by autoclaving. Store at RT.
7. M9 Buffer (1 L): Dissolve 3 g KH_2PO_4, 6 g Na_2HPO_4, 5 g NaCl, 1 mL 1 M $MgSO_4$ in deionized water (final volume 1 L). Sterilize by autoclaving. Store at RT.
8. Bleaching solution (20 mL): 2 mL of 5 M KOH, 3 mL of sodium hypochlorite, 15 mL of water (see Note 1).
9. Lysis buffer stock solution (1 L): 1 mL of 1 M KAc, 300 µL of 1 M HEPES–KOH pH 7.5, 20 µL of 1 M $Mg(Ac)_2$. Sterilize by filtration. Store at 4°C.
10. Complete lysis buffer (10 mL): 9.40 mL lysis buffer stock solutions, 10 µL 1 M DTT, 50 µL triton X-100, 1 tablet of protease inhibitors (Complete Mini EDTA-free, Roche). Add 2% [v/v] of RNase inhibitor (SUPERaseIn, Ambion) when indicated.
11. Homogenizer: Wheaton dounce tissue grinders 1 mL (Fisher).

2.2. Immobilized 2′-O-Methylated Oligonucleotide Matrices

1. 2′-*O*-methylated oligonucleotides were synthesized by Integrated DNA Technologies (IDT). The modification is represented in Fig. 2.

   Unrelated oligo: 5′-Bio-$_mC_mA_mU_mC_mA_mC_mG_mU_mA_mC_mG_mC_mG_mG_mA_mA_mU_mA_mC_mU_mU_mC_mG_mA_mA_mA_mU_mG_mU_mC$-3′;

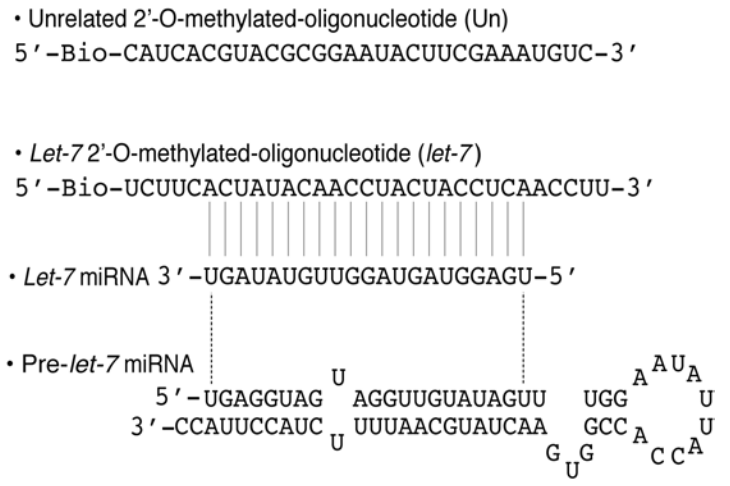

Fig. 2. *Let-7* precursor microRNA is a substrate for the cleavage activity of Dicer to form mature *let-7* microRNA, which is fully complementary to 2′-*O*-methylated oligonucleotides used to pull-down *let-7* RISC complex.

and *let-7* complementary microRNA oligo: 5′-Bio-$_{m}$U$_{m}$C$_{m}$U$_{m}$U$_{m}$C$_{m}$A$_{m}$C$_{m}$U$_{m}$A$_{m}$U$_{m}$A$_{m}$C$_{m}$A$_{m}$A$_{m}$C$_{m}$C$_{m}$U$_{m}$A$_{m}$C$_{m}$U$_{m}$-A$_{m}$C$_{m}$C$_{m}$U$_{m}$C$_{m}$A$_{m}$A$_{m}$C$_{m}$C$_{m}$U$_{m}$U-3′ (see Notes 2–5).

2. Dynabeads M-280 streptavidin (Invitrogen): To pull-down the RISC, the modified oligonucleotide is biotinylated at the 5′ end and then coupled to magnetic beads through streptavidin monolayer attached to the surface of beads (see Notes 6 and 7).
3. Dynal MPC-S (Invitrogen): We used a magnetic particle concentrator (referred as magnet) compatible with microcentrifuge tube (1.5 mL tube). Dynabeads are separated from the solution when the tube is inserted into the magnet and the magnetic slide is inserted. Bead-bound material is then attracted to the side of the tube.

2.3. SDS–Polyacrylamide Gel Electrophoresis

1. Resolving buffer 4× (1 L): 182 g Tris (hydroxymethyl) aminomethane, 4 g Sodium Dodecyl Sulfate (SDS) in deionized water. Adjust pH to 8.8 with concentrated HCl. Sterilize by filtration. Store at RT.
2. Stacking buffer 4× (1 L): 60 g Tris (hydroxymethyl) aminomethane, 4 g SDS in deionized water. Adjust pH to 6.8 with concentrated HCl. Sterilize by filtration. Store at RT.
3. Running buffer 10× (1 L): 30.3 g Tris (hydroxymethyl) aminomethane, 144.1 g glycine, 10 g SDS in deionized water. Store at RT (see Note 8).
4. 29:1, 40% Acrylamide/bis solution (J.T Baker). (This is a neurotoxic reagent when unpolymerized, handle with care).

5. *N*,*N*,*N*,*N*′-Tetramethyl-ethylenediamine (TEMED) (this is a corrosive and irritant reagent: handle with care).
6. Ammonium persulfate (APS) 10% (10 mL): 10 g $(NH_4)_2S_2O_8$ in cold deionized water and freeze as 1 mL aliquots at –20°C.
7. Prestained molecular weight markers: Kaleidoscope marker (Bio-Rad).
8. Laemmli buffer 4× (20 mL): 4 mL 1 M Tris (hydroxymethyl) aminomethane–HCl pH 6.8, 0.04 g bromophenol blue, 8 mL glycerol, 1.6 g SDS, and 8 mL 1 M Dithiothreitol (DTT). Store at –20°C as 1 mL aliquots.
9. Ethanol 95%.

2.4. Western Blotting for Argonautes Associated to the RISC

1. Transfer buffer (1.6 L): 5.86 g glycine, 11.64 g Tris (hydroxymethyl) aminomethane, 0.75 g SDS. Store at RT.
2. Methanol.
3. Nitrocellulose Hybond-ECL membrane (Amersham) and Blotting pad (VWR).
4. TBS-T (1 L): 6.05 g Tris (hydroxymethyl) aminomethane, 8.76 g NaCl, 1 mL Tween-20. Adjust pH to 7.5 with concentrated HCl. Store at 4°C.
5. Blocking solution: 5% [w/v] nonfat dry milk in TBS-T.
6. Primary antibody: anti-GFP antibody (Roche) diluted in TBS-T supplemented with 5% [w/v] nonfat dry milk (see Note 9).
7. Secondary antibody: Peroxydase-conjugated Anti-mouse IgG (Roche) diluted in TBS-T supplemented with 5% [w/v] nonfat dry milk.
8. Enhanced chemiluminescence (ECL) reagent (Perkin Elmer) and hyperfilm ECL (Amersham).

2.5. Total RNA Extraction

1. TRI-Reagent solution (Sigma). (The TRI-Reagent solution contains phenol and guanidine thiocyanate, handle with care).
2. Chloroform (chloroform can be fatal if swallowed, inhaled, or absorbed. Manipulate with care in a fume hood).
3. Isopropanol 75% [v/v] and ethanol 75% [v/v].
4. Freshly autoclaved deionized water.
5. 1.5 mL RNase-free microcentrifuge tubes.

2.6. Analysis of Short RNA Integrity by 12% Mini-Polyacrylamide Gel Electrophoresis

1. SequaGel Sequencing System kit (National Diagnostic): (1) SequaGel Concentrate (1 L: 37.5 g of acrylamide, 12.5 g of methylene bis-acrylamide, and 7.5 M urea in a deionized aqueous solution), (2) SequaGel Diluent (7.5 M urea in deionized water), and (3) SequaGel Buffer [0.89 M

Tris–Borate–20 mM EDTA buffer pH 8.3 (10× TBE) and 7.5 M urea] (see Note 10).

2. TEMED.
3. APS 10% (10 mL): 10 g $(NH_4)_2S_2O_8$ in cold water and freeze in 1 mL aliquots at −20°C.
4. Formamide-dye loading buffer: 98% [w/v] deionized formamide, 10 mM EDTA pH 8, 0.025% [w/v] xylene cyanol, and 0.025% [w/v] bromophenol blue.
5. TBE buffer 10× (1 L): 108 g Tris (hydroxymethyl) aminomethane and 40 mL of 0.5 M Na_2EDTA, 55 g boric acid. Adjust to pH 8. Sterilize by autoclaving. Store at RT.
6. Ethidium bromide (EtBr) solution at 5 μg/mL (EtBr is a mutagenic agent, so handle with care).

2.7. Quantitative Real-Time PCR for Let-7 MicroRNA

1. Real-Time PCR machine: 7900HT Fast Real-Time PCR system (Applied Biosystems).
2. MicroAmp Fast optical 96-well reaction plate (Applied Biosystems).
3. Optical adhesive covers (Applied Biosystems).
4. MicroRNAs Primers: We used TaqMan probes-based chemistry. The primers were obtained from Applied Biosystems and correspond to mature *let-7* microRNA (Assay ID: 000377). We used the short nuclear RNA *sn2841* as an endogenous control (Assay ID: 001759).
5. Reverse Transcription Assays: TaqMan microRNA transcription kit (Applied Biosystems).
6. PCR reaction: TaqMan 2× Universal PCR Master Mix, No AmpErase UNG (Applied Biosystems).

3. Methods (see Note 11)

For this protocol, we took *let-7* microRNA-associated with ALG-1 RISC as an example to demonstrate the efficiency of the pull-down using 2′-*O*-methylated oligonucleotides affinity matrices. A transgenic *C. elegans* strain expressing ALG-1 protein tagged at the N terminus with the green fluorescent protein (GFP) was used as described in ref. (3). An extract was generated using staged animals as starting material, a pull-down assay targeting *let-7* microRNA was performed, and the associated GFP::ALG-1 protein was detected by western blot. As a negative control, we used an unrelated 2′-*O*-methylated oligonucleotide that does not share base complementarity with any known microRNA. To confirm *let-7* microRNA depletion, we quantified *let-7* in the

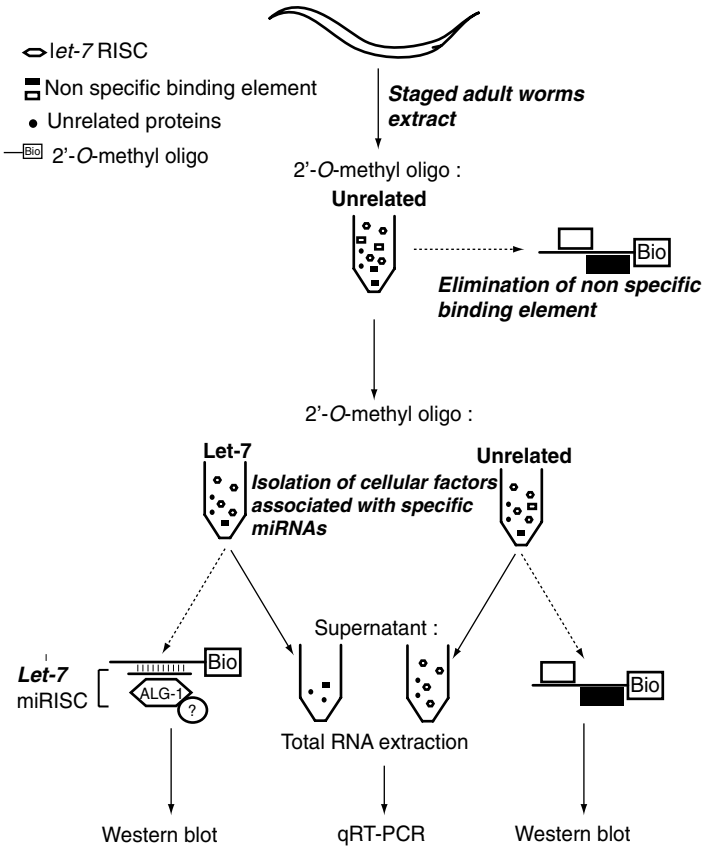

Fig. 3. Experimental procedure. This scheme provides an overview of the technical steps in this method (1) Growing a population of staged *Caenorhabditis elegans*; (2) Extraction of animal proteins; (3) Pull-down of the *let-7* microRNA-associated RISC; (4) Detection of ALG-1 protein by western blot; (5) Analysis of the efficiency of this method by quantification of the level of *let-7* miRNA by qRT-PCR.

recovered unbound fractions by quantitative real-time PCR (qRT-PCR). We also verified the 5.8S and 5S RNA integrity by EtBr staining from total RNA preparations. Figure 3. summarizes the experimental procedure followed.

3.1. Preparation of Agar NGM Plate Seeded with Concentrated OP50

1. Pour 20 mL of NGM medium in 15 cm diameter Petri dishes aseptically, cover with the lids, and let dry overnight.
2. Inoculate one colony of OP50 bacteria into 1 L of TB medium. Incubate 16 h at 37°C under agitation.
3. Split the overnight culture in two sterile centrifuge bottles (700 mL) and spin for 30 min at 3,500 × *g*.
4. Resuspend the pellet with 20 mL of M9 and transfer into 50 mL Falcon tube.

5. Wash three times with sterile M9 and spin for 10 min at 4,500 × *g*.
6. Resuspend the pellet in four volumes of M9. Vortex vigorously to obtain a homogenized OP50 solution.
7. Dispense uniformly 2 mL of concentrated food on each plate, and let them dry in a sterile field with the lid open.
8. Store the seeded plates at 4°C for up to for several days.

3.2. Preparation of a Synchronous *C. elegans* population

All the following centrifugation steps are done at 2,800 × *g* for 30 s. Manipulation must be done in a sterile field (flame).

1. Transfer starved animals from three 35 mm plates to one 150 mm plate. Once population reach adult stage (hermaphrodites bearing fertilized eggs), transfer gravid adult population of *C. elegans* in a 15 mL sterile Falcon tube using the M9 solution.
2. Wash three times by successively transferring 10 mL of M9 and centrifuging to pellet the animals.
3. Remove the supernatants completely and add 10 mL of freshly prepared bleaching solution.
4. Shake vigorously for 5 min and monitor the lysis of worm cuticles by observing the content of the tube under a stereomicroscope.
5. Once half of the worm cuticles are destroyed, centrifuge, remove the supernatant, and add 10 mL of fresh bleaching solution.
6. Shake vigorously. After an additional 1–2 min, most of the animals should be dissolved, leaving only the embryos (eggs) (see Note 12).
7. Centrifuge, remove the supernatant, and wash the eggs three times with 10 mL of M9.
8. Let the eggs hatch in 10 mL of M9 at 20°C under gentle rotation overnight.
9. On the next day, estimate the number of newly hatched larvae (L1) by counting under a stereomicroscope the amount of animals in 1 µL aliquot of homogenous solution (triplicate). Centrifuge the L1 animals, wash, and resuspend them to obtain approximately 300 animals/µL in M9. Dispense 500 µL (around 150,000 animals total) on a large OP50-seeded plate, and grow the animals at 20°C up to the young adult stage (approximately 50 h).
10. Wash the young adults from the plate with sterile M9 and transfer the animals to a 15 mL Falcon tube.
11. Centrifuge and wash three times with M9. Resuspend in 10 mL of M9, and let the suspension rotate gently for 1 h to

completely eliminate the bacteria from the gut of the animals.

12. Centrifuge, eliminate the supernatant, and freeze the pellet of young adults at −80°C until use.

3.3. Preparation of the Crude C. elegans Extract

1. Thaw a pellet of 150,000 young adults at room temperature.
2. Wash the pellet three times with three volumes of complete lysis solution.
3. Add ½ volume of complete lysis solution and transfer into a Wheaton Dounce Tissue grinder.
4. Grind for around 7 min on ice and monitor the lysis efficiency under the microscope by transferring 2 µL of extract on a glass slide. Continue until the worm cuticles are destroyed.
5. Transfer the lysate in a 1.5 mL tube and spin at 17,000 × *g* for 15 min at 4°C.
6. Transfer the supernatant to a fresh 1.5 mL tube on ice. This is the crude *C. elegans* extract.
7. Determine the protein concentration of the crude *C. elegans* extract using one of the standard colorimetric assays, such as Lowry, Biuret, or Bradford (about 10 mg of total protein should be obtained from 150,000 young adults animals).

3.4. Let-7 MicroRNA Pull-Down and RISC Analysis Using 2′-O-Methylated Oligonucleotide Affinity Matrices (see Note 13)

1. Resuspend the magnetic beads from the stock tube by pipetting up and down 20 times.
2. Transfer 60 µL of homogenized bead suspension in a 1.5 mL tube, place the tube into the magnet for 1 min, and discard the supernatant (see Note 14). The beads are washed twice with four volumes of lysis solution containing 2% [v/v] RNase inhibitor.
3. Add 120 µL of the biotinylated unrelated 2 -*O*-methyl oligonucleotide at 1 µM concentration. Incubate for 45 min at RT with gentle rotation (see Note 15). Place the tube in a magnet for 1 min and discard the supernatant.
4. Wash the coated beads twice in stock lysis solution with 2% [v/v] RNase inhibitor.
5. Place the tube in the magnet for 1 min and discard the supernatant.
6. Dilute the quantified crude *C. elegans* extract to a working solution of 13.3 mg/mL.
7. Add 4 mg of crude *C. elegans* extract (300 µL of 13.3 mg/mL suspension) in a 1.5 mL tube containing the unrelated (control) 2′-*O*-methylated oligonucleotide bound to the beads.

8. Incubate at RT with gentle rotation for 45 min. During this incubation, prepare the *let-7*-complementary oligo, and the unrelated matrices (see Note 16).
9. Transfer 30 µL of each bead suspensions into two separate 1.5 mL tubes. Wash the beads and coat with 60 µL of either the unrelated or the *let-7* complementary 2′-*O*-methylated oligonucleotides for 45 min at RT, as described in steps 2–5. Keep the coated beads on ice until used. Discard the buffer just before starting step 10.
10. Once the incubation time of the extract is complete (step 8), place the tube on the magnet for 1–2 min and transfer half of the cleared supernatant either to the unrelated or to the *let-7* coated beads (step 9). Incubate at room temperature with gentle rotation for 45 min (see Note 17).
11. Place the tubes on the magnet for 1–2 min and then transfer the supernatants to new 1.5 mL tubes. Keep the supernatants on ice until total RNA extraction and qRT-PCR analysis.
12. Wash the beads twice with three volumes of stock lysis solution containing 2% [v/v] of RNase inhibitor.
13. Resuspend the beads in Laemmli 2× loading buffer and boil them 10 min before loading on 8% SDS–Polyacrylamide gel (SDS–PAGE) electrophoresis (see Subheading 3.5). As input control, load 100 µg of total proteins from the crude *C. elegans* extract (resuspended and boiled in Laemmli 2× loading buffer).

3.5. SDS–PAGE (8%) Electrophoresis

1. The SDS–PAGE electrophoresis is performed with the "Mini-PROTEAN Tetra Cell" system (Bio-Rad). Ensure that the glass plates are clean. Before use, it is recommended to wash them with detergent first, then with ethanol 95%, and finally to let them dry completely.
2. Prepare a 1.5 mm thick, 8% gel by mixing 2.5 mL of 4× resolving buffer with 2 mL of 40% acrylamide/bis-acrylamide solution, 5 mL of water, 100 µL of APS 10%, and 10 µL of TEMED. Pour the gel while leaving space for the stacking gel (around 1–2 cm) and overlay with 95% ethanol. Let the gel polymerize for 30 min.
3. Discard the layer of ethanol 95% on the gel.
4. Prepare a 6% stacking gel by mixing 1.25 mL of 4× stacking buffer with 750 µL of 40% acrylamide/bis-acrylamide solution, 2.9 mL of water, 50 µL of APS 10%, and 5 µL of TEMED. Pour the stacking gel, and insert the comb. Let the stacking gel polymerize for 30 min.
5. Prepare the running buffer by dissolving 100 mL of 10× stock solution with 900 mL of water.

6. Once the stacking gel is polymerized, transfer the gel assembly in the tank and fill with running buffer.
7. Remove the comb carefully and wash the wells with running buffer using a 10 mL syringe fitted with a 22-gauge needle.
8. Boil your samples for 1 min, spin 30 s at 17,000 × *g*, and load the total sample in the wells. Load one well with a prestained molecular weight marker (see Note 18).
9. Connect the gel chamber to a power supply and run at 160 V for 1.5 h, or until the blue dye front runs off the gel.

3.6. Western Blotting for ALG-1 Protein

1. The samples that are resolved by SDS–PAGE are transferred using a semidry transfer apparatus (Trans-Blot SD semidry Transfer cell, Bio-Rad).
2. Prepare working transfer buffer solution (setup buffer) by mixing 200 mL of transfer buffer with 50 mL of methanol.
3. Carefully remove the gel from the glass plate assembly and put the gel in a clean dish containing 50 mL of setup buffer.
4. Cut a sheet of nitrocellulose membrane and two blotting pads of slightly larger dimensions than the size of the separating gel, and soak in the setup buffer.
5. Prepare a sandwich assembly with one wet blotting pad covered with the nitrocellulose membrane. Carefully transfer the resolving gel on the top of the membrane and cover with a second soaked blotting pad. Ensure that no bubbles are trapped in the resulting sandwich by gently rolling a 15 mL Falcon tube on the top of the assembly.
6. Connect to a power supply and run at 15 V for 50 min.
7. Once the transfer is complete, disassemble the sandwich and wash the nitrocellulose membrane with TBS-T.
8. Incubate the membrane in 25 mL of TBS-T containing 5% (w/v) dry milk for 1 h at RT with gentle agitation.
9. Discard the blocking buffer, and incubate the membrane with a 1:3,000 dilution of the anti-GFP antibody in TBS-T containing 5% [w/v] dry milk overnight at 4°C on a rocking platform.
10. Remove the primary antibody solution and wash the membrane three times with TBS-T for 10 min each.
11. The secondary antibody, an HRP-coupled anti-mouse, is diluted at 1:10,000 in TBS-T and added to the membrane for 45 min at room temperature on a rocking platform.
12. Remove the secondary antibody, and wash the membrane three times for 10 min each with TBS-T.
13. Mix equal volumes of ECL reagent (2 mL each) and keep the mixture at room temperature until used.

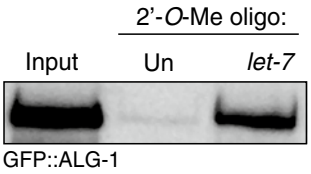

Fig. 4. Western blot analysis of the GFP-tagged ALG-1 protein associated with *let-7* microRNA. The input represents 100 μg of total protein. Each matrix [unrelated (Un) or *let-7* biotinylated 2′-*O*-methylated oligonucleotides] was mixed with 2 mg of protein and pull-down was conducted using Dynabeads coupled to streptavidin. Notice that ALG-1 is detected only in the *let-7* complementary 2′-*O*-methylated oligonucleotide pulldowns.

14. Cut out two clean acetate sheets with dimensions just larger than the size of the nitrocellulose membrane.
15. Fix a laboratory film (Parafilm) on the working bench and place the 4 mL of mixed ECL reagent on the top.
16. Transfer the membrane protein up side down on the ECL drop and incubate for 1 min.
17. Put the membrane side up on the clean acetate sheet and place the other acetate sheet over membrane and smooth out air bubbles.
18. Place the membrane between acetate sheets protector (as in a sandwich), into an autoradiography cassette and head to the dark room with X-ray films for developing.
19. In the dark room, place the film in an autoradiography cassette for a suitable exposure time (1–2 min for GFP::ALG-1 in our experiment). An example of the result is shown in Fig. 4.

3.7. Total RNA Extraction

1. Add three volumes of TRI-Reagent in 1.5 mL tubes containing either 2 mg of protein from the input crude *C. elegans* extract or the supernatant (unbound) samples recovered from the unrelated and the *let-7* matrices. Vortex for 30 s.
2. Add one volume of chloroform, vortex for 10 s and allow to sit at RT for 3 min.
3. Centrifuge the tubes at 13,000 × *g* for 15 min at 4°C.
4. Remove the top aqueous layer and transfer to a fresh 1.5 mL RNase-free tube (do not disturb or retrieve the interphase).
5. Add an equal volume of isopropanol, mix well, and incubate at RT for 10 min.
6. Centrifuge at 13,000 × *g* for 15 min at 4°C.
7. Discard the supernatant and wash the RNA pellet carefully with 300 μL of 75% ethanol.
8. Spin at 7,500 × *g* for 5 min at 4°C.

9. Discard the supernatant, air dry the RNA pellet with the open cap at RT for 5–10 min.
10. Dissolve the pellet in deionized, autoclaved water (around 100–200 µL). To dissolve the pellet, heat at 65°C for 10 min and homogenize the RNA solution by pipetting up and down.
11. The concentration of the purified RNA is determined by measuring the absorbance at 260 nm in a spectrophotometer.
12. Monitor the short RNA quality by running 15 µg of total RNA on 12% mini-polyacrylamide gel electrophoresis (see Subheading 3.8).

3.8. Preparation of 12% Polyacrylamide Gel Electrophoresis

1. The 12% mini-PAGE is performed with the same clean material used for SDS–PAGE assembly.
2. Prepare a 1.5 mm thick, 12% mini-PAGE gel by mixing 4.8 mL of SequaGel concentrate, 4.2 mL of SequaGel Diluent, 1 mL of SequaGel buffer, 80 µL of APS 10%, and 4 µL of TEMED. Pour the gel and insert the comb. Let the gel polymerize for 1 h.
3. Carefully remove the comb and pre-run the gel for 30 min at 150 V in 0.5× TBE before loading the samples.
4. While pre-running, prepare the RNA samples. Add ½ volume of formamide-dye loading buffer with 15 µg of total RNA.
5. Heat the RNA samples at 65°C for 15 min.
6. Once the pre-run is complete, wash the wells with 0.5× TBE buffer using a 10-mL syringe fitted with a 22-gauge needle.
7. Load the warm samples and run at 150 V until the bromophenol blue dye is at the bottom.
8. After completion of the run, allow the plates to cool 10–15 min before separation.
9. Carefully remove the gel from the glass plate assembly and put it in clean dish containing 50 mL of 5 µg/µL EtBr diluted in 0.5× TBE. Incubate for 15 min with gentle shaking.
10. Discard the EtBr solution and wash the membrane with 0.5× TBE.
11. Take a picture of the stained gel with a UV transilluminator to record EtBr-stained RNA fluorescence. An example of a typical experimental result is shown in Fig. 5.

3.9. Quantitative Real-Time PCR for Let-7 MicroRNA

1. Dilute the total RNA samples in water to obtain a 2 ng/µL solution.
2. Perform reverse transcription reaction to convert specific microRNAs to complementary DNA with the TaqMan MicroRNA Reverse Transcription (RT) kit, using either *let-7*

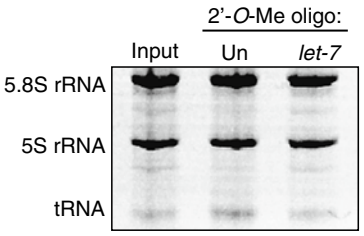

Fig. 5. Assessment of the integrity of the 5.8S and 5S rRNAs in the unbound fractions recovered from either the unrelated (Un) or *let-7* complementary matrices. *Discrete bands* are visible, demonstrating the integrity of the short RNA preparations.

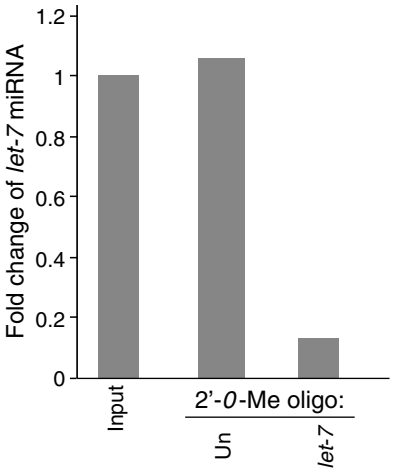

Fig. 6. qRT-PCR analysis of the *let-7* miRNA remaining in the unbound fractions recovered from either the unrelated (Un) or the *let-7* complementary matrices. When using the *let-7* complementary matrix, almost 90% of the mature *let-7* miRNA is depleted from the starting material. This demonstrates the efficiency and the specificity of the affinity chromatography.

microRNA-specific primer or the *sn2841* short RNA primer as an endogenous control. We use 10 ng of total RNA per reaction.

3. Perform Quantitative RT-PCR analyses of *let-7*, and *sn284* with TaqMan microRNA Assays kit following manufacturer procedures.
4. Data analysis was performed using the comparative C_t method using the endogenous control to normalize the level of microRNA.
5. A typical experimental result is shown in Fig. 6.

4. Notes

1. Be aware that sodium hypochlorite solution becomes less effective with time. Volume can be changed from 2 to 5 mL to obtain a complete lysis of *C. elegans* cuticules with an older solution.
2. Biotinylated 2′-*O*-methylated oligonucleotides can be designed to pull-down any small RNA-specific complex. The nucleotide sequences must be fully complementary to the chosen small RNA, and five extra nucleotides are added on each side of the complementary region to increase the stability of the small RNA complex-oligonucleotide association and the efficiency of the pull-down.
3. Ensure that the RNA molecule has been purified by HPLC techniques.
4. Upon reception of the synthesized modified RNA oligonucleotides, aliquot at 100 μM in deionized, freshly autoclaved water (use RNase-free tubes). Store aliquots at –20°C.
5. 2′-*O*-methylated oligonucleotides are stable in water solution at 4°C for up to 2 weeks, and stable for at least 6 months if stored at –20°C. Dried oligos stored at –20°C in a nuclease-free environment should be stable for several years.
6. It is very important to store the vial containing beads upright to keep them in liquid suspension. The performance will decrease if the beads air dry. Do not freeze.
7. Dynabeads are not supplied in RNase-free solutions, it is very important to use buffer containing nuclease inhibitors during the binding and washing steps.
8. Running buffer can be used for up to two runs, if it is cooled down at room temperature between successive runs.
9. The same primary antibody diluted in TBS-T and supplemented with dry milk can be reused two or three times. This solution can be stored at 4°C for several days or at –20°C for 2–3 weeks.
10. As urea may precipitate if these solutions are refrigerated, the solution should be stored in a tightly capped container and in a dark area at room temperature. However, the urea can be rapidly redissolved when warmed to room temperature.
11. For this protocol manuscript, we used the nematode *C. elegans* as a biological sample. The RISC pull-down assay using 2′-*O*-methylated oligonucleotides as affinity matrices can easily be applied to any other biological samples. The binding of RNA molecules to the beads should be optimized for a lysis buffer adequate for the specific biological sample used.

12. Do not allow the reaction to proceed for longer than 3 min as this will result in death of the embryos.
13. For better results and to avoid the microRNA/RISC/protein degradation, the pull-down assay should be performed (if possible) directly after the crude *C. elegans* extract is prepared.
14. We used 30 µL of suspension solution containing 10 mg/mL of beads for 2 mg of protein extract.
15. The binding capacities of beads are around to 200 pmol of RNA molecule for 1 mg of beads. Thirty microliter of suspension solution corresponds to 300 µg of beads, so 60 pmol of 2′-*O*-methylated oligonucleotide molecules are necessary for the binding. This is why the oligonucleotide solution is diluted to 1 pmol/µL (1 µM final).
16. Some proteins can interact more strongly than others with the matrix. To limit nonspecific binding, you may increase the quantity of beads bound to the unrelated oligo in the first step (clearing step) or repeat this step two or three times.
17. If the cell extract is too viscous, some beads may not be separated from the suspension by the magnet. To circumvent this problem, centrifugation may be used to pellet the beads.
18. Sometimes, a small amount of beads are loaded on the gel, along with the samples. This does not prevent the proper running process.

Acknowledgments

We are grateful to the members of our laboratory for comments on this methods manuscript. Nematode strain, N2 was provided by the *Caenorhabditis* Genetics Center, which is funded by the NIH National Center for Research Resources (NCRR). Our research is funded work by the Canadian Institutes of Health Research (CIHR), the Natural Sciences and Engineering Research Council of Canada, and the Cancer Research Society. M.J.S. is a CIHR New Investigator.

References

1. Stefani, G., and Slack, F. J. (2008) Small noncoding RNAs in animal development, Nat Rev Mol Cell Biol **9**, 219–230.
2. Hutvagner, G., and Simard, M. J. (2008) Argonaute proteins: key players in RNA silencing, Nat Rev Mol Cell Biol **9**, 22–32.
3. Hutvágner, G., Simard, M. J., Mello, C. C., and Zamore, P. D. (2004) Sequence-specific inhibition of small RNA function, PLoS Biol **2**, E98.
4. Inoue, H., Hayase, Y., Imura, A., Iwai, S., Miura, K., and Ohtsuka, E. (1987) Synthesis and hybridization studies on two

complementary nona(2′-O-methyl)ribonucleotides, Nucleic Acids Res **15**, 6131–6148.

5. Fabian, M. R., Mathonnet, G., Sundermeier, T., Mathys, H., Zipprich, J. T., Svitkin, Y. V., Rivas, F., Jinek, M., Wohlschlegel, J., Doudna, J. A., Chen, C. Y., Shyu, A. B., Yates, J. R., 3rd, Hannon, G. J., Filipowicz, W., Duchaine, T. F., and Sonenberg, N. (2009) Mammalian miRNA RISC recruits CAF1 and PABP to affect PABP-dependent deadenylation, Mol Cell **35**, 868–880.
6. Aoki, K., Moriguchi, H., Yoshioka, T., Okawa, K., and Tabara, H. (2007) In vitro analyses of the production and activity of secondary small interfering RNAs in *C. elegans*, EMBO J **26**, 5007–5019.
7. Yigit, E., Batista, P. J., Bei, Y., Pang, K. M., Chen, C. C., Tolia, N. H., Joshua-Tor, L., Mitani, S., Simard, M. J., and Mello, C. C. (2006) Analysis of the *C. elegans* Argonaute family reveals that distinct Argonautes act sequentially during RNAi, Cell **127**, 747–757.
8. Mayr, C., Hemann, M. T., and Bartel, D. P. (2007) Disrupting the pairing between let-7 and Hmga2 enhances oncogenic transformation, Science **315**, 1576–1579.